PERFORMANCE ANALYSIS OF DEEP LEARNING MODELS ON SKIN CANCER IMAGE CLASSIFICATION IN DIFFERENT COLOUR SPACES

THESIS SUBMITTED IN
PARTIAL FULFILLMENT OF THE REQUIREMENTS
FOR THE AWARD OF THE DEGREE OF

Master of Technology
in
VLSI Design and Microelectronics Technology
(Electronics and Telecommunication Engineering Department)
Jadavpur University

June, 2023

by

ANISHA PAUL
Class Roll No: 002010703020
Examination Roll No: M6VLS23013
Registration No: 154122 of 2020-2021

Under the guidance of
Prof. Sheli Sinha Chaudhuri

Department of Electronics and Telecommunication Engineering
Jadavpur University
Kolkata - 700032
West Bengal, India

DECLARATION OF ORIGINALITY AND COMPLIANCE OF ACADEMIC ETHICS

I hereby declare that this thesis contains previous work and original work by the undersigned candidate, as part of my Master of Technology in VLSI Design and Microelectronics Technology in the Department of Electronics and Telecommunication Engineering. All information in this document has been obtained and presented in accordance with academic rules and ethical conduct. I also declare that I have thoroughly cited and referenced all material and findings which are not original to this research, as provided by these rules and conduct.

Name : Anisha Paul

Exam Roll No : M6VLS23013

Thesis Title : PERFORMANCE ANALYSIS OF DEEP LEARNING MODELS ON SKIN CANCER IMAGE CLASSIFICATION IN DIFFERENT COLOUR SPACES

Signature of Candidate

FACULTY OF ENGINEERING & TECHNOLOGY
JADAVPUR UNIVERSITY

CERTIFICATE

This is to certify that the thesis entitled — "PERFORMANCE ANALYSIS OF DEEP LEARNING MODELS ON SKIN CANCER IMAGE CLASSIFICATION IN DIFFERENT COLOUR SPACES" has been carried out by ANISHA PAUL bearing Class Roll No: 002010703020, Examination Roll No.: M6VLS23013 and Registration No: 154122 of 2020-2021, under my guidance and supervision and be accepted in partial fulfillment of the requirement for the degree of **Master of Techolonoly** in **VLSI Design and Microelectronics Technology** in the Department of Electronics and Telecommunication Engineering.

Dr. Sheli Sinha Chaudhuri   *S. S. Chaudhuri   13/6/23*
Professor
Dept. of Electronics & Tele-Comm. Engg.
JADAVPUR UNIVERSITY
Kolkata-700 032

Prof. Sheli Sinha Chaudhuri
Supervisor
Department of Electronics and
Telecommunication Engineering
Jadavpur University

Manotosh Biswas   14/06/23

Prof. Manotosh Biswas
Head of the Department
Department of Electronics and
Telecommunication Engineering
Jadavpur University

Ardhendu Ghoshal   14/06/23

Prof. Ardhendu Ghoshal
Dean
Faculty of Engineering & Technology
Jadavpur University
Kolkata – 700032

MANOTOSH BISWAS
Professor and Head
Electronics and Telecommunication Engineering
University, Kolkata - 32

DEAN
Faculty of Engineering & Technology
JADAVPUR UNIVERSITY
KOLKATA-700 032

FACULTY OF ENGINEERING & TECHNOLOGY
JADAVPUR UNIVERSITY

CERTIFICATE OF APPROVAL
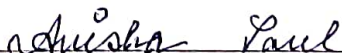
The thesis titled **"PERFORMANCE ANALYSIS OF DEEP LEARNING MODELS ON SKIN CANCER IMAGE CLASSIFICATION IN DIFFERENT COLOUR SPACES"** is hereby approved as a creditworthy study of an engineering subject conducted and presented satisfactorily to warrant its acceptance as a precondition to the degree for which it was submitted. It is understood that the undersigned does not automatically support or accept any argument made, opinion expressed, or inference drawn in it by this approval, but only approves the thesis for the reason it was submitted.

**Committee on Final
Examination for Evaluation of
the Thesis**

Signature of External Examiner

Signature of Supervisor

ACKNOWLEDGEMENTS

Anisha Paul

VLSI Design & Microelectronics Technology

Electronics & Telecommunication Engineering Department

Jadavpur University

Kolkata-32, West Bengal, India

Abstract

Skin cancer classification work is chosen for thesis projects due to its importance in healthcare, the rising incidence of skin cancer, and the potential for improved outcomes through accurate and automated classification systems. In this thesis work, I have extensively analyze the effect of utilizing different color spaces beyond the widely employed RGB model in deep convolutional neural networks (CNNs) for cancer cell classification. I trained and tested five popular deep-learning models on a diverse set of eleven color spaces, including RGB, HED, HSV, LAB, RGBCIE, XYZ, YCBCR, YDBDR, YIQ, YPBPR, and YUV. The results consistently demonstrated that the YUV, LAB, and YIQ color spaces exhibited superior performance compared to other color models in most instances. The YUV color space, by separating luminance and chromaticity components, enabled me to focus on distinct aspects of the images, leading to improved accuracy in capturing subtle differences in cell structures and textures. The LAB color space, representing colors based on perceptual qualities and separating lightness from opponent color channels, proved advantageous in capturing subtle color variations indicative of malignancy. Additionally, the YIQ color space's separation of intensity and chromatic information provided valuable cues for discriminating cancerous cells.

These findings highlight the significance of considering alternative color spaces in deep learning-based cancer cell classification tasks. By exploring beyond the traditional RGB color space, I discovered that the YUV, LAB, and YIQ spaces offer valuable features that can enhance accuracy and performance in cancer cell classification. The use of these color spaces enables the models to capture important visual information specific to cancer cells, thereby improving the overall classification accuracy and potentially assisting in more accurate diagnosis and treatment decisions. . Keywords: Skin Cancer classification, Image Classification, Color Space, Deep learning.

Contents

List of Tables

List of Figures

Chapter 1

Introduction

Skin cancer classification is indeed an important application of machine learning in healthcare.Machine learning algorithms can be utilized to examine images of skin lesions and categorize them into various forms of skin cancer, such as melanoma, basal cell carcinoma, and squamous cell carcinoma. Early and accurate detection of skin cancer is crucial for timely treatment and improved patient outcomes. Skin cancer classification using machine learning combines the power of automation, data analysis, and image recognition to improve the accuracy, efficiency, and accessibility of skin cancer diagnosis. By leveraging technology, it has the potential to enhance healthcare outcomes, support dermatologists, and positively impact public health efforts.

Skin cancer classification using machine learning is a significant and valuable application in healthcare. By analyzing images of skin lesions, ML algorithms can aid in early skin cancer detection, which can greatly improve patient outcomes. This approach addresses the visual complexity of skin lesions and provides objective and consistent analysis, assisting dermatologists in making accurate diagnoses. The scalability of ML algorithms allows for the analysis of large volumes of images, making it beneficial in areas with limited access to dermatological expertise. These systems save time by expediting the screening process and providing decision support to dermatologists. By reaching a wider population, ML-based classification systems can have a positive impact on public health initiatives related to skin cancer prevention and early detection. Overall, this application combines automation, data analysis, and image recognition to enhance the accuracy, efficiency, and accessibility of skin cancer diagnosis.

1.1   BASIC APPLICATIONS

Deep Learning (DL) is a subfield of machine learning that focuses on using artificial neural networks with multiple layers to learn and extract hierarchical representations

of data. DL has a wide range of applications across various domains. Some basic applications of Deep Learning:

- Image and Video Recognition: DL models, particularly Convolutional Neural Networks (CNNs), excel in tasks such as image classification, object detection, facial recognition, and scene understanding. DL models have achieved remarkable performance in competitions like ImageNet, enabling advanced image analysis and understanding.

- Natural Language Processing (NLP): DL techniques have revolutionized NLP tasks, including language translation, sentiment analysis, named entity recognition, text generation, and question answering. Recurrent Neural Networks (RNNs) and Transformer models, such as the popular BERT and GPT architectures, have significantly advanced language understanding and generation.

- Speech Recognition and Synthesis: DL models have been successful in speech recognition tasks, such as converting spoken language into written text. They are also used in text-to-speech synthesis, converting written text into natural-sounding speech. Deep learning architectures like Recurrent Neural Networks (RNNs) and Long Short-Term Memory (LSTM) networks are commonly used for these tasks.

- Autonomous Vehicles: DL plays a vital role in enabling autonomous vehicles to perceive and understand the environment. DL models process data from various sensors such as cameras, lidar, and radar to detect objects, recognize traffic signs, predict trajectories, and make real-time driving decisions.

- Recommender Systems: DL models are used to build powerful recommender systems that can provide personalized recommendations based on user preferences and behaviour. These systems are widely used in e-commerce platforms, streaming services, social media, and content platforms.

- Generative Models: DL has advanced the field of generative modelling, allowing the creation of realistic synthetic images, videos, and text. Models like Generative Adversarial Networks (GANs) and Variational Autoencoders (VAEs) can generate new samples that resemble real data, with applications in art, entertainment, and data augmentation.

- Healthcare: DL is making significant contributions to healthcare, including medical image analysis, disease diagnosis, drug discovery, and genomics. DL models can analyze medical images, such as X-rays and MRIs, to detect diseases, assist in diagnosis, and predict patient outcomes.

- Robotics: DL is used in robotics to enable perception, control, and decision-making tasks. DL models can process sensor data, such as vision and tactile feedback, to

understand the robot's environment, manipulate objects, and perform complex tasks autonomously.

- Robotics: DL is used in robotics to enable perception, control, and decision-making tasks. DL models can process sensor data, such as vision and tactile feedback, to understand the robot's environment, manipulate objects, and perform complex tasks autonomously.

- Gaming and Reinforcement Learning: DL techniques have been successful in training agents to play complex games through reinforcement learning. DL models, combined with reinforcement learning algorithms, can learn optimal strategies and achieve superhuman performance in games like chess, Go, and video games.

This thesis focuses on how deep learning models are performing on different color spaces. Color is a very important role in human life or the universe. If I mixed all the color together it gives a white color, which means the sum of all colors is equal to white. I hereby present the relevant existing research works,that influenced me to take up this thesis work.

I could see different types of color and different colors used in different fields. P.Ganesanet et al. conducts a survey of color spaces and the reutilization for image segmentation [1]. M. Tkalčič et al. explores the various color spaces utilized in the fields of electrical engineering and image processing. It examines the perceptual, historical, and practical factors that have contributed to the development and application of each color space. [2]. Some of the paperwork for evaluating the color space and M. Asmare et al proposed that the YUV color space has been perfectly reconstructed while in image enhancement HSI performs the best in eight colors. Also, this paper evaluates eight color spaces and their conversion accuracy and structural similarity measure [3]. A. Zeileis et al. discussed the color space R package offers a versatile set of tools for selecting specific colors or color palettes, manipulating those colors, and using them in statistical graphics and data visualizations. [4]. Another proposal by R. Kuehni et al. is the concept of color space and its various subdivisions. It illustrates the evolution of a colorimetric model and explores challenges related to colour-matching functions, distinct hues, the Helmholtz-Kohlrausch effect, and the enhancement of lightness and chroma. Additionally, it introduces a novel approach to measuring lightness and dealing with the sharpening of lightness [5]. C. Ballester et al. state studies the impact of different color spaces on deep learning-based image colorization. By employing the same deep neural network architecture, it compares the outcomes obtained using RGB, YUV, and Lab color spaces. The results indicate that there is no unanimous agreement on the superiority of any specific color space [6].

Richard Zhang et al. proposed a deep learning technique presented in this study for user-guided image colorization. The proposed system utilizes a Convolutional Neural Network

(CNN) to map a grayscale image, along with sparse and local user hint colorized output. By leveraging a large-scale dataset, CNN combines low-level cues and high-level semantic information to effectively incorporate user edits into the final colorization result [7].

For Color Space, another application is in the transport system, traffic light and Hyun-Koo Kim et al. investigate how the objective of the research is to explore the design of a high-performance traffic light detection system using deep learning techniques. The study investigates the effectiveness of six different color spaces and three types of network models in achieving optimal results. The findings indicate that the combination of the RGB color space and the faster R-CNN model yields the best performance in detecting traffic lights [8]. Hani K. Al-Mohair conducted a study using Deep Learning models and color spaces to detect skin texture, skin cancer, and skin-related problems on a large scale. The study evaluated the performance of various color spaces for skin detection and found that the YIQ color space exhibited the highest degree of distinction between skin and non-skin pixels, indicating its superior effectiveness in accurately detecting skin regions. [9].

In the purpose of using the color space there are many advantages and disadvantages. For that, Edgar Chavolla et al. used a Machine Learning algorithm for on K means++ clustering for object recognition and tracking and the paper looks at the research that h investigates the strengths and limitations of different color spaces in image color clustering segmentation. It examines how the choice of a specific color space impacts the performance of a widely used clustering machine learning algorithm. By evaluating the outcomes, the study aims to determine the benefits and drawbacks associated with each color space representation with respect to skin cancer images in achieving accurate and effective segmentation of the region of interest from the color images of the skin of patients' image color clustering segmentation [10].

Chapter 2

Motivation & Contribution

2.1 Motivation

Skin cancer classification using machine learning holds tremendous significance in the field of healthcare. One of the primary reasons is the ability to achieve early detection of skin cancer, which is crucial for successful treatment and improved patient outcomes. By analyzing skin lesion images, machine learning algorithms can identify potential cancerous growths at an early stage when they are most treatable. This early detection can significantly increase the chances of successful interventions and save lives.

A key advantage of using machine learning for skin cancer classification is the accuracy and objectivity it brings to the diagnostic process. Dermatologists face challenges in differentiating between benign and malignant lesions due to the visual complexity and subtle variations. Machine learning algorithms, trained on large datasets of annotated skin lesion images, can learn patterns and features that aid in accurate diagnosis. By providing objective and consistent analysis, these algorithms can complement the expertise of dermatologists, leading to more reliable diagnoses and reducing the risk of misdiagnosis.

Scalability and accessibility are other crucial aspects where machine learning excels in skin cancer classification. With the ability to process and analyze a vast volume of skin lesion images efficiently, machine learning algorithms can handle the increasing demand for automatic screening and diagnosis. This scalability is particularly valuable in regions with limited access to dermatologists or areas with high patient loads. Automated classification systems can prioritize cases based on risk assessment, providing preliminary evaluations and extending access to skin cancer screening to a larger population. This improves the efficiency and reach of healthcare services, ensuring that more individuals have access to timely and accurate skin cancer diagnoses.
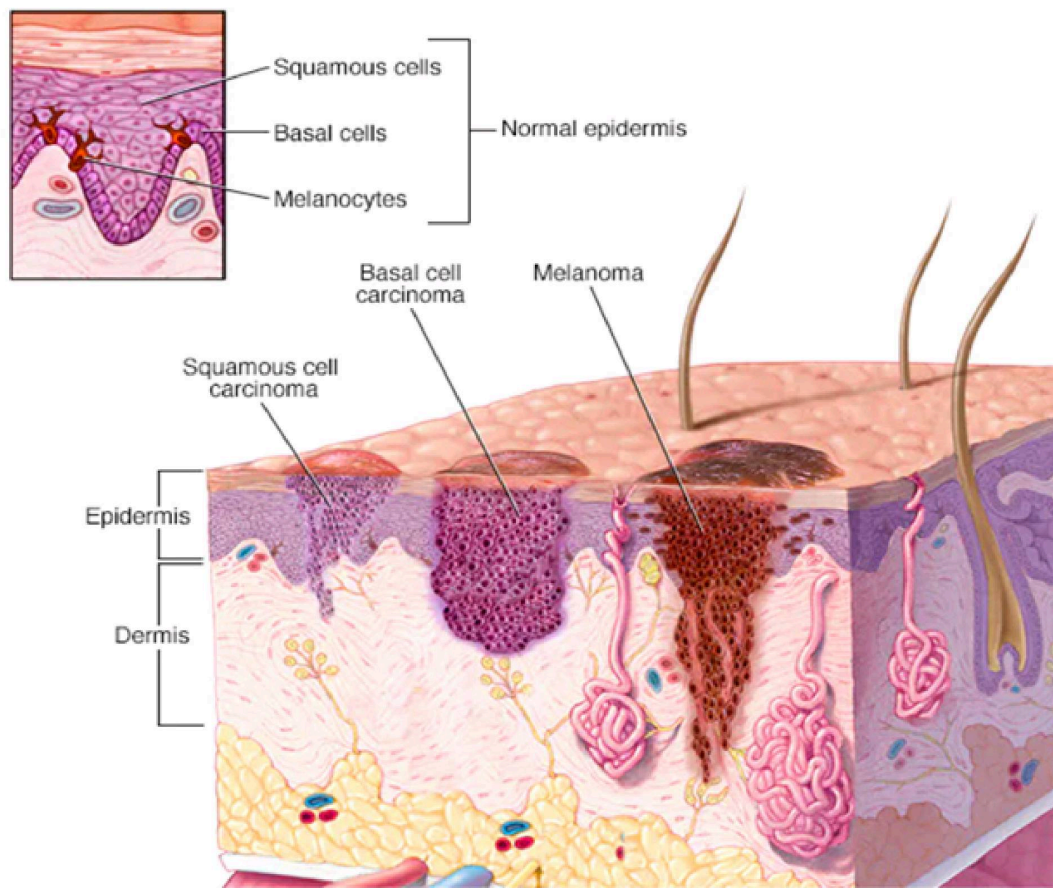
FIGURE 2.1: Layering of Skin

Machine learning-based classification systems also serve as invaluable decision-support tools for dermatologists. By providing additional insights and objective assessments, these systems can assist dermatologists in making more informed decisions regarding further examinations, biopsies, or referrals to specialists. This integration of machine learning into the clinical workflow empowers dermatologists with improved diagnostic accuracy, enabling better patient management and personalized treatment plans.

The impact of skin cancer classification using machine learning extends beyond individual patients and healthcare professionals. Skin cancer is a global public health issue of considerable importance and early detection plays a vital role in prevention and reducing the overall burden of the disease. Machine learning-based classification systems have the potential to reach a broader population, including individuals who may not have easy access to specialized healthcare services. By promoting early detection through automated screening and diagnosis, these systems contribute to public health initiatives focused on preventing and reducing the prevalence and impact of skin cancer. Ultimately, these advancements can lead to earlier treatment, reduced healthcare costs, and improved overall public health outcomes. Skin cancer classification using machine learning offers a multitude of advantages in healthcare. The ability to achieve early detection, enhance diagnostic accuracy, improve scalability and accessibility, provide decision support, and

positively impact public health make it an essential tool in the fight against skin cancer. By leveraging the power of machine learning, this can improve patient outcomes, empower healthcare professionals, and make significant strides in preventing and managing skin cancer.

2.2   Contribution

Performing inference with MobileNet using the YUV colour space involves a specific workflow and considerations.Since MobileNet is typically trained and expects RGB images as input, one needs to convert the input RGB images to the YUV color space before inference. This conversion can be done using appropriate image processing libraries or frameworks like OpenCV or PIL (Python Imaging Library).

Convert the RGB image to YUV by applying the YUV transformation to separate the luminance (Y) channel from the chrominance (U and V) channels. This step involves converting the RGB pixel values to YUV values using appropriate conversion formulas. Once the RGB image is converted to YUV, you can perform inference using the MobileNet model. Pass the Y channel (luminance) as input to the model. This process will involve loading the MobileNet model, feeding the input image, and obtaining the inference results, such as class predictions or feature representations. After obtaining the inference results from MobileNet, you can apply any necessary post-processing steps depending on your specific application. This could include tasks like object detection, semantic segmentation, or any other relevant processing based on the obtained predictions or feature maps.

YUV color space with MobileNet on a Raspberry Pi can offer certain benefits, such as reduced bandwidth or emphasis on luminance, it's crucial to assess the trade-offs in terms of computational overhead and overall performance. Additionally, optimizing the inference pipeline, considering hardware accelerators, or model quantization techniques can further enhance the efficiency of the inference process on the Raspberry Pi.

Chapter 3

Literature Survey

3.1 Application in Details

Image classification is a process of categorizing an image into a predefined set of classes based on its visual content. This task is usually performed by a machine learning algorithm to analyse various classes of images.

Deep learning algorithms work by building and training artificial neural networks that are composed of multiple layers of interconnected nodes. These nodes are modelled after the neurons in the human brain, and they are organized into input, hidden, and output layers. During the training phase, the neural network is presented with a set of labelled examples, or training data, which consists of input data and the corresponding desired output. The network adjusts the weights and biases of the nodes in each layer based on the error between the predicted output and the actual output.
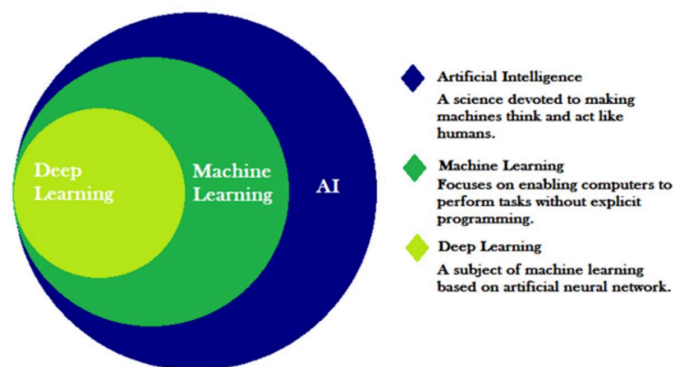
FIGURE 3.1: Section of AI,ML,DL

This process is called backpropagation, and it involves propagating the error backwards through the network, from the output layer to the input layer. By adjusting the weights

and biases of the nodes in each layer, the network learns to recognize patterns and relationships in the data, and it can make more accurate predictions over time.

Once the network has been trained, it can be used to make predictions on new, unseen data. The input data is fed into the input layer of the network, and it propagates through the hidden layers until it reaches the output layer, which produces the predicted output. One of the main advantages of deep learning is that it can automatically extract features from raw data, without the need for manual feature engineering. This allows the network to learn complex patterns and relationships in the data that may not be apparent to human experts.

However, deep learning also has some limitations, such as the need for large amounts of data and computational resources, as well as the difficulty in interpreting the decisions made by the network.
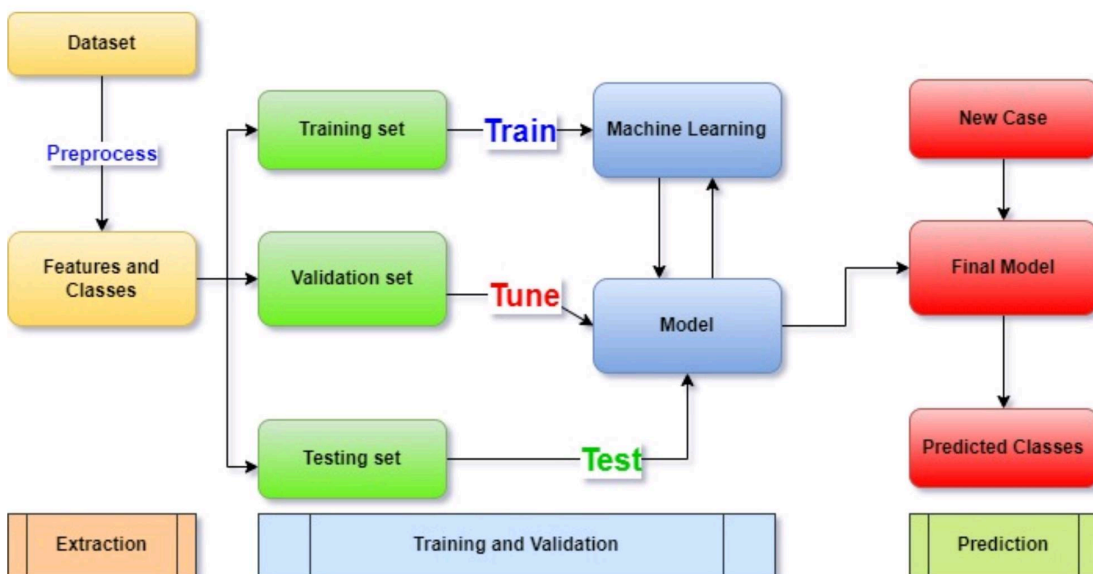
FIGURE 3.2: Deep Learning Workflow

Deep learning, on the other hand, can learn a hierarchy of features from the raw pixel values of the images. The initial layers of the network learn simple features, such as edges and corners, while the later layers learn more complex features, such as shapes and textures. By combining these features, the network can classify the images with a high degree of accuracy.

Convolutional neural networks (CNNs) are powerful algorithms for image classification. They extract features through convolutional and pooling layers and use fully connected layers for classification. CNNs learn hierarchical representations and have achieved remarkable performance. However, they require large labeled datasets and can be computationally expensive. CNNs have revolutionized computer vision tasks.

Many approaches are there to classify an image but one of the best common method is convolutional neural networks (CNNs). CNNs are deep learning models that analyzing an image cause it can extract the relevant features automatically which is needed for classification.

Steps for classification of image using CNN To classify an image using CNNs many steps are there:

1. Data preparation: In this step collect the data and prepares the dataset and label the data according to the class.

2. Model training: This involves training a CNN on the labelled dataset to learn to recognize the patterns and features associated with each class.

3. Model evolution: It evaluates the trained models and identifies which model gives the best performances on a separate set of images that were not used during training.

4. Prediction: Once the model were trained and evaluated, it easy to predict the class of new images based on their visual content. CNN:Convolution Neural Network is constructed by multiple building blocks, such as convolution layers, pooling layers, and fully connected layers. This is designed for automatically and easily extract the main features of an image through a backpropagation algorithm.

CNNs is widely used in image analysis in medicine, detecting objects in a self-driving car, social media face recognition, OCR (optical character recognition) and image recognition.

The first two layers which are the convolution layer and pooling layer used for feature extraction from an image and the third layer, fully connected layers is maps the extracted features into final output. A convolution layer is a main or key role in CNN, which is combined of a stack of mathematical operations, such as convolution, a specialized type of linear operation. In digital images, pixel values are 2-dimensional array numbers and a small parameter called the kernel, an optimizable feature extractor which makes CNNs high quality and efficient for image processing and is applied in every image position.

3.2   Current Challenges

Despite the significant progress made in image classification using deep learning, there are still several challenges that need to be addressed. Some of the current challenges are:

- Data quality and quantity: Deep learning algorithms require large amounts of high-quality labelled data to learn meaningful representations. However, obtaining and
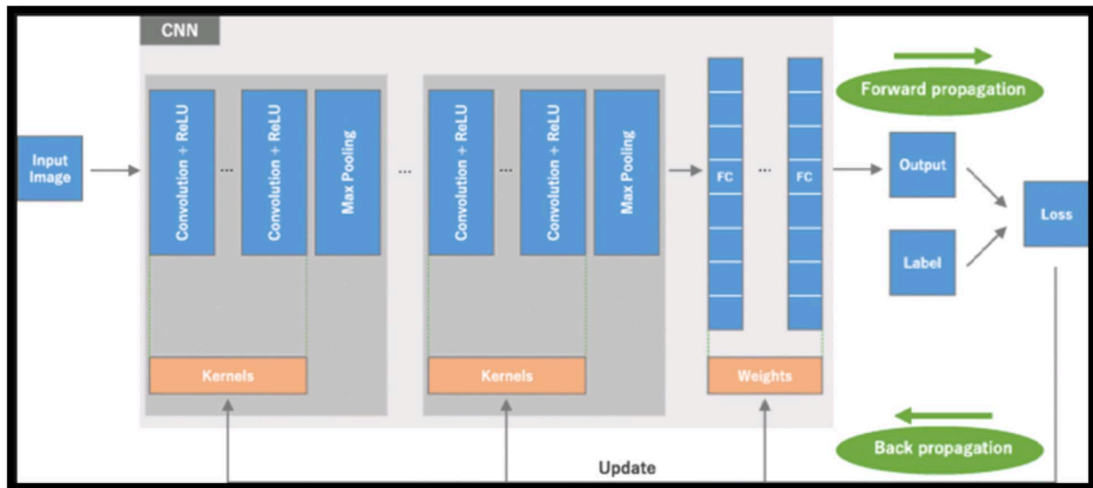
FIGURE 3.3: Architecture of Convolution Neural Network

annotating large datasets can be time-consuming and expensive, particularly for certain applications such as medical imaging.

- Generalization: Deep learning algorithms may over fit the training data and perform poorly on new, unseen data. This can be addressed through techniques such as regularization, data augmentation, and transfer learning, but it remains a significant challenge.

- Explainability: Deep learning models can be difficult to interpret, particularly when they are composed of many layers and millions of parameters. Understanding how the model arrived at its decision is important for applications such as medical diagnosis, where the reasoning behind the decision is crucial.

- Privacy and security: Deep learning models trained on sensitive data, such as medical records or personal images, can raise privacy and security concerns. Techniques such as federated learning and differential privacy can help address these concerns, but they remain an active area of research.

- Robustness: Deep learning models can be vulnerable to adversarial attacks, where small perturbations to the input can cause the model to make incorrect predictions. Developing robust models that are resistant to such attacks is an ongoing challenge.

3.3 Existing Papers

Here I am discussing some of the paper which are related with Skin Cancer and Color Space

2016

In N. Codella et al. proposed this paper proposes this study suggests an integrated system that combines deep learning and traditional machine learning methods to enhance the accuracy of melanoma detection in dermoscopy images. The system is assessed using a comprehensive dataset of dermoscopic images, and it showcases improved performance levels compared to existing approaches [11].

2016

In A. Mahbod et al. research to introduce an automated computerized approach for classifying skin lesions, utilizing optimized deep features extracted from various well-known convolutional neural networks (CNNs) at different levels of abstraction. The method demonstrates excellent classification performance, achieving an area under the receiver operating characteristic curve of 83.83% for melanoma classification and 97.55% for seborrheic keratosis classification [12].

In Yuexiang Li et al. proposed two deep learning methods to address three main tasks in skin lesion image processing: lesion segmentation, lesion dermoscopic feature extraction, and lesion classification. The proposed frameworks were evaluated on the ISIC 2017 dataset and achieved promising accuracies [13].

In Andre Esteva et al. discuss the dermatologist-level classification of skin cancer with deep neural networks. It demonstrates that a convolutional neural network can be trained to classify skin cancer with a level of competence comparable to dermatologists [14]. In Alper Arik et al. propose a system that uses deep learning methods for the classification of skin lesions for melanoma detection [15].

2016

In K. Hosny et al. propose an automated skin lesion classification method using a pre-trained deep learning network and transfer learning. The proposed model presented in the study is trained and evaluated using the ph2 dataset. To assess the performance of the proposed method, widely recognized quantitative measures such as accuracy, sensitivity, specificity, and precision are utilized. The achieved values for these metrics are 98.61% for accuracy, 98.33% for sensitivity, 98.93% for specificity, and 97.73% for precision [16].

Y. Fujisawa et al. discuss how a deep-learning-based, computer-aided classifier can improve the sensitivity and specificity of skin cancer screening [17].

S. Fooladi et al. use deep learning to detect and classify skin cancer. It uses a dataset of 70 images of melanoma and 100 images of benign moles. 80% of the images are used for training and 20% for testing [18].

Ahmet Demir et al. use deep learning architectures to classify images of skin cancer as benign or malignant. It finds that the ResNet-101 architecture has an accuracy rate of 84.09% and the Inception-v3 architecture has an accuracy rate of 87.42% [19].

In their study, Abeer Afifi Mohamed et al. introduce a novel approach for skin lesion classification using convolutional neural networks (CNNs). Their proposed system achieves an impressive accuracy of 97.78% in accurately predicting the presence of melanoma in dermoscopic lesions. This research demonstrates the effectiveness and reliability of CNNs in dermatological diagnosis [20]. Pratik Kanani et al. explore the application of Deep Learning in detecting skin cancer using Google Colab. They highlight the capability of deep learning models to autonomously learn features from data and emphasize that deep learning outperforms traditional artificial intelligence and machine learning methods in skin cancer detection. This study underscores the potential of deep learning techniques in improving the accuracy and effectiveness of skin cancer diagnosis [21].

In Seeja R D et al. the primary aim of this research is to enhance the accuracy of melanoma classification through the implementation of an automatic skin lesion segmentation system based on deep learning techniques. The segmentation process utilizes a U-net algorithm, which is a Convolutional Neural Network (CNN) approach. The extracted features from this segmentation method are then utilized as input for classifiers such as Support Vector Machine (SVM), Random Forest (RF), K-Nearest Neighbor (KNN), and Naïve Bayes (NB) to classify skin images as either melanoma or benign lesions [22].

In Md. Muzahidul Islam Rahi et al. discuss the use of deep neural networks for the detection of skin cancer. It compares the performance of different algorithms and finds that the resnet algorithm achieves the highest accuracy [23].

In Catarina Barata et al. proposes to use a hierarchical deep-learning architecture to mimic the medical strategy of diagnosing skin lesions. It provides an evaluation of the criteria that must be considered in the development of such systems [24].

Garg et al. introducing a novel framework, this study suggests the utilization of the VGG-16 CNN model for categorizing cancer images. The framework was trained using publicly available skin cancer images from the ISIC archive and achieved an impressive accuracy of 97.81% in its classification performance [25].

In Teck Yan Tan et al. presenting an intelligent system for aiding in skin cancer detection, this research proposes the integration of asymmetry, border irregularity, color, dermoscopic structure features, along with texture features to represent skin lesions. Subsequently, a deep convolutional neural network is employed to classify the lesions accurately [26].

2016

A.Khamparia et al. introduce an innovative framework driven by deep learning and the Internet of Health and Things (IoHT), this study focuses on the classification of skin lesions in images. The framework leverages transfer learning to extract meaningful features from images using pre-trained architectures. By integrating with an IoHT

framework, the proposed system offers remote assistance to medical specialists, facilitating the diagnosis and treatment of skin cancer [27].

Ravi Manne et al. this research investigate the application of convolutional neural networks (CNNs) in classifying skin cancer. It explores the evolution of CNNs in effectively categorizing different types of skin cancer and discusses the strengths and weaknesses associated with utilizing CNNs for this purpose [28].

Mohammad Ali kadampur et al. discuss a model-driven architecture in the cloud that uses deep learning algorithms to predict skin cancer. The models were tested on standard datasets and had an accuracy of 99.77% [29].

A.A. proposes a deep-learning model for skin cancer detection from skin lesion images. It uses a transfer learning method with AlexNet as the pre-trained model. Using a confidence score threshold of 0.5, a classification accuracy of 84%, a sensitivity of 81%, and a specificity of 88% was obtained [30].

Rehan Ashraf et al. develop deep convolutional neural network-based technique to extract spatial information for skin cancer classification. The experiments show that the classification accuracy is about 93.29

Md. Farhad Hossin et al. discuss a model that predicts melanoma skin cancer by evaluating dermoscopic images with the help of deep learning. It uses a multi-layered CNN approach with multiple regularization techniques and achieves an accuracy of 93.58% [32].

Abhishek C. Salian et al. This paper discusses using deep learning architectures to classify skin lesions. It finds that different types of skin lesions can be classified with an accuracy of above 80% [33].

2016

Mehwish Dildar et al. conduct a comprehensive systematic review focused on deep learning techniques for early detection of skin cancer. Their study includes an analysis of research papers published in reputable journals, presenting their findings through various tools such as graphs, tables, and frameworks. The review provides valuable insights into the advancements, techniques, and approaches in deep learning for the early detection of skin cancer, contributing to the understanding and development of effective diagnostic tools in this field [34].

O.S.Kareem et al. this paper provides a comprehensive overview of various techniques used for detecting skin cancer from images. It examines the current state-of-the-art models that are effective in automatically identifying melanoma from skin images. The study suggests that the classification and segmentation results obtained from skin lesion images can be improved by employing an ensemble deep learning algorithm [35].

In J.Bethanney Janney et al. using deep learning algorithms to detect skin cancer. It compares the effectiveness of two different approaches and finds that both are equivalent to those of dermatologists [36]. In Hongfeng Li reviews the recent works on skin disease diagnosis with deep learning. This article examines the difficulties encountered in the field of skin disease diagnosis using deep learning and proposes potential avenues for future research. It highlights the challenges that arise when applying deep learning techniques to accurately diagnose various skin diseases. Additionally, the paper puts forth suggestions for future research directions, aiming to address these challenges and further enhance the performance and applicability of deep learning in skin disease diagnosis [37].

In Husam Khalaf Salih Juboori discusses a system for the identification of skin cancer at an early stage. The system is based on a deep learning technique and an entity encoding scheme. It can provide more discriminatory information despite its limited training examples [38].

2016

In Vandana Rawat et al. comparative study of various skin cancer techniques using deep learning. It analyzes the performance of various deep learning methods and focuses on a comparative study of various algorithms of deep learning [39].

Yinhao Wu et al. present a comprehensive overview of recent advancements in deep learning algorithms for skin cancer classification. Their study focuses on the successful application of convolutional neural networks in this domain and highlights key challenges such as data imbalance, data limitation, domain adaptation, model robustness, and model efficiency. By summarizing these frontier problems, the authors provide valuable insights into the current state of deep learning-based approaches for skin cancer classification and shed light on areas that require further research and development [40]. In S. Sweta et al. This paper discusses using deep learning to diagnose skin cancer. It describes how the accuracy of the diagnosis is 82 percent [41].

In Walaa Gouda et al. uses deep learning to detect skin cancer. It uses the ISIC2018 dataset, which includes 3533 skin lesions. The CNN model is used and shows an 83.2In Sidratul Montaha et al. proposes a shallow convolutional neural network (SCNN_12) model to classify the lesions into benign and malignant. It uses the 'box blur' downscaling method to reduce the overall training time and space complexity significantly. The model was able to achieve an accuracy of 98.87

In R.S.Kumar et al. uses Convolutional Neural Network (CNN) to identify and diagnose skin cancer. It gives an accuracy of 88% for classifying the training dataset as either benign or malignant [44].

As shown in the above table The ISIC (International Skin Imaging Collaboration) dataset is one of the prominent datasets in skin cancer research, comprising over 20,000 images of various sizes. This dataset encompasses both dermoscopy and clinical images
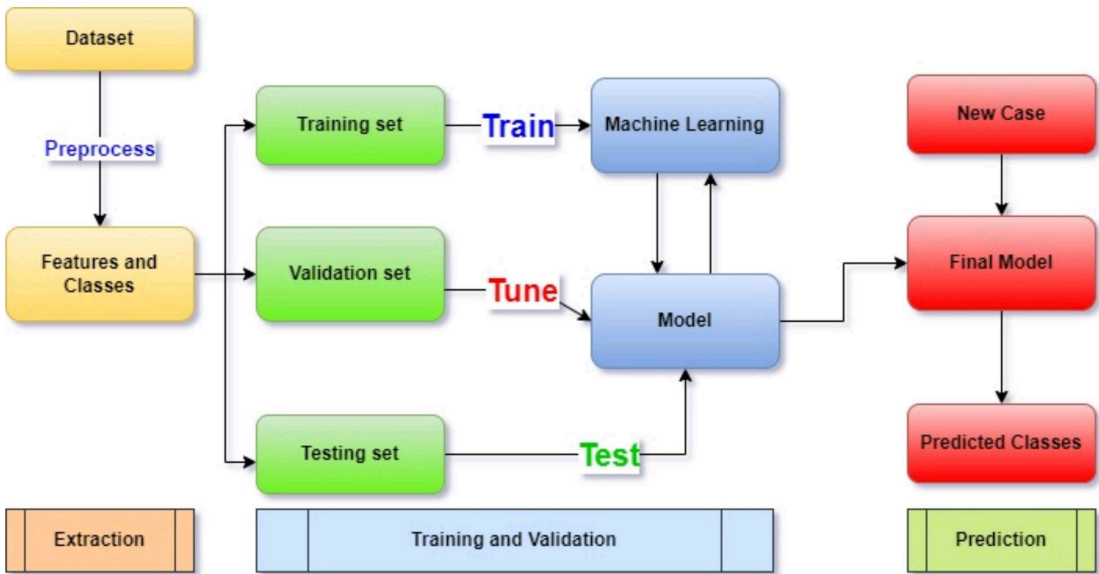
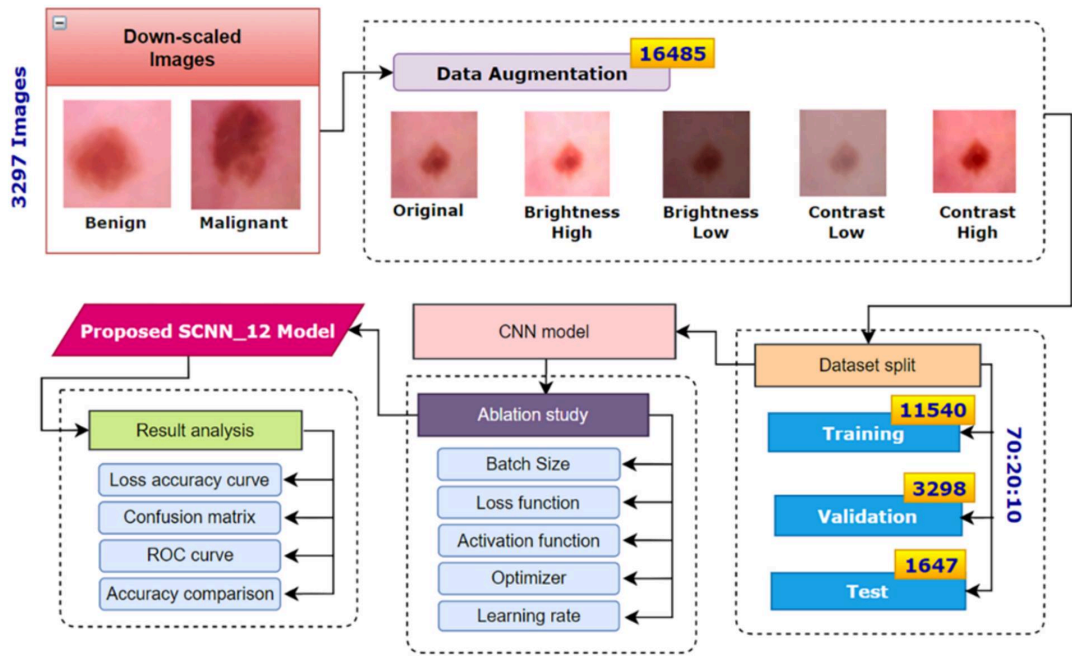FIGURE 3.4: Workflow of machine learning

FIGURE 3.5: Cancer Cell Classification Using Deep Learning

TABLE 3.1: Image Classification Dataset

Dataset	Data Volume		Image type		Others
	>20,000	Various sizes	Dermoscopy and clinical image	Melanoma,seborrheic keratosis, benign nevi	Segmentation mask provided
PH2	200	768x560	Dermoscopy image	Common nevi, melanomas, atypical nevi	-
HAM10000	10,015	800x600	Dermoscopy image	Pigmented lesions	-
IAD	2800	Various sizes	Dermoscopy and clinical image	Melanoma and benign lesion	-
Hallym	152	Various sizes	Clinical image	Basal cell carcinoma	-
Dermnet	23,000	Various sizes	Dermoscopy,pathology and clinical image	23 categories	-
Ref.	>18,930	Various sizes	Clinical image	23 categories	-
AtlasDerm	11,057	Various sizes	Clinical image	All kinds of skin diseases	-
Derm101	Thousands	Various sizes	Clinical image	All kinds of skin diseases	-
7-point criteria evaluation dataset	>2000	Various sizes	Dermoscopy and clinical image	Melanoma and non-melanoma	Structured metadata provided
MED-NODE	170	Various sizes	Clinical image	Melanoma and nevi	-

and covers diseases such as melanoma, seborrheic keratosis, and benign nevi. Additionally, the ISIC dataset provides segmentation masks, allowing researchers to delve into precise lesion delineation and analysis.

The PH2 dataset, consisting of 200 dermoscopy images, offers high-resolution images with dimensions of 768x560. It includes various types of skin lesions, including common nevi, melanomas, and atypical nevi. The HAM10000 dataset, on the other hand, provides a substantial collection of 10,015 dermoscopy images with an image resolution of 800x600. It focuses specifically on pigmented lesions, enabling researchers to explore the intricacies of melanoma and other pigmented skin conditions.

Another dataset worth mentioning is the IAD (Image Archive Database), which encompasses approximately 2,800 dermoscopy and clinical images. The IAD dataset focuses on differentiating melanoma from benign lesions and serves as a valuable resource for evaluating classification models in this specific context.

The Hallym dataset contributes 152 clinical images specifically targeting basal cell carcinoma, enabling researchers to develop and evaluate algorithms for the detection and classification of this particular type of skin cancer.

For a broader perspective on skin diseases, the Dermnet dataset offers a comprehensive collection of 23,000 images in various formats, including dermoscopy, pathology, and clinical images. Covering a wide range of skin diseases, this dataset provides an opportunity to explore classification models across different disease categories. In addition to these datasets, there are other resources available, such as the Ref. dataset, which provides a substantial number of clinical images spanning 23 categories of skin diseases. The AtlasDerm dataset offers 11,057 clinical images representing various skin conditions, while the Derm101 dataset consists of thousands of clinical images covering a wide array of skin diseases. Furthermore, datasets like the 7-point criteria evaluation dataset focus on evaluating melanoma and non-melanoma cases. With over 2,000 dermoscopy and clinical images, this dataset includes structured metadata, facilitating in-depth analysis and algorithm evaluation based on specific diagnostic criteria.

Lastly, the MED-NODE dataset contributes 170 clinical images centered around melanoma and nevi, serving as an additional resource for developing and testing classification models in this domain.

Chapter 4

Proposed Method

4.1 Working Principle

A specific method of representing and structuring colors in a digital image or video is known as a color space. This refers to a mathematical model which are mapped to numerical values. Different color space are used in image processing, including RGB (Red, Green, Blue), HSV (Hue, Saturation, Value), and LAB (Lightness, a(green to red), b(blue to yellow). Each color space has its own unique properties and can be used for different purposes. This section provides an overview of the eleven color space such as RGB, HED, HSV, LAB, RGBCIE, XYZ, YCBCR, YDBDR, YPBPR, YIQ, YUV.

4.2 Color Model and Spaces

4.2.1 RGB

RGB color space is the most commonly used color space in image classification. It represents color as a combination of red, green, and blue values. In this color space, each pixel in an image is represented by three numbers ranging from 0 to 255, which corresponds to the intensity of the red, green, and blue colors.

RGB (Red, Green, Blue) is a color model used to represent and display colors in digital devices, such as computer monitors, televisions, and cameras. It is based on the additive color theory, which suggests that when red, green, and blue light are combined at full intensity, they create pure white light.

In the RGB color space, colors are represented by three values that indicate the intensity of each primary color. Each value ranges from 0 to 255, where 0 represents no intensity and 255 represents full intensity. For example, pure red would be represented as (255,

0, 0) in RGB, indicating that the red component has full intensity and the green and blue components have no intensity.
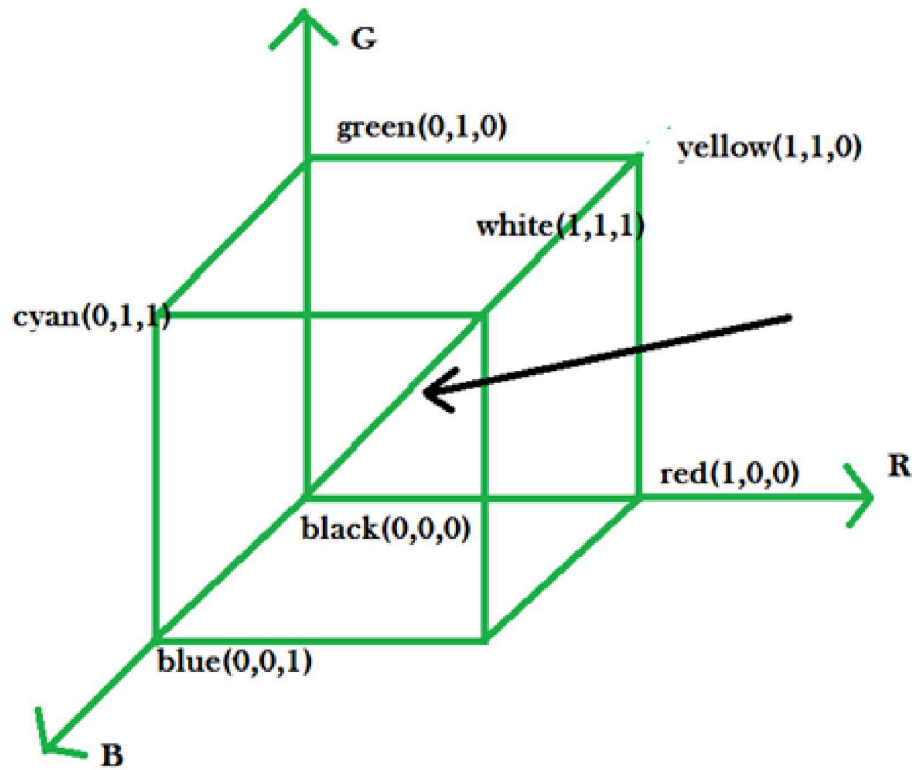
FIGURE 4.1: RGB in graphical view

The RGB color space can produce a wide range of colors using just three primary colors, making it a popular choice for digital devices. However, it is not ideal for printing, as the ink used in printers is based on the subtractive color model, which is different from the additive color model used in RGB. Therefore, RGB colors may appear differently when printed.

There are several variations of the RGB color space, including sRGB, Adobe RGB, and ProPhoto RGB. sRGB is the most widely used RGB color space and is commonly used for web graphics and digital images. Adobe RGB has a larger color gamut than sRGB and is used in professional photography and graphic design. ProPhoto RGB has an even larger color gamut and is used for high-end printing and professional photography.

In addition to the RGB color space, there are other color models used in digital imaging, such as CMYK (Cyan, Magenta, Yellow, Black) for printing and HSL/HSV (Hue, Saturation, Lightness/Value) for color selection and adjustment. Each color model has its strengths and weaknesses and is suited for different applications.
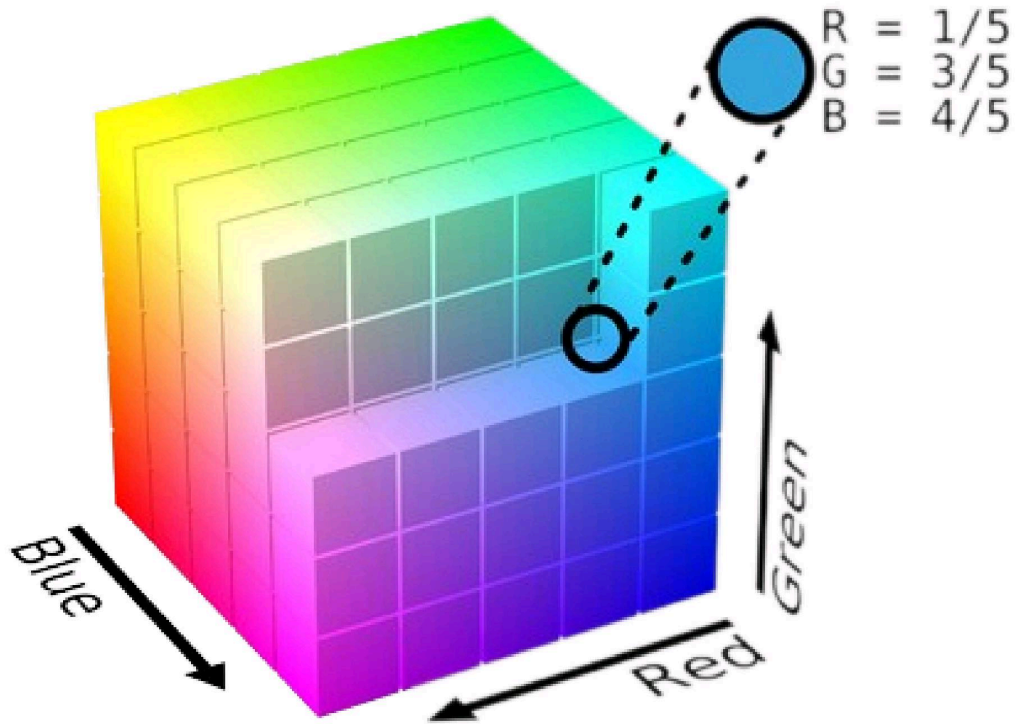
FIGURE 4.2: RGB color space

4.2.2 HSV

HSV (Hue, Saturation, and Value) is a color space that is commonly used in computer graphics, image processing, and color analysis. The HSV color space represents colors in terms of their hue, saturation, and value, providing a more intuitive way of describing color than the RGB color space.

Hue refers to the color of the light, and is measured in degrees around a color wheel. In the HSV color space, hues range from 0 to 360 degrees, with red at 0 degrees, green at 120 degrees, and blue at 240 degrees.

Saturation refers to the purity of the color, or how much gray is mixed with the hue. Saturation ranges from 0 (gray) to 100 (fully saturated).Value refers to the brightness of the color, or how much light is reflected. Value ranges from 0 (black) to 100 (white). RGB to HSV calculated as:

R' = R/255

G' = G/255

B' = B/255

Cmax = max(R', G', B')

Cmin = min(R', G', B')

Δ = Cmax - Cmin Hue calculation:

$$H := \begin{cases} 0, & \text{if } C = 0 \\ 60° \cdot \left(\frac{G-B}{C} \mod 6\right), & \text{if } V = R \\ 60° \cdot \left(\frac{B-R}{C} + 2\right), & \text{if } V = G \\ 60° \cdot \left(\frac{R-G}{C} + 4\right), & \text{if } V = B \end{cases} \tag{4.1}$$

Saturation calculation:

$$S_V := \begin{cases} 0, & \text{if } V = 0 \\ \frac{C}{V}, & \text{otherwise} \end{cases} \tag{4.2}$$

$$S_L := \begin{cases} 0, & \text{if } L = 0 \text{ or } L = 1 \\ \frac{C}{1-|2V-C-1|} = \frac{2(V-L)}{1-|2L-1|} = \frac{V-L}{\min(L,1-L)}, & \text{otherwise} \end{cases} \tag{4.3}$$

Value calculation: V = Cmax
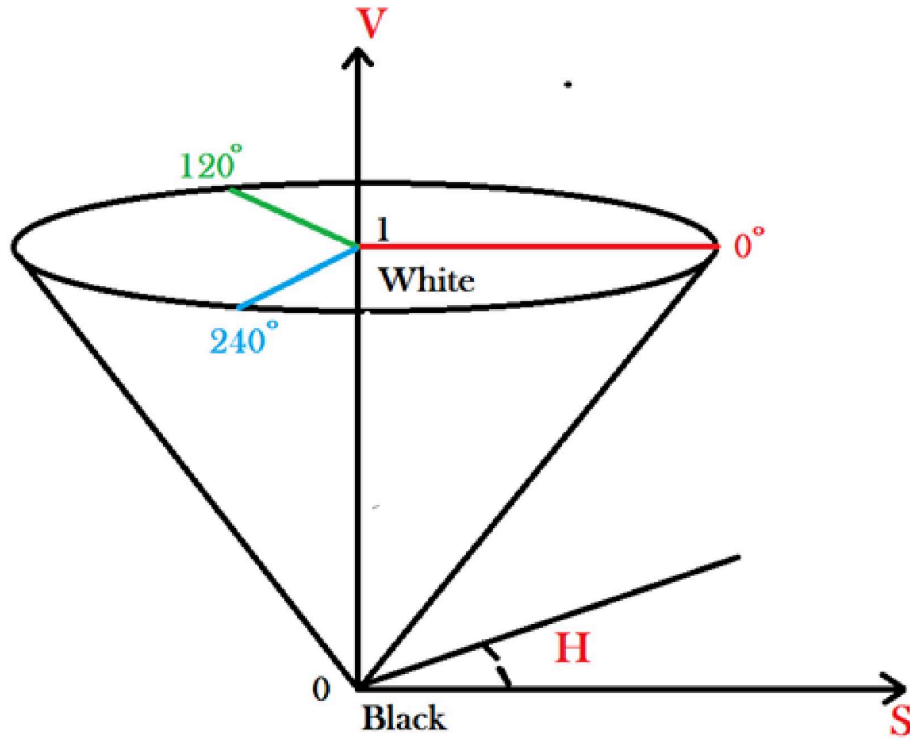
FIGURE 4.3: HSV color space in graphical view

In the HSV color space, colors are represented as a cylindrical coordinate system, with the hue angle around the center axis and the saturation and value axes extending outward from the center. This allows for easy manipulation of colors by changing their hue,

saturation, or value independently. The conversion from RGB to HSV is a non-linear transformation that involves normalizing the RGB values to a range of 0 to 1, and then calculating the hue, saturation, and value based on the normalized values. The formula for converting RGB to HSV can vary depending on the software or application used, but typically involves some form of normalization and calculation of the hue, saturation, and value components. The HSV color space is useful for a variety of color-related tasks, such as color selection, color manipulation, and color segmentation. For example, in computer graphics, the HSV color space can be used to create color palettes that are more aesthetically pleasing or to adjust the brightness and saturation of images. In image processing and computer vision, the HSV color space can be used for color-based segmentation and object detection, as it provides a more intuitive way of describing color than the RGB color space.
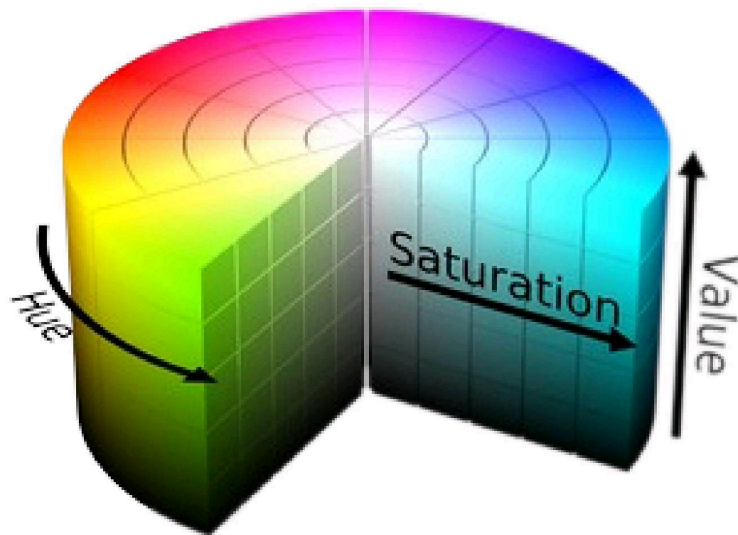
FIGURE 4.4: HSV color space

HSV color space, on the other hand, represents color as a combination of hue, saturation, and value. Hue represents the color itself, saturation represents the purity of the color, and value represents the brightness of the color.

LAB color space is another color space that is widely used in image processing. It is based on the opponent process theory of color vision, which states that there are three pairs of complementary colors: red-green, blue-yellow, and black-white. In this color space, the values of L, a, and b represent the lightness, red-green axis, and blue-yellow axis, respectively.

4.2.3   XYZ

The XYZ color space, introduced by the International Commission on Illumination (CIE) in 1931, is a widely used and influential color model in the field of color science. It provides a mathematical representation of human perception of colors and serves as a foundation for various color-related applications.

In the XYZ color space, colors are defined by three components: X, Y, and Z. These components represent the tristimulus values of the color, which quantify the amount of three primary colors required to reproduce the color. The X, Y, and Z values are determined based on the spectral power distribution of the light source and the sensitivity of the human visual system to different wavelengths.

The Y component in the XYZ color space represents the brightness or luminance of the color. It quantifies the perceived intensity of the color and plays a crucial role in determining the overall visual appearance of an image or scene. The X and Z components represent the chromaticity or color information of the color. They capture the relative balance of the different primary colors and specify the color's hue and saturation.

One of the key advantages of the XYZ color space is its device-independence. It is designed to be independent of any specific color reproduction system or display device. This allows for consistent color representation and communication across different devices, ensuring that colors appear the same regardless of the medium or technology used.

The XYZ color space encompasses the entire range of human vision and includes both real and imaginary colors. The real colors represent actual visible colors that can be reproduced by light sources, while the imaginary colors are beyond the range of human perception and do not correspond to any physical emission spectra. Although imaginary colors are not perceptible, they are mathematically defined within the XYZ color space to ensure a comprehensive and consistent color model.

RGB to XYZ calculated as:

$$\begin{bmatrix} R \\ G \\ B \end{bmatrix} = \frac{1}{3400850} \begin{bmatrix} 8041697 & -3049000 & -1591847 \\ -1752003 & 4851000 & 301853 \\ 17697 & -49000 & 3432153 \end{bmatrix} \begin{bmatrix} X \\ Y \\ Z \end{bmatrix}$$

The XYZ color space has been widely adopted as a fundamental reference in color science and related fields. It serves as the basis for defining other color spaces, such as the CIE RGB color space and the CIE Lab color space. These color spaces are derived from the XYZ color space using specific transformations that optimize color representation for different purposes, such as additive color mixing or perceptual uniformity.

In practical applications, the XYZ color space is often utilized alongside other color spaces for various color-related tasks. Color space conversions are commonly performed to translate colors between XYZ and other color models, such as RGB, CMYK, or Lab. These conversions allow for seamless integration with existing color workflows and enable accurate color measurement, analysis, manipulation, and reproduction. RGB to HSV calculated as:

4.2.4 YCBCR

YCBCR (also written as YĆBCR or YCbCr) is a color space that is commonly used in digital video and image processing. It is similar to YUV, but with a slightly different color conversion formula. The YCBCR color space consists of three channels: Y, CB, and CR. The Y channel represents the luma or brightness component, and is calculated in the same way as in the YUV color space. The CB and CR channels represent the chroma or color information, and are calculated as the difference between the luma component and the blue and red components, respectively.
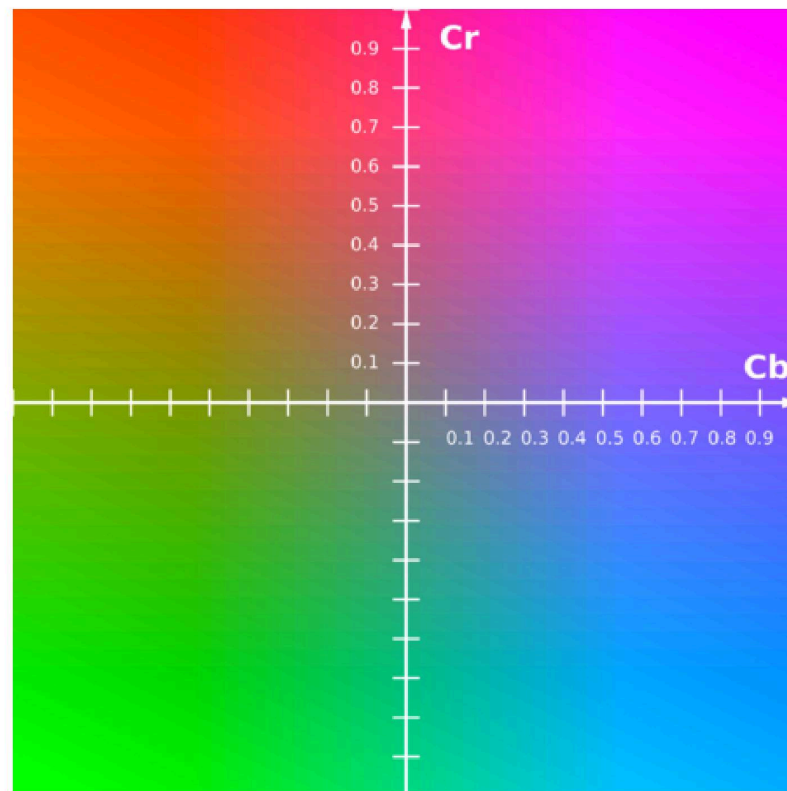

FIGURE 4.5: YCBR color space

The conversion from RGB to YCBCR is typically performed using a matrix multiplication, with different matrices used for different video standards. For example, the ITU-R BT.601 standard uses a conversion matrix that is optimized for standard definition television, while the ITU-R BT.709 standard uses a conversion matrix that is optimized for

high definition television. The YCBCR color space is widely used in digital video compression and transmission, as it allows for efficient coding of color information. Similar to YUV, the chroma channels (CB and CR) can be subsampled to reduce the amount of data needed to represent the color information, while the luma channel (Y) is typically left at full resolution to preserve image quality.

YCBCR to RGB calculated as:

$$
\begin{aligned}
Y' &= 16 + \frac{65.738 \cdot R'_D}{256} + \frac{129.057 \cdot G'_D}{256} + \frac{25.064 \cdot B'_D}{256} \\
C_B &= 128 - \frac{37.945 \cdot R'_D}{256} - \frac{74.494 \cdot G'_D}{256} + \frac{112.439 \cdot B'_D}{256} \\
C_R &= 128 + \frac{112.439 \cdot R'_D}{256} - \frac{94.154 \cdot G'_D}{256} - \frac{18.285 \cdot B'_D}{256}
\end{aligned}
\tag{4.4}
$$

The YCBCR color space is also used in digital image processing, where it can be used for tasks such as color correction and manipulation. In this context, the Y channel can be used to adjust the brightness and contrast of an image, while the CB and CR channels can be used to adjust the color balance and saturation.

4.2.5 YPBPR

YPBPR is a color space that is commonly used in analog and digital video applications. It is similar to YCBCR and YUV, but with a different color conversion formula.

The YPBPR color space consists of three channels: Y, PB, and PR. The Y channel represents the luma or brightness component, and is calculated in the same way as in the YCBCR and YUV color spaces. The PB and PR channels represent the chroma or color information, and are calculated as the difference between the luma component and the blue and red components, respectively.

YPBPR is typically used in analog video applications, where the color information is carried on separate cables from the brightness information. The Y channel is carried on one cable, while the PB and PR channels are carried on two separate cables. In digital video applications, YPBPR is often used as an intermediate color space for processing video signals before they are converted to another color space, such as RGB or YCBCR.

The conversion from RGB to YPBPR is typically performed using a matrix multiplication, with different matrices used for different video standards. For example, the SMPTE 170M standard uses a conversion matrix that is optimized for standard definition television, while the SMPTE 240M standard uses a conversion matrix that is optimized for high definition television.

RGB to YPBPR calculated as:

$$Y' = K_R \cdot R' + K_G \cdot G' + K_B \cdot B'$$
$$P_B = \frac{1}{2} \cdot \frac{B' - Y'}{1 - K_B} \tag{4.5}$$
$$P_R = \frac{1}{2} \cdot \frac{R' - Y'}{1 - K_R}$$

The YPBPR color space is also used in digital image processing, where it can be used for tasks such as color correction and manipulation. In this context, the Y channel can be used to adjust the brightness and contrast of an image, while the PB and PR channels can be used to adjust the color balance and saturation.

4.2.6 RGBCIE

RGBCIE is a color space that combines the RGB (Red, Green, Blue) and CIE (Commission Internationale de l'Eclairage) color spaces. It is a popular color space used in digital imaging and color management systems.

The RGB color space is based on the additive color model, where colors are created by combining red, green, and blue light. The CIE color space, on the other hand, is a mathematical model that describes how humans perceive color. It is based on the XYZ color space, which defines a set of color values that correspond to the three types of cone cells in the human eye that are responsible for color vision.

The RGBCIE color space combines the RGB color space and the CIE color space to create a more accurate and comprehensive color representation system. It adds two additional color channels to the standard RGB model, which represent the chromaticity and luminance of a color.

The first additional channel, the chromaticity channel, represents the hue and saturation of a color. It is based on the CIE xy chromaticity diagram, which maps all visible colors onto a two-dimensional plane. The chromaticity channel in the RGBCIE color space uses these coordinates to represent the color's hue and saturation. The second additional channel, the luminance channel, represents the brightness or intensity of a color. It is based on the CIE Y luminance function, which defines the perceived brightness of a color. The luminance channel in the RGBCIE color space uses this function to represent the color's brightness or intensity. By combining the RGB color space and the CIE color space, the RGBCIE color space provides a more comprehensive representation of color than the standard RGB model. It allows for more accurate color selection, manipulation, and reproduction in digital imaging and color management systems. The RGBCIE color space is used in a variety of applications, including digital photography, video, and color management software. It is also used in color calibration systems, where it is used to accurately match colors between different devices, such as monitors and printers.
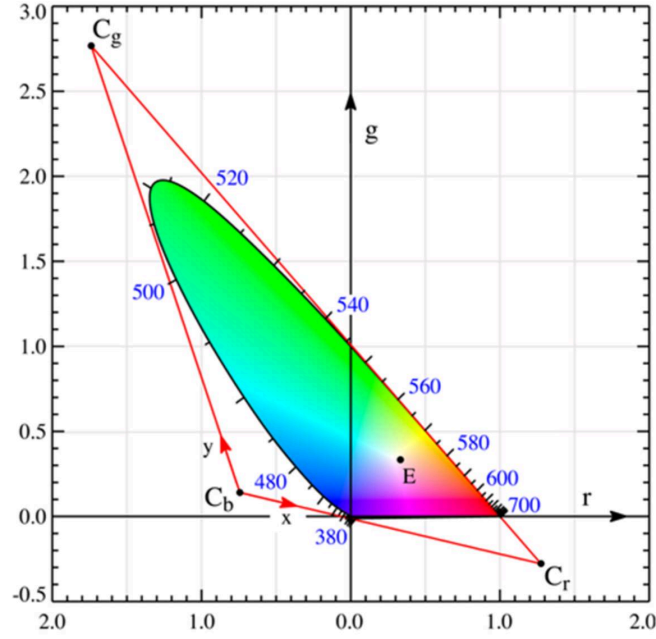
FIGURE 4.6: RGBCIE ccolor space

4.2.7 LAB

LAB (or sometimes written as CIELAB) is a color space that was developed by the International Commission on Illumination (CIE) as a device-independent way to describe colors. It is based on the CIE 1931 XYZ color space, which defines a set of color values that correspond to the three types of cone cells in the human eye that are responsible for color vision.

The LAB color space consists of three channels: L, a, and b. The L channel represents the lightness or brightness of a color, and ranges from 0 (black) to 100 (white). The channel represents the color on a red-green axis, with positive values representing red and negative values representing green. The b channel represents the color on a blue-yellow axis, with positive values representing yellow and negative values representing blue.

The LAB color space is device-independent, which means that it is not affected by the characteristics of the device used to create or display the color. This makes it a useful color space for color management, where it is used to accurately match colors between different devices, such as monitors and printers.

One of the key advantages of the LAB color space is that it is designed to be perceptually uniform, meaning that equal differences in color values are perceived as equal differences in color by the human eye. This makes it easier to make precise color adjustments and corrections, as changes in the LAB values correspond more closely to changes in human perception of color.

FIGURE 4.7: LAB color space

FIGURE 4.8: LAB color space in graphical view

The LAB color space is used in a variety of applications, including digital imaging, graphic design, and color management. It is particularly useful in color 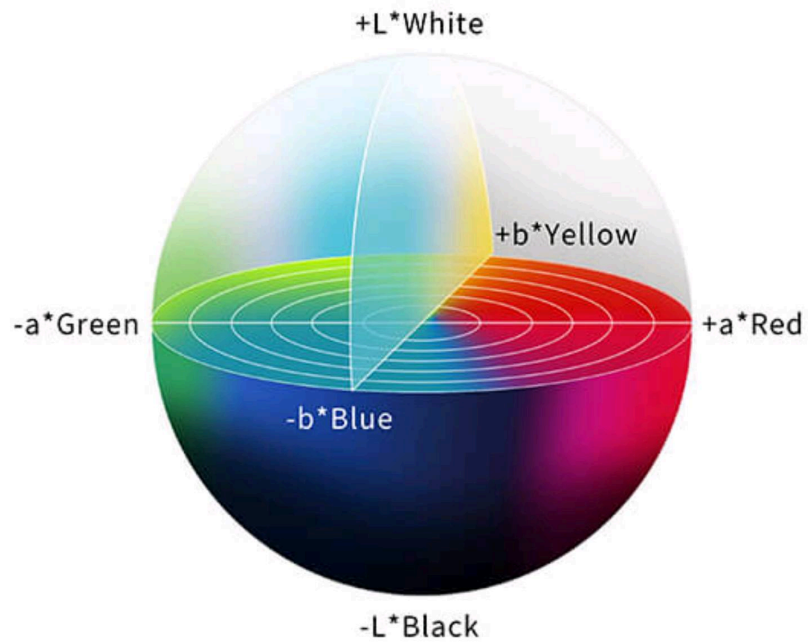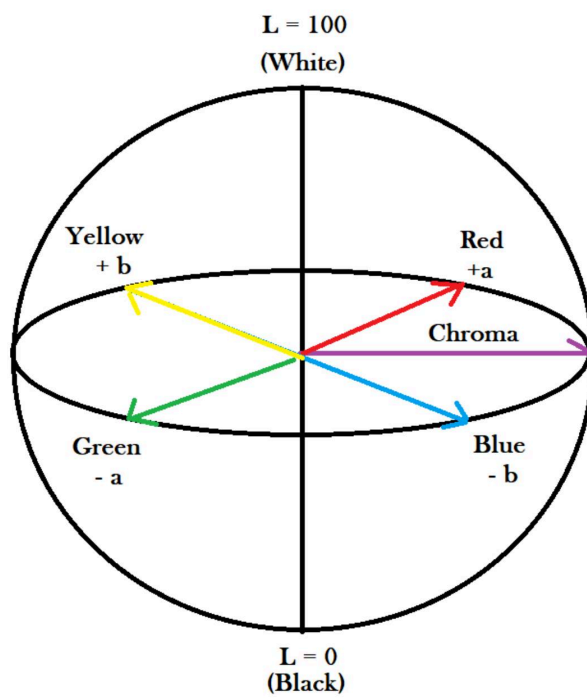correction and color matching applications, where it allows for precise adjustments to be made to the colors in an image or design.

RGB to LAB calculated as:

$$
\begin{aligned}
L^\star &= 116 \ f\left(\frac{Y}{Y_{\mathrm{n}}}\right) - 16 \\
a^\star &= 500 \left(f\left(\frac{X}{X_{\mathrm{n}}}\right) - f\left(\frac{Y}{Y_{\mathrm{n}}}\right)\right) \\
b^\star &= 200 \left(f\left(\frac{Y}{Y_{\mathrm{n}}}\right) - f\left(\frac{Z}{Z_{\mathrm{n}}}\right)\right)
\end{aligned}
\tag{4.6}
$$

$$
f(t) = \begin{cases}
\sqrt[3]{t} & \text{if } t > \delta^3 \\
\dfrac{t}{3\delta^2} + \dfrac{4}{29} & \text{otherwise}
\end{cases}
\tag{4.7}
$$
$$
\delta = \tfrac{6}{29}
$$

4.2.8 HED

HED (Hematoxylin-Eosin-DAB) is a color space that is commonly used in biomedical image analysis. It is a three-channel color space that separates an image into three channels corresponding to the staining components of hematoxylin (blue-purple), eosin (pink), and DAB (brown). Hematoxylin is a basic dye that stains the nuclei of cells blue-purple, while eosin is an acidic dye that stains the cytoplasm and extracellular matrix pink. DAB (3,3'-diaminobenzidine) is a chromogen that is commonly used for immunohistochemistry staining, and produces a brown reaction product when bound to an antibody.

The HED color space is created by transforming an RGB image into an optical density space, where the values of each channel represent the logarithm of the ratio of the light transmitted through the stained tissue to the light transmitted through an unstained reference. The transformation is performed using a color deconvolution algorithm, which separates the image into the three channels corresponding to the staining components. Once the image is in the HED color space, the channels can be used for various image analysis tasks. For example, the hematoxylin channel can be used to segment nuclei in an image, while the eosin and DAB channels can be used to segment other structures or to detect specific features such as blood vessels or cancer cells.

The HED color space is widely used in biomedical image analysis, particularly in histology and pathology applications. It allows for accurate segmentation of different tissue components, which can be used for diagnosis and prognosis of diseases such as cancer.

Additionally, the HED color space can be combined with other imaging modalities such as fluorescence or multiphoton imaging to provide a more complete picture of cellular and tissue structures.

4.2.9 YDBDR

YDbDr (also known as Y'Db'Dr or YDbDr) is a color space that is commonly used in analog video and digital video compression. It is a three-channel color space that separates the image into the luminance (Y) and two color difference channels (Db and Dr).

The Y channel represents the luminance, or brightness, of the image, while the Db and Dr Channels represent the color difference between the blue and the luminance, and the red and the luminance, respectively.

The YDbDr color space is derived from the YUV color space, which separates the image into the luminance (Y) and two color difference channels (U and V). The YUV color space was originally developed for analog television broadcasting and is still widely used in video compression standards such as MPEG and H.264.

The conversion from YUV to YDbDr involves a simple matrix transformation that preserves the luminance information and changes the color difference information to be more compatible with digital video compression. The conversion from RGB to YDbDr can also be performed using a matrix transformation.

RGB to YDBDR calculated as:

$$
\begin{bmatrix} Y \\ D_B \\ D_R \end{bmatrix} = \begin{bmatrix} 0.299 & 0.587 & 0.114 \\ -0.450 & -0.883 & 1.333 \\ -1.333 & 1.116 & 0.217 \end{bmatrix} \begin{bmatrix} R \\ G \\ B \end{bmatrix} \quad (4.8)
$$

The YDbDr color space is useful for video compression because it separates the luminance information, which is more important for image quality, from the color information, which can be compressed more aggressively without sacrificing perceived image quality. Additionally, the Db and Dr channels are less correlated with each other than the U and V channels in YUV, which can further improve compression efficiency.

4.2.10 YIQ

YIQ color space is a color representation system used in the analog NTSC television broadcasting system. It was developed by the National Television System Committee

(NTSC) to enable the transmission of color TV signals over existing black-and-white TV channels.

The YIQ color space represents colors as a combination of three components: Y, I, and Q. The Y component represent the luminance or brightness of the color, whereas the I and Q components represent the chrominance or color information. The I component represents the difference between the red and the luminance, and the Q component represents the difference between the blue and the luminance.
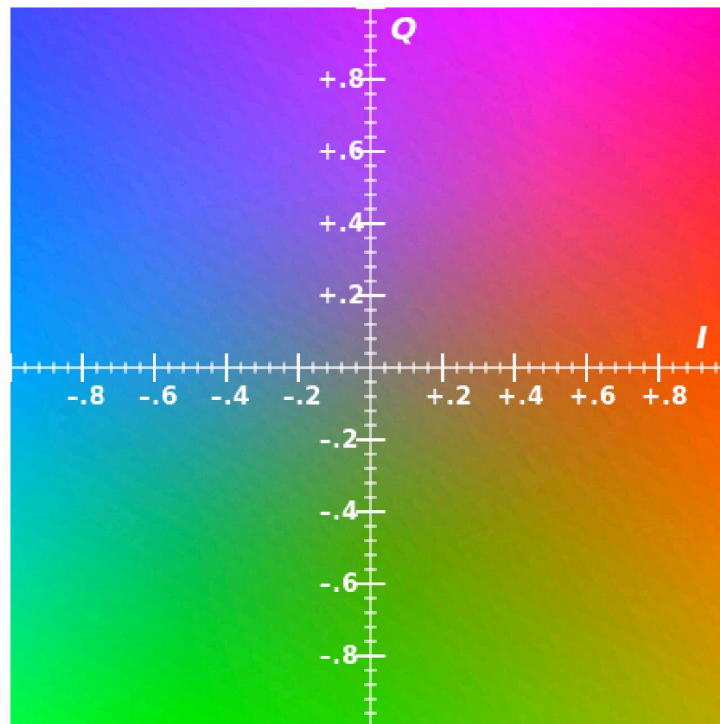
FIGURE 4.9: YIQ color space in graphical view

In the YIQ Y represents the black-and-white portion of a signal, I and Q represents the information of a color. It means that color TV signals can be transmitted over the same channel as black-and-white signals, which was important for the transition from black-and-white to color TV. Changing the range in the orange–blue(I) to the purple-green range(Q), in this condition human eye is more sensitive. Broadcast NTSC limits I to 1.3 MHz and Q to 0.4 MHz.

Because of the high costing in implementation some television can perform the true I and Q decoding. Another advantage of the YIQ color space is that it is perceptually uniform. This means that equal changes in the I and Q components result in equal perceptual changes in color. This makes it easier to manipulate and process color images and videos in a way that preserves their visual appearance.

RGB to YIQ calculated as:

$$\begin{bmatrix} Y \\ I \\ Q \end{bmatrix} \approx \begin{bmatrix} 0.299 & 0.587 & 0.114 \\ 0.5959 & -0.2746 & -0.3213 \\ 0.2115 & -0.5227 & 0.3112 \end{bmatrix} \begin{bmatrix} R \\ G \\ B \end{bmatrix} \tag{4.9}$$

In the YIQ color space, the Y component represents the black-and-white portion of the signal, while the I and Q components represent the color information. The I and Q components are usually normalized to the range of -0.5 to +0.5, so they can be transmitted as analog signals over the same channel as the Y component.

One of the advantages of the YIQ color space is that it is perceptually uniform. This means that equal changes in the I and Q components result in equal perceptual changes in color. This makes it easier to manipulate and process color images and videos in a way that preserves their visual appearance.

4.2.11   YUV

A colour image pipeline frequently uses the YUV colour model. As opposed to a "direct" RGB representation, it allows for a smaller bandwidth for the chrominance components when encoding a colour image or video. The designations YUV and YUV have historically been used to refer to a particular analogue encoding of colour information in broadcast systems. Currently, colorspaces that are encoded using YCbCr are referred to as YUV in the computer industry.

One luminance component (Y), which represents actual linear-space brightness, and two chrominance components, designated as U (blue projection) and V (red projection), respectively, are defined by the YUV model. Different colour spaces and the RGB model can both be converted using this method.

YUV is a color space that is widely used in video and digital image processing. It is based on the concept of separating color information (chrominance) from brightness information (luminance) in an image or video signal.

The YUV color space consists of three channels: Y, U, and V. The Y channel represents the luminance or brightness of the image, and is often referred to as the luma component. The U and V channels represent the chrominance or color information, and are often referred to as the chroma components.

RGB to YUV calculated as:
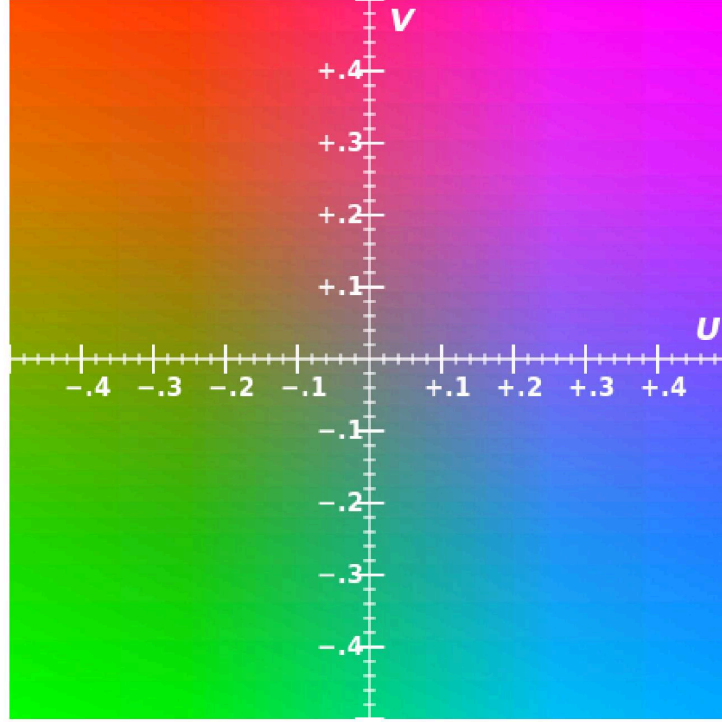
FIGURE 4.10: YUV color space

$$W_R = 0.299,$$

$$W_G = 1 - W_R - W_B = 0.587,$$

$$W_B = 0.114, \qquad (4.10)$$

$$U_{\max} = 0.436,$$

$$V_{\max} = 0.615.$$

$$Y' = W_R R' + W_G G' + W_B B' = 0.299R' + 0.587G' + 0.114B',$$

$$U = U_{\max} \frac{B' - Y'}{1 - W_B} \approx 0.492(B' - Y'), \qquad (4.11)$$

$$V = V_{\max} \frac{R' - Y'}{1 - W_R} \approx 0.877(R' - Y').$$

The Y channel is calculated as a weighted sum of the red, green, and blue values of a pixel, with higher weights given to the green component, as the human eye is more sensitive to green light. The U and V channels represent the difference between the blue and luma channel, and the red and luma channel, respectively. This allows for a compact representation of color information, as the U and V channels can be represented with less data than the full RGB color space. The YUV color space is used in video compression and transmission, as it allows for more efficient coding of color information. By separating the luminance and chrominance components, it is possible to apply different levels of compression to each component, with less compression applied to the luminance channel to preserve the image quality.

The YUV color space is also used in digital image processing, where it can be used for tasks such as color correction and manipulation. In this context, the Y channel can be used to adjust the brightness and contrast of an image, while the U and V channels can be used to adjust the color balance and saturation.

4.3   IMAGE CLASSIFICATION ALGORITHM

4.3.1   MOBILENET

MobileNet is a convolutional neural network (CNN) architecture that has gained popularity for its suitability in mobile and embedded devices. It was developed by Google researchers in 2017, focusing on optimizing for low latency and low power consumption. One of the key features of MobileNet is its use of depthwise separable convolutions, which significantly reduces the number of parameters and computations required while maintaining accuracy. Different versions of MobileNet, such as V1, V2, and V3, offer trade-offs between speed and accuracy. The versatility of MobileNet has made it widely used in various computer vision applications, including image classification, object detection, and semantic segmentation. Its efficiency has made it particularly suitable for deploying deep learning models on resource-constrained devices like smartphones, drones, and embedded systems. MobileNet is often combined with other techniques, such as quantization and pruning, to further reduce the model size and enhance its performance on mobile devices. This architecture has played a significant role in enabling the development of efficient and accurate deep learning models tailored for mobile and embedded applications. Its main advantage lies in its efficiency, which has made it a popular choice in the realm of mobile and embedded devices.

MobileNet offers several advantages that make it a highly desirable architecture for various applications:

Firstly, it is lightweight and efficient due to the utilization of depthwise separable convolutions. This design choice significantly reduces the number of parameters, making it highly suitable for resource-constrained devices like smartphones and embedded systems. The efficient nature of MobileNet allows for optimal usage of limited memory and processing power.

Secondly, MobileNet achieves high accuracy despite its compact size and efficiency. It has demonstrated state-of-the-art performance on multiple computer vision tasks, including image classification and object detection. This makes it a powerful choice for a wide range of applications where accurate predictions are crucial.

Thirdly, MobileNet offers flexibility. It can be tailored to different use cases and requirements by adjusting the size and depth of the network layers. This adaptability allows

developers to fine-tune the architecture based on the specific domain or task at hand, ensuring optimal performance and efficiency.

Additionally, MobileNet enables fast inference due to its lightweight design. The reduced computational complexity allows for real-time processing of data, making it well-suited for applications that require quick and responsive decision-making, such as video analysis or augmented reality.
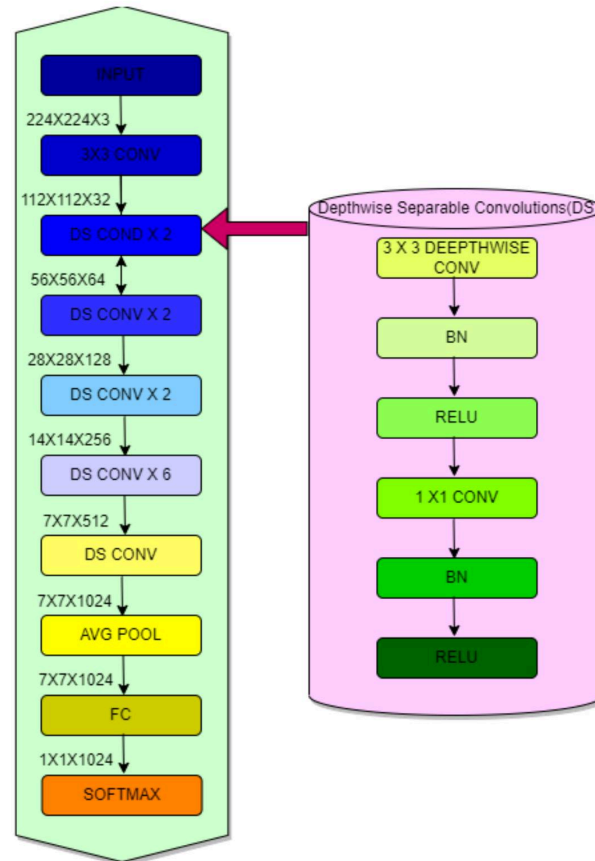
FIGURE 4.11: Architechture of Mobilenet network

4.3.2 RESNET50

ResNet50 is a renowned deep neural network architecture widely utilized for image classification and various computer vision tasks. Here are some key points about ResNet50:

• ResNet50 is a variant of the ResNet architecture created by Microsoft researchers Kaiming He, Xiangyu Zhang, Shaoqing Ren, and Jian Sun in 2015.

• It consists of 50 layers, making it a deep neural network that incorporates residual connections. These connections enable the model to learn more complex representations and enhance accuracy.

● ResNet50 is trained on the ImageNet dataset, which encompasses millions of images across numerous categories.

● In 2015, ResNet50 achieved state-of-the-art performance on the ImageNet classification task, establishing it as a prominent baseline model in computer vision research.

● ResNet50 has demonstrated remarkable performance on various computer vision tasks, including object detection, segmentation, and image captioning.

● The architecture of ResNet50 revolves around residual blocks, which include shortcut connections allowing information to bypass certain layers. This addresses the challenge of vanishing gradients encountered in deep neural networks.

● ResNet50 is commonly employed as a feature extractor in transfer learning, where the model is fine-tuned on a new dataset specific to a particular task. This approach proves beneficial when dealing with limited data or when pre-trained models are not readily available.
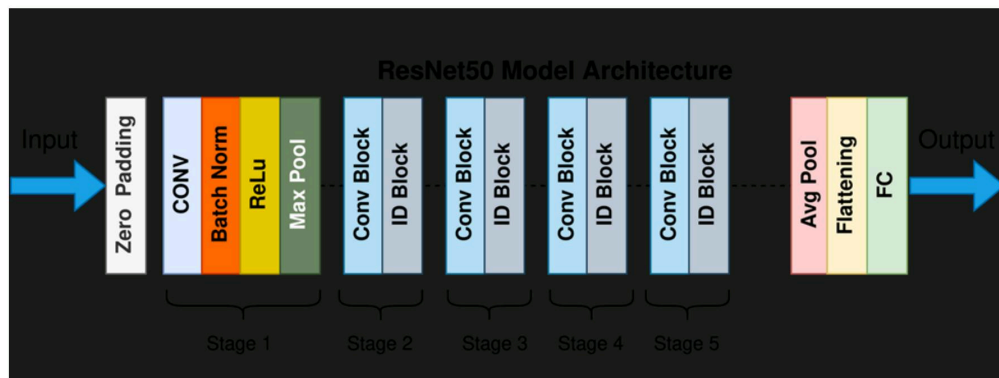
FIGURE 4.12: Architechture of Resnet50 network

ResNet50 offers several notable advantages in the realm of computer vision:

● Ability to Train Very Deep Networks: ResNet50's architecture enables the training of extremely deep neural networks, up to 50 layers deep, while effectively addressing the vanishing gradient problem. This empowers the model to learn intricate and abstract features, enhancing its performance on complex computer vision tasks.

● High Accuracy: ResNet50 has demonstrated exceptional accuracy on various computer vision tasks, including image classification and object detection. Its state-of-the-art results establish it as a powerful architecture capable of achieving top-notch performance in diverse applications.

● Transfer Learning Capabilities: ResNet50's success on ImageNet, a comprehensive image recognition database, has made it a favored choice for transfer learning. By utilizing pre-trained ResNet50 models and fine-tuning them on specific tasks, researchers and practitioners can leverage the network's learned features to improve accuracy and expedite training on smaller datasets.

• Wide Adoption and Support: ResNet50 enjoys widespread adoption and is supported by popular deep learning libraries like Keras, TensorFlow, and PyTorch. This widespread availability and support make it easily accessible and straightforward to implement in various applications, fostering its broad usage and further development in the research community.

4.3.3   INCEPTION_V3

Inception v3 is a deep convolutional neural network architecture that was introduced by Google in 2015. It is an extension of the original Inception architecture, also known as GoogLeNet. Inception v3 has achieved state-of-the-art performance on a number of computer vision tasks, including image classification and object detection. One of the key innovations in Inception v3 is the use of "inception modules", which are designed to efficiently capture spatial correlations at different scales. An inception module consists of several convolutional layers of different filter sizes and pooling operations, which are concatenated together to produce the output. This allows the network to learn both local and global features from the input image. Inception v3 also includes other techniques to improve its performance, such as factorized convolutions, which reduce the number of parameters and increase computational efficiency, and batch normalization, which helps to stabilize the training process and improve generalization. Overall, Inception v3 is a powerful deep learning architecture that has been widely adopted in the computer vision community, and has been used in a variety of applications, including image recognition, object detection, and image segmentation. The main advantage of InceptionV3 is its ability to balance accuracy and efficiency, making it a powerful architecture for a wide range of computer vision tasks.

InceptionV3 offers several notable advantages:

• Efficient Architecture: InceptionV3 utilizes Inception modules, which consist of parallel convolutional layers with different filter sizes. This design achieves a fine balance between accuracy and efficiency, allowing InceptionV3 to deliver strong performance on image classification tasks while keeping the number of parameters and computation time relatively low.

• High Accuracy: InceptionV3 has demonstrated state-of-the-art results across various computer vision tasks, including image classification, object detection, and semantic segmentation. Its ability to achieve top-level performance makes it a powerful architecture suitable for a wide range of applications.

• Transfer Learning Capabilities: Leveraging its success on large-scale image recognition databases like ImageNet, InceptionV3 is commonly employed as a pre-trained network for transfer learning. By utilizing pre-trained InceptionV3 models and fine-tuning them
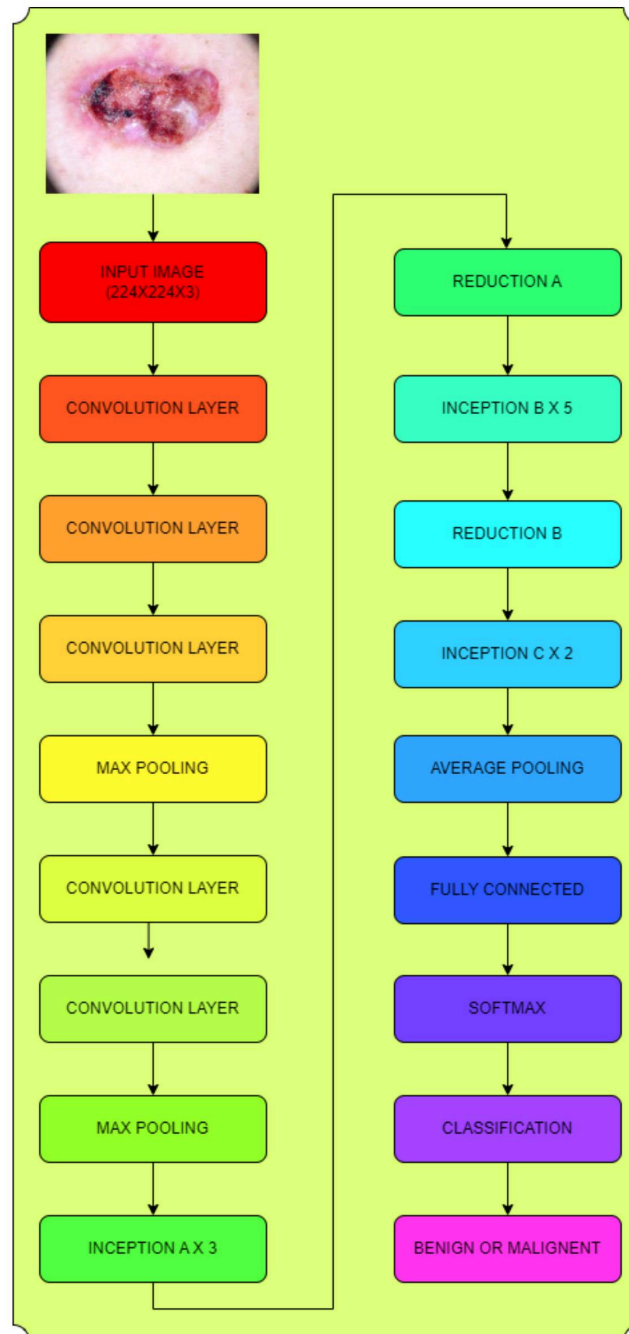
FIGURE 4.13: Architechture of Inceptionv3 network

on specific tasks, researchers and practitioners can expedite training and achieve improved accuracy, particularly on smaller datasets.

• Widely Adopted and Supported: InceptionV3 enjoys broad adoption and is well-supported by popular deep learning libraries such as Keras, TensorFlow, and PyTorch. This widespread adoption and support facilitate its seamless implementation and usage across various applications, fostering its continued development and utilization within the research community.

4.3.4 XCEPTION

Xception is a deep learning model architecture that was introduced in 2016 by Fran cois Chollet, the creator of the Keras library. Xception stands for "Extreme Inception" and is based on the Inception architecture, which is a popular deep neural network architecture used for image classification tasks. Xception takes the idea of Inception modules one step further by replacing the traditional convolutional layers with depthwise separable convolutions. These convolutions break down the standard convolution into two separate layers, one for channel-wise feature learning and another for spatial feature learning, which can be computed separately. This reduces the number of parameters in the network and makes training faster and more efficient.

The Xception architecture has achieved state-of-the-art results on a range of image classification tasks, including the ImageNet dataset, which is a large-scale visual recognition challenge. The Xception architecture has also been used in other computer vision tasks, such as object detection, segmentation, and face recognition.

The Xception architecture has several advantages over other deep neural network architectures:

• Enhanced Efficiency: Xception leverages depthwise separable convolutions, reducing the number of parameters in the network. This results in improved efficiency and faster training, making it well-suited for resource-constrained environments such as mobile devices and embedded systems.

• Superior Accuracy: Xception has demonstrated state-of-the-art performance across various computer vision tasks, including image classification, object detection, and semantic segmentation. By employing depthwise separable convolutions, Xception facilitates effective feature learning, leading to enhanced accuracy.

• Versatility: While commonly used in computer vision, Xception's benefits extend beyond this domain. It can be successfully applied in other areas, such as natural language processing and speech recognition, showcasing its versatility and adaptability to diverse tasks and domains.
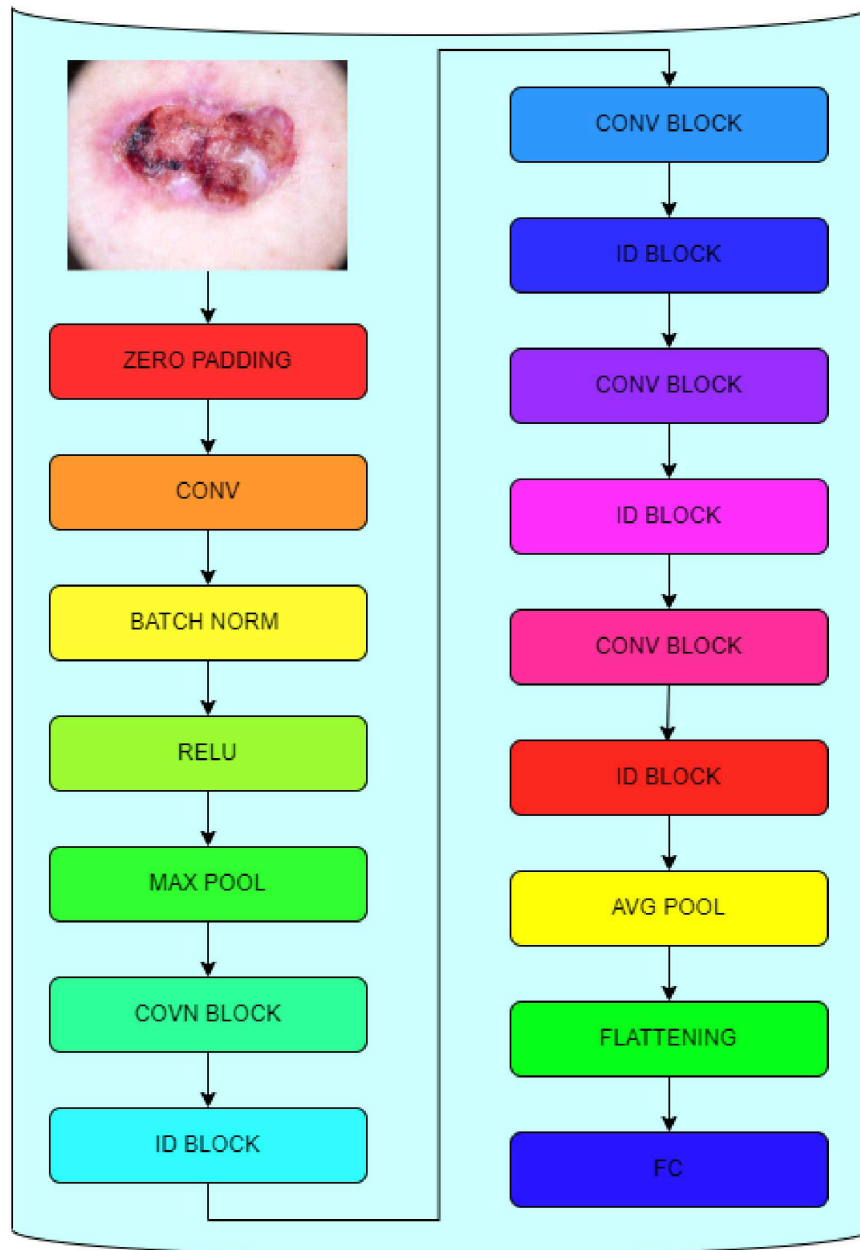
FIGURE 4.14: Architechture of Xception network

• Interpretable Design: Xception's modular architecture lends itself to enhanced interpretability compared to other deep neural network architectures. This feature is particularly valuable in applications where understanding the decision-making process is crucial, such as healthcare and finance.

4.3.5 DENSENET121

DenseNet121 is a deep neural network architecture that was introduced in 2017 by researchers at Facebook AI Research. The main advantage of DenseNet121 is its ability

to reduce the number of parameters in the network while maintaining high accuracy, making it a powerful architecture for image classification tasks.
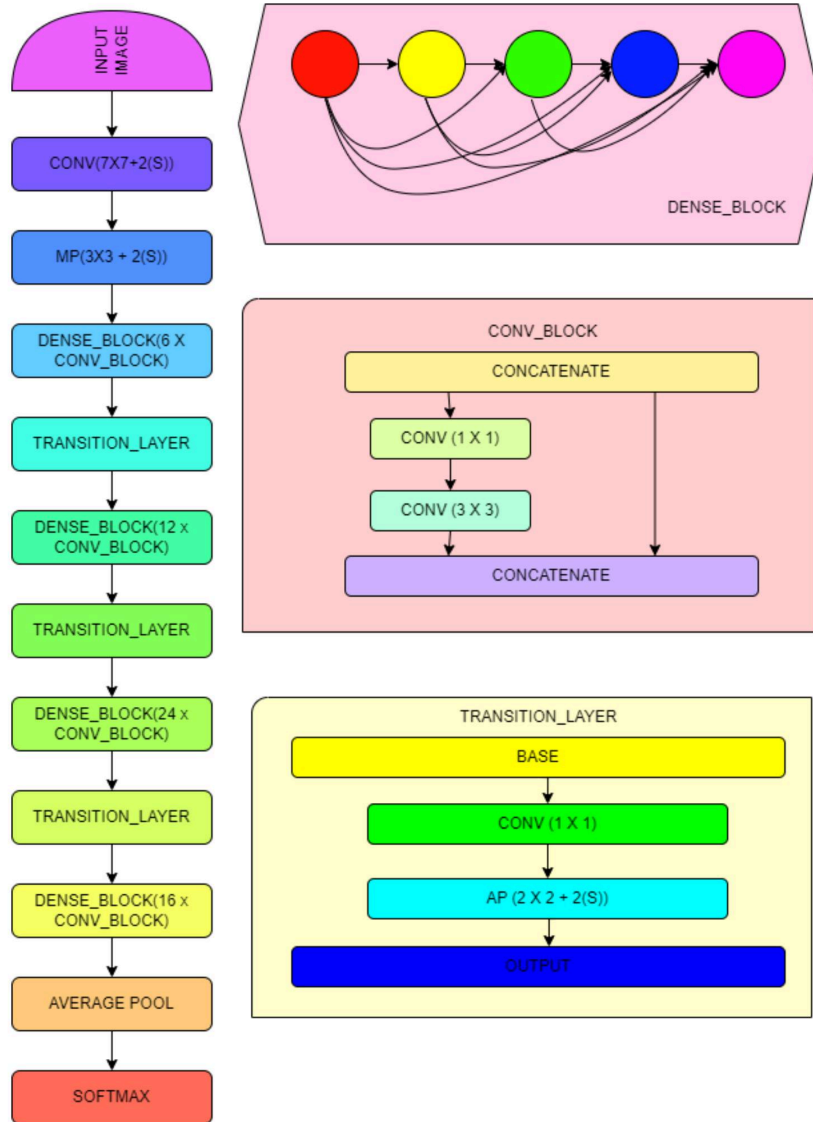
FIGURE 4.15: Architechture of Densenet151 network

Some of the advantages of DenseNet121 are:

• Parameter Efficiency: DenseNet121 uses a unique dense connectivity pattern, where each layer receives inputs from all previous layers, to reduce the number of parameters in the net- work. This allows for better parameter sharing and feature reuse, leading to higher accuracy and faster training.

• High Accuracy: DenseNet121 has achieved state-of-the-art results on a range of computer vision tasks, including image classification and object detection. This makes it a powerful architecture for a variety of applications.

• Transfer Learning: Because of its success on large-scale image recognition databases such as ImageNet, DenseNet121 is often used as a pre-trained network for transfer

learning on other computer vision tasks. This allows for faster training and better accuracy on smaller datasets.

• Widely Adopted: DenseNet121 is a widely adopted architecture and is supported by popular deep learning libraries such as Keras, TensorFlow, and PyTorch. This makes it easy to implement and use in a variety of applications. Overall, DenseNet121 is a powerful architecture that provides parameter efficiency while maintaining high accuracy, making it a popular choice for image classification tasks. Its success on large-scale image recognition databases, transfer learning capabilities, and wide adoption make it a versatile architecture for various computer vision applications.

4.4   ISIC DATASET

ISIC (the International Skin Imaging Collaboration) dataset is a large collection of dermoscopic images of skin. This is a large-scale publicly available dataset which contains more than 20,000 images internationally. The ISIC dataset was first published in 2016 for a public benchmark challenge on dermoscopy images. The main motive of this dataset is to promote and development of automated diagnosis algorithms in the matter of segmentation, feature detection and classification. In 2017, ISIC dataset was going to the next challenge which is extended the dataset with 2000 images for training with masks for segmentation, masks for feature extraction and annotation for classification. At that time the images are categorized into three classes but now this dataset is known as Multi-class classification with nine classes in train and testing purposes:

• Actinic keratosis

• Basal cell carcinoma

• Dermatofibroma

• Melanoma

• Nevus

• Pigmented benign keratosis

• Seorrheic keratosis

• Squamous cell carcinoma

• Vascular lesion.

Summary of the ISIC 2016-2020 dataset (image counts do not include mask and super pixel images)

DATASET	TRAIN	TEST	TOTAL
ISIC2016	900	379	1279
ISIC2017	2000	600	2600
ISIC2018	10,015	1512	11,527
ISIC2019	25,331	8238	33,569
ISIC2020	33,126	10,982	44,108

The dataset for skin cancer classification comprises five different datasets: ISIC2016, ISIC2017, ISIC2018, ISIC2019, and ISIC2020. Each dataset has been carefully curated and labeled to provide samples for training and testing ML models. The ISIC2016 dataset consists of 1,279 samples, with 900 samples allocated for training and 379 samples for testing. Moving on to the ISIC2017 dataset, it contains a larger set of 2,600 samples, with 2,000 samples designated for training and 600 samples for testing. The ISIC2018 dataset offers an even larger collection of skin cancer images, with a total of 11,527 samples. Out of these, 10,015 samples are reserved for training purposes, and the remaining 1,512 samples are used for testing. The ISIC2019 dataset provides an extensive dataset with 33,569 samples, divided into 25,331 training samples and 8,238 testing samples. Lastly, the ISIC2020 dataset encompasses 44,108 samples, with 33,126 samples used for training and 10,982 samples for testing.

Chapter 5

Experimental Setup & Results

5.1 EVALUATION MATRIC

Accuracy is defined as the ratio of them of true positive and true negative to the sum of true positive, true negative, false positive, and, false negative.

FIGURE 5.1: Evolution Matrices

5.1.1 ACCURACY

Accuracy is a widely used evaluation metric for classification models that measures the ratio of correctly classified instances to the total number of instances. It provides an overall assessment of the model's performance and is expressed as a percentage. While accuracy is a valuable metric, it should be interpreted with caution, especially in scenarios with imbalanced datasets or when considering the performance of specific classes. It is advisable to complement accuracy with other evaluation metrics such as

precision, recall, F1 score, and AUC-ROC to obtain a more comprehensive understanding of the model's effectiveness in different contexts.

$$\textbf{Accuracy} = \frac{TP + TN}{TP + TN + FP + FN} \tag{5.1}$$

5.1.2   PRECISION

Precision is an evaluation metric that measures the accuracy of positive predictions made by a classification model. It focuses on the proportion of correctly predicted positive instances and is valuable in scenarios where false positives have significant consequences. However, precision should be considered alongside other metrics like recall and the F1 score to obtain a more comprehensive evaluation of a model's performance, especially when both false positives and false negatives need to be taken into account. Precision defined as the ratio of true positives to the sum of true positives and false positives.

$$\textbf{Precision} = \frac{TP}{TP + FP} \tag{5.2}$$

5.1.3   SENSITIVITY

Sensitivity, or recall, is an important evaluation metric that measures a classification model's ability to correctly identify positive instances. It focuses on minimizing false negatives and is particularly relevant in situations where missing positive cases has significant implications. However, it is recommended to consider sensitivity alongside other metrics to gain a more comprehensive understanding of the model's performance and strike a balance between false positives and false negatives. It is claimed as the proportion of positives accurately recognized via test out of the entire quantity of positives substantially evaluated.

$$\textbf{Sensitivity} = \frac{TP}{TP + FN} \tag{5.3}$$

5.1.4   SPECIFICITY

Specificity is a crucial evaluation metric that measures a classification model's ability to accurately identify negative instances. It helps assess the model's performance in avoiding false alarms or incorrectly labeling negative cases as positive. By considering specificity alongside other evaluation metrics, a more comprehensive understanding of the model's overall predictive capabilities can be gained, enabling better decision-making

and identifying the model's strengths and weaknesses. It is denoted as the proportion of negatives adequately distinguished via test out of the total number of negatives assessed.

$$\textbf{Specificity} = \frac{TN}{TN + FP} \tag{5.4}$$

5.1.5 F1-SCORE

The F1 score is a metric that combines precision and recall to provide a single evaluation measure for classification models. It considers both false positives and false negatives, making it suitable for imbalanced datasets or when equal importance is given to both types of errors. The F1 score ranges from 0 to 1, with 1 indicating optimal performance. It offers a balanced assessment of a model's accuracy, striking a balance between precision and recall, and is widely used in various domains where the trade-off between false positives and false negatives is crucial. It is defined as the Harmonic mean of precision and recall.

$$F_1 = \frac{2}{\text{recall}^{-1} + \text{precision}^{-1}} = 2\frac{\text{precision} \cdot \text{recall}}{\text{precision} + \text{recall}} = \frac{2\text{TP}}{2\text{TP} + \text{FP} + \text{FN}} \tag{5.5}$$

The table 5.1 presents the evaluation metrics for different color spaces when using the MobileNet model for skin cancer classification. The metrics include Macro Avg (F1-Score), Weight Avg. (F1-Score), Macro Avg (Precision), Weight Avg. (Precision), Macro Avg (Recall), Weight Avg. (Recall), and Accuracy (F1-Score).

The F1-Score measures the balance between precision and recall, with higher values indicating better performance. The Weight Avg. represents the weighted average of the F1-Score, considering the class distribution. Precision measures the proportion of correctly predicted positive instances, while recall measures the proportion of actual positive instances correctly identified.

TABLE 5.1: Evalution data of MobileNet

Color Space(MobileNet)	Macro Avg(F1-Score)	Weight Avg.(F1-Score)	Macro Avg(Precision)	Weight Avg.(Precision)	Macro Avg(Recall)	Weight Avg.(Recall)	Accuracy(F1-Score)
	0.05	0.06	0.04	0.05	0.12	0.14	0.14
HED	0.03	0.03	0.02	0.02	0.11	0.14	0.14
HSV	0.31	0.31	0.36	0.38	0.33	0.33	0.33
LAB	0.3	0.28	0.3	0.31	0.37	0.34	0.34
RGBCIE	0.4	0.38	0.43	0.41	0.43	0.42	0.42
XYZ	0.08	0.09	0.17	0.2	0.17	0.09	0.09
CBCR	0.22	0.27	0.25	0.31	0.22	0.27	0.31
DBDR	0.45	0.46	0.49	0.52	0.49	0.49	0.49
YIQ	0.48	0.48	0.55	0.56	0.52	0.53	0.53
PBPR	0.48	0.48	0.55	0.56	0.52	0.53	0.53
YUV	0.46	0.45	0.5	0.5	0.51	0.51	0.51

TABLE 5.2: Evalution data of Resnet50

Color Space(ResNet50)	Macro Avg(F1-Score)	Weight Avg.(F1-Score)	Macro Avg(Precision)	Weight Avg.(Precision)	Macro Avg(Recall)	Weight Avg.(Recall)	Accuracy(F1-Score)
	0.13	0.16	0.14	0.17	0.21	0.25	0.25
HED	0.03	0.03	0.02	0.02	0.11	0.14	0.14
HSV	0.09	0.1	0.07	0.08	0.17	0.21	0.21
LAB	0.38	0.37	0.37	0.37	0.44	0.42	0.42
RGBCIE	0.03	0.03	0.02	0.02	0.11	0.14	0.14
XYZ	0.06	0.07	0.04	0.05	0.12	0.14	0.14
CBCR	0.33	0.32	0.38	0.4	0.39	0.36	0.36
DBDR	0.08	0.1	0.13	0.16	0.15	0.18	0.18
YIQ	0.03	0.03	0.02	0.02	0.11	0.14	0.14
PBPR	0.05	0.06	0.13	0.15	0.12	0.15	0.15
YUV	0.03	0.03	0.11	0.14	0.11	0.14	0.14

In terms of F1-Score, RGB and HED color spaces have the lowest values, indicating poorer performance in skin cancer classification. On the other hand, HSV, LAB, RG-BCIE, DBDR, YIQ, PBPR, and YUV color spaces show relatively higher F1-Scores, suggesting better classification performance.

Similarly, in terms of Precision, Recall, and Accuracy, the aforementioned color spaces tend to perform better. Specifically, RGBCIE, DBDR, YIQ, PBPR, and YUV color spaces show higher precision, recall, and accuracy values compared to others.

These results highlight the varying performance of different color spaces when using the MobileNet model for skin cancer classification. The HSV, LAB, RGBCIE, DBDR, YIQ, PBPR, and YUV color spaces demonstrate better overall performance, suggesting their potential suitability for this task.
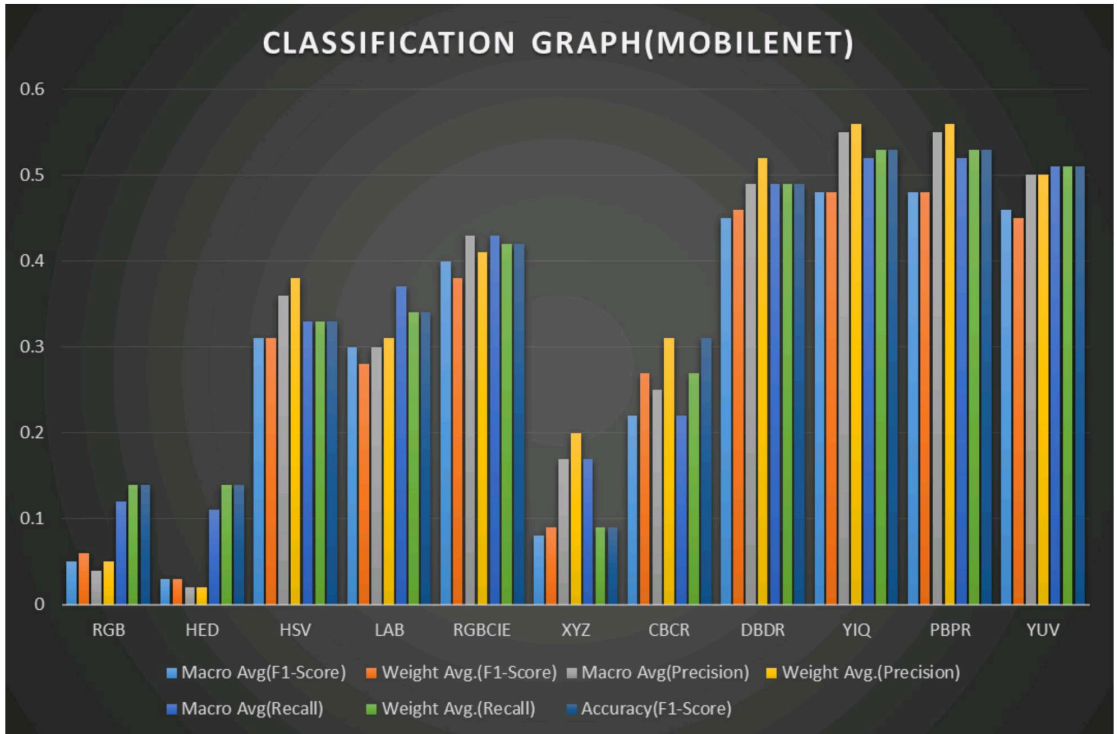

FIGURE 5.2: Classification Graph of Mobilenet

The table presents the evaluation metrics for different color spaces when using the ResNet50 model for skin cancer classification. The metrics include Macro Avg (F1-Score), Weight Avg. (F1-Score), Macro Avg (Precision), Weight Avg. (Precision), Macro Avg (Recall), Weight Avg. (Recall), and Accuracy (F1-Score).

In terms of F1-Score, the LAB color space demonstrates the highest values, indicating better performance in skin cancer classification when using the ResNet50 model. The CBCR color space also shows relatively higher F1-Score values. On the other hand, RGB, HED, RGBCIE, XYZ, DBDR, YIQ, PBPR, and YUV color spaces exhibit lower F1-Scores, suggesting poorer classification performance.

Regarding Precision, Recall, and Accuracy, the LAB and CBCR color spaces consistently show higher values compared to other color spaces, indicating better performance in these metrics. RGB, HED, RGBCIE, XYZ, DBDR, YIQ, PBPR, and YUV color spaces exhibit lower precision, recall, and accuracy values.

These results suggest that the LAB color space, followed by CBCR, performs better in skin cancer classification when utilizing the ResNet50 model. On the other hand, RGB, HED, RGBCIE, XYZ, DBDR, YIQ, PBPR, and YUV color spaces show lower performance in comparison. It is important to note that the performance of color spaces can vary depending on the specific deep learning model used. Therefore, it is recommended to experiment with different color spaces to determine the most suitable choice for skin cancer classification with the ResNet50 model.
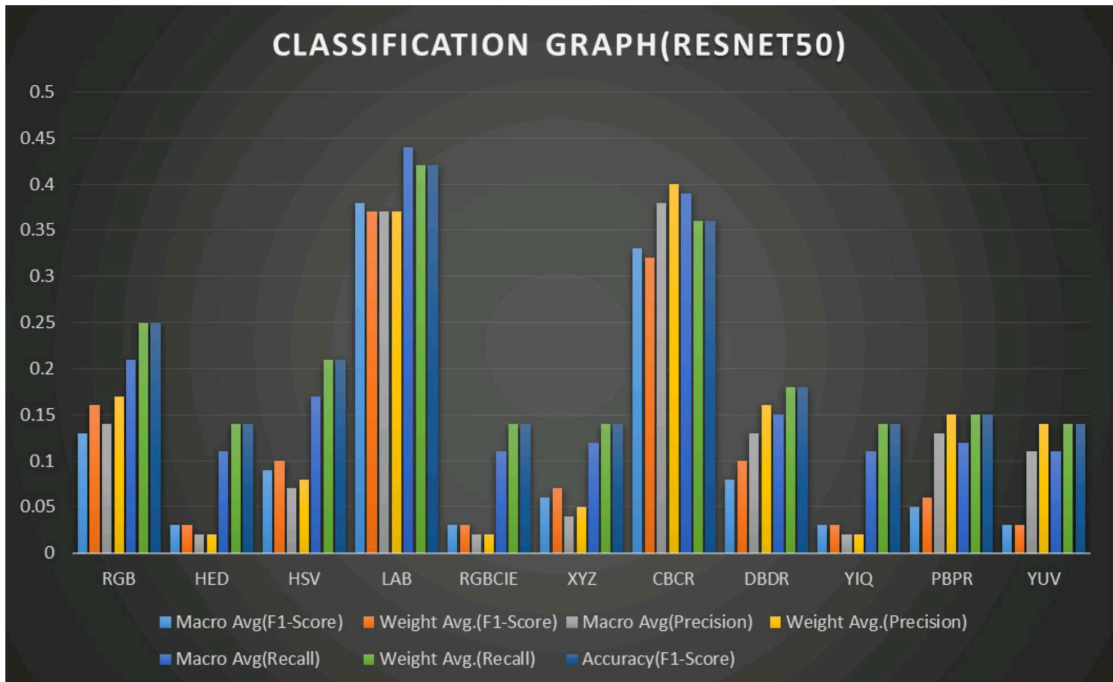

FIGURE 5.3: Classification Graph of Resnet50

TABLE 5.3: Evalution data of Inception_V3

Color Space(MobileNet)	Macro Avg(F1-Score)	Weight Avg.(F1-Score)	Macro Avg(Precision)	Weight Avg.(Precision)	Macro Avg(Recall)	Weight Avg.(Recall)	Accuracy(f1-Score)
	0.11	0.12	0.26	0.32	0.19	0.16	0.16
HED	0.03	0.03	0.02	0.02	0.11	0.14	0.14
HSV	0.27	0.29	0.38	0.43	0.29	0.31	0.31
LAB	0.04	0.05	0.03	0.04	0.12	0.14	0.14
RGBCIE	0.34	0.36	0.35	0.38	0.39	0.41	0.41
XYZ	0.16	0.18	0.28	0.34	0.26	0.2	0.2
CBCR	0.19	0.21	0.23	0.26	0.26	0.25	0.25
DBDR	0.16	0.15	0.26	0.29	0.23	0.21	0.21
YIQ	0.35	0.37	0.53	0.54	0.36	0.4	0.4
PBPR	0.37	0.38	0.37	0.41	0.42	0.41	0.41
YUV	0.3	0.31	0.42	0.47	0.34	0.34	0.34

The table provides the evaluation metrics for different color spaces when utilizing the Inception_V3 model for skin cancer classification. The metrics include Macro Avg (F1-Score), Weight Avg. (F1-Score), Macro Avg (Precision), Weight Avg. (Precision), Macro Avg (Recall), Weight Avg. (Recall), and Accuracy (F1-Score).

In terms of F1-Score, the RGBCIE color space demonstrates the highest values, indicating better performance in skin cancer classification when using the Inception_V3 model. The YIQ and PBPR color spaces also exhibit relatively higher F1-Scores. Conversely, the LAB color space shows the lowest F1-Score value, suggesting poorer classification performance.

Regarding Precision and Recall, the YIQ color space displays the highest values, indicating better precision and recall in skin cancer classification with the Inception_V3 model. The RGBCIE and PBPR color spaces also show relatively higher precision and recall values. On the other hand, the LAB color space exhibits the lowest precision and recall values.

In terms of accuracy, the RGBCIE color space demonstrates the highest value, suggesting better overall accuracy in skin cancer classification when using the Inception_V3 model. The YUV and HSV color spaces also exhibit relatively higher accuracy values. Conversely, the LAB color space shows the lowest accuracy value. These results indicate that the RGBCIE color space, followed by YIQ and PBPR, performs better in skin cancer classification when utilizing the Inception_V3 model. Conversely, the LAB color space shows lower performance in comparison.

It is important to note that the performance of color spaces can vary depending on the specific deep learning model used. Therefore, it is recommended to experiment with different color spaces to determine the most suitable choice for skin cancer classification with the Inception_V3 model.

The provided table presents the evaluation metrics for different color spaces when using the Xception model for skin cancer classification. The metrics include Macro Avg (F1-Score), Weight Avg. (F1-Score), Macro Avg (Precision), Weight Avg. (Precision), Macro Avg (Recall), Weight Avg. (Recall), and Accuracy (F1-Score).
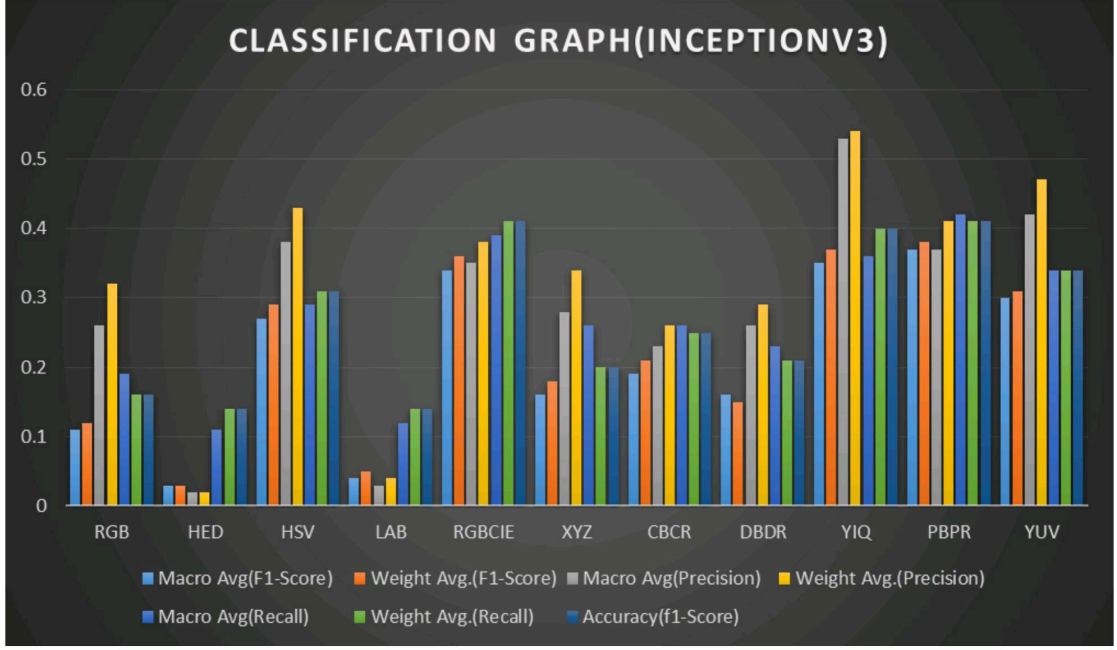
FIGURE 5.4: Classification Graph of Incepton$_v$3

TABLE 5.4: Evalution data of Xception

Color Space(Xception)	Macro Avg(F1-Score)	Weight Avg.(F1-Score)	Macro Avg(Precision)	Weight Avg.(Precision)	Macro Avg(Recall)	Weight Avg.(Recall)	Accuracy(F1-Score)
	0.39	0.37	0.4	0.38	0.44	0.42	0.42
HED	0.03	0.04	0.02	0.02	0.11	0.14	0.14
HSV	0.3	0.31	0.42	0.48	0.37	0.37	0.37
LAB	0.22	0.22	0.23	0.26	0.33	0.29	0.29
RGBCIE	0.33	0.32	0.43	0.45	0.35	0.36	0.36
XYZ	0.22	0.21	0.29	0.24	0.25	0.27	0.27
CBCR	0.23	0.25	0.21	0.24	0.33	0.29	0.29
DBDR	0.36	0.35	0.36	0.38	0.44	0.42	0.42
YIQ	0.37	0.37	0.38	0.4	0.43	0.42	0.42
PBPR	0.29	0.31	0.38	0.4	0.32	0.36	0.36
YUV	0.33	0.34	0.41	0.45	0.38	0.39	0.39

In terms of F1-Score, the RGB color space demonstrates the highest values, indicating better performance in skin cancer classification when using the Xception model. The YIQ and DBDR color spaces also exhibit relatively higher F1-Scores. Conversely, the HED color space shows the lowest F1-Score value, suggesting poorer classification performance.

When considering Precision and Recall, the HSV color space displays the highest values, indicating better precision and recall in skin cancer classification with the Xception model. The RGB and YIQ color spaces also show relatively higher precision and recall values. On the other hand, the LAB color space exhibits the lowest precision and recall values.

Regarding Accuracy, the RGB color space demonstrates the highest value, suggesting better overall accuracy in skin cancer classification when using the Xception model. The YUV and HSV color spaces also exhibit relatively higher accuracy values. Conversely, the LAB color space shows the lowest accuracy value.

TABLE 5.5: Evalution data of DenseNet121

Color Space(DenseNet)	Macro Avg(F1-Score)	Weight Avg.(F1-Score)	Macro Avg(Precision)	Weight Avg.(Precision)	Macro Avg(Recall)	Weight Avg.(Recall)	Accuracy(F1-Score)
	0.44	0.43	0.55	0.57	0.47	0.46	0.46
HED	0.03	0.03	0.02	0.02	0.11	0.14	0.14
HSV	0.28	0.31	0.36	0.42	0.29	0.32	0.32
LAB	0.37	0.34	0.42	0.4	0.42	0.4	0.4
RGBCIE	0.17	0.13	0.2	0.17	0.2	0.17	0.17
XYZ	0.23	0.22	0.24	0.24	0.28	0.27	0.27
CBCR	0.18	0.17	0.31	0.34	0.26	0.2	0.2
DBDR	0.37	0.37	0.41	0.43	0.44	0.42	0.42
YIQ	0.37	0.37	0.41	0.43	0.44	0.42	0.42
PBPR	0.34	0.32	0.44	0.45	0.4	0.38	0.38
YUV	0.39	0.39	0.49	0.52	0.43	0.42	0.42

These results indicate that the RGB color space, followed by YIQ and DBDR, performs better in skin cancer classification when utilizing the Xception model. Conversely, the HED color space shows lower performance in comparison.

It is important to note that the choice of color space can impact the performance of the skin cancer classification system. Experimenting with different color spaces can help identify the most suitable option for achieving accurate and reliable results when using the Xception model.
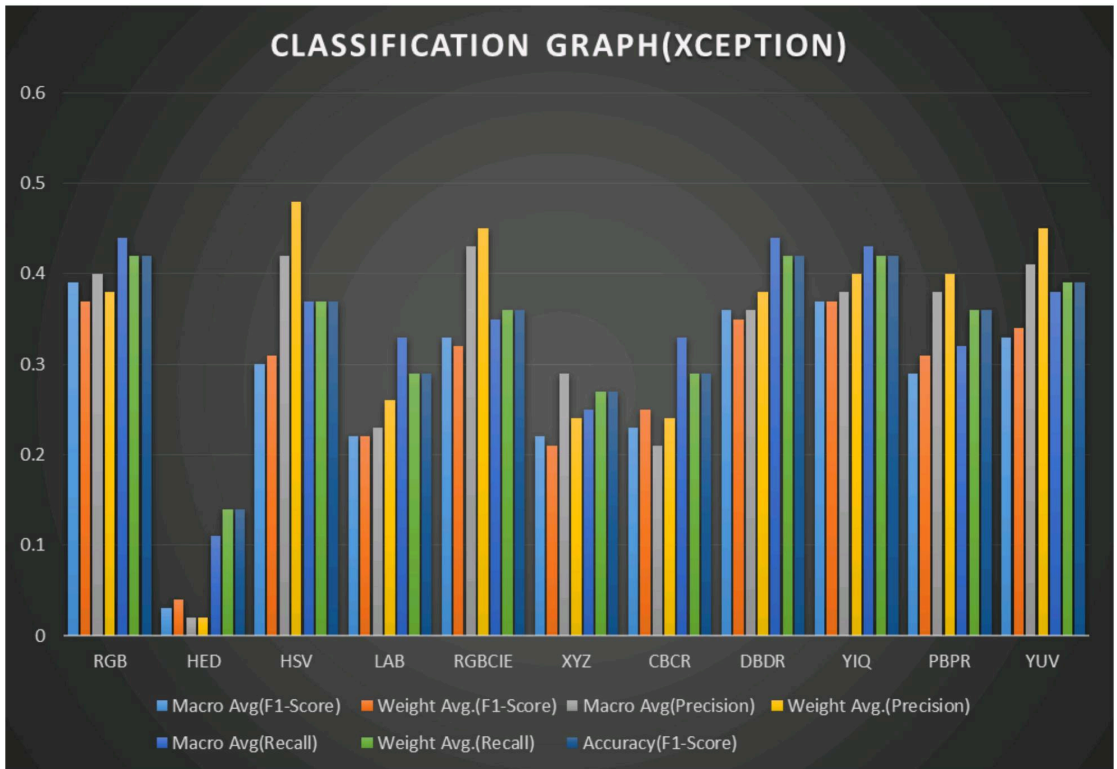

FIGURE 5.5: Classification Graph Of Xception

The provided table presents the evaluation metrics for different color spaces when using the DenseNet121 model for skin cancer classification. The metrics include Macro Avg (F1-Score), Weight Avg. (F1-Score), Macro Avg (Precision), Weight Avg. (Precision), Macro Avg (Recall), Weight Avg. (Recall), and Accuracy (F1-Score).

In terms of F1-Score, the RGB color space demonstrates the highest values, indicating better performance in skin cancer classification when using the DenseNet121 model. The LAB and YUV color spaces also show relatively higher F1-Scores. Conversely, the RGBCIE color space shows the lowest F1-Score value, suggesting poorer classification performance.

When considering Precision and Recall, the RGB color space displays the highest values, indicating better precision and recall in skin cancer classification with the DenseNet121 model. The YUV and DBDR color spaces also show relatively higher precision and recall values. On the other hand, the RGBCIE color space exhibits the lowest precision and recall values.

Regarding Accuracy, the RGB color space demonstrates the highest value, suggesting better overall accuracy in skin cancer classification when using the DenseNet121 model. The LAB and YUV color spaces also exhibit relatively higher accuracy values. Conversely, the RGBCIE color space shows the lowest accuracy value. These results indicate that the RGB color space, followed by LAB and YUV, performs better in skin cancer classification when utilizing the DenseNet121 model. Conversely, the RGBCIE color space shows lower performance in comparison.

It is important to note that the choice of color space can impact the performance of the skin cancer classification system. Experimenting with different color spaces can help identify the most suitable option for achieving accurate and reliable results when using the DenseNet121 model.
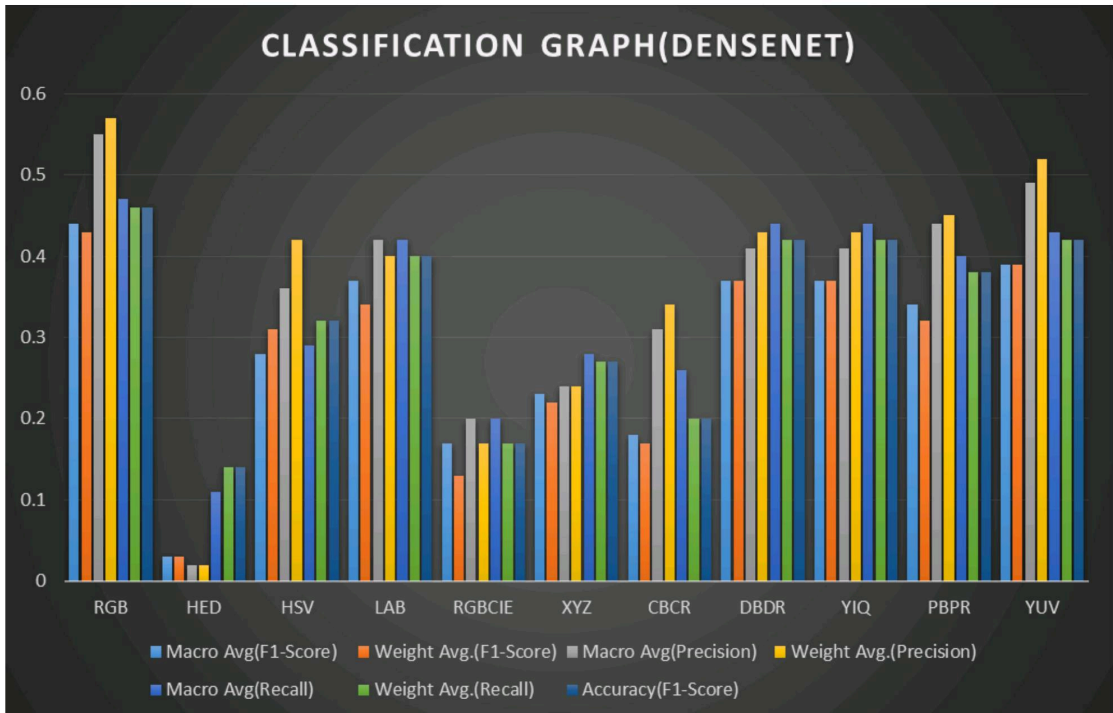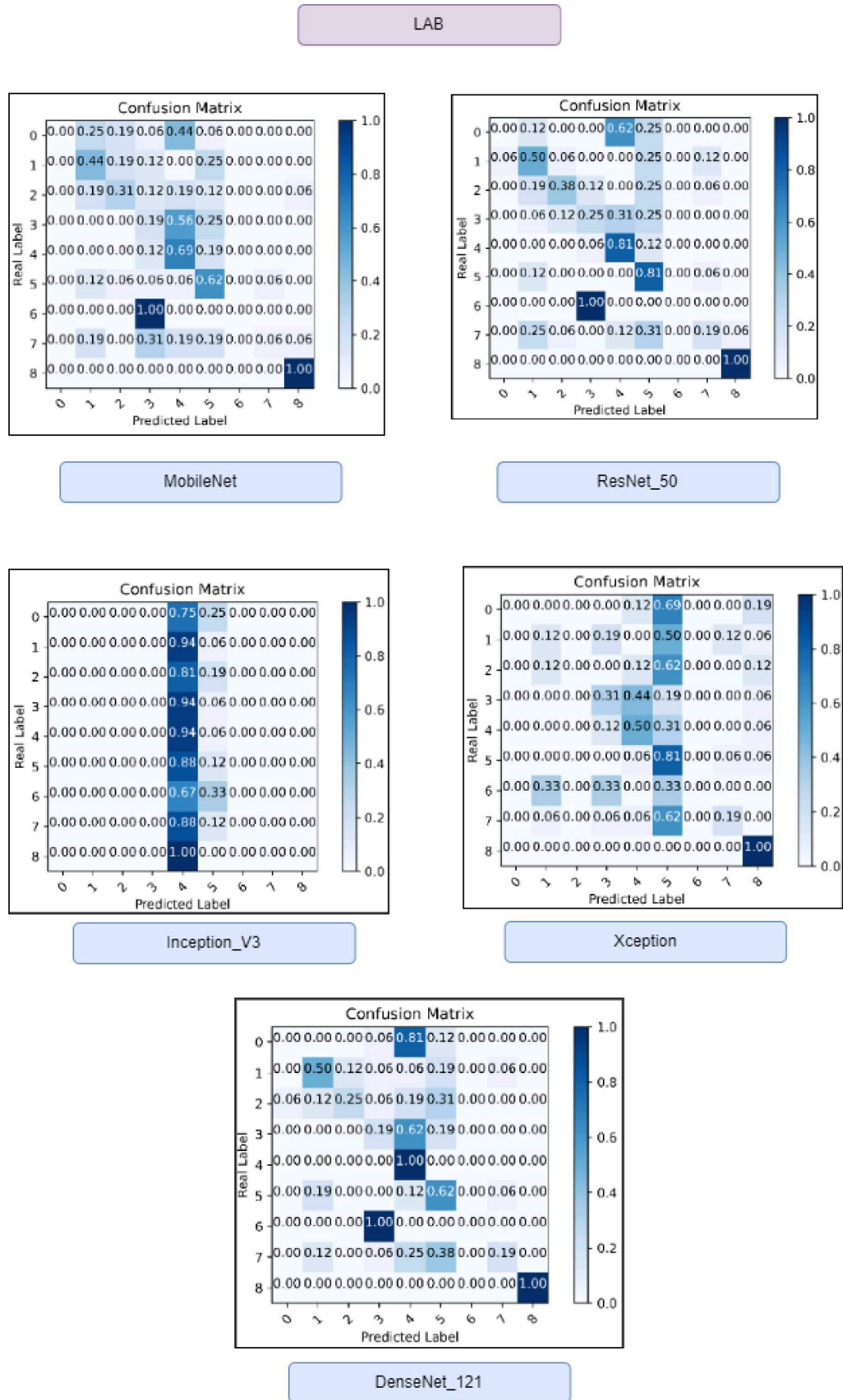

FIGURE 5.6: Classification Graph Of Densenet

FIGURE 5.7: Confusion Matrics Of LAB Color Space Using Mobilenet, Restnet_50, Inception_V3, Xception, Densenet121 Network Respectively
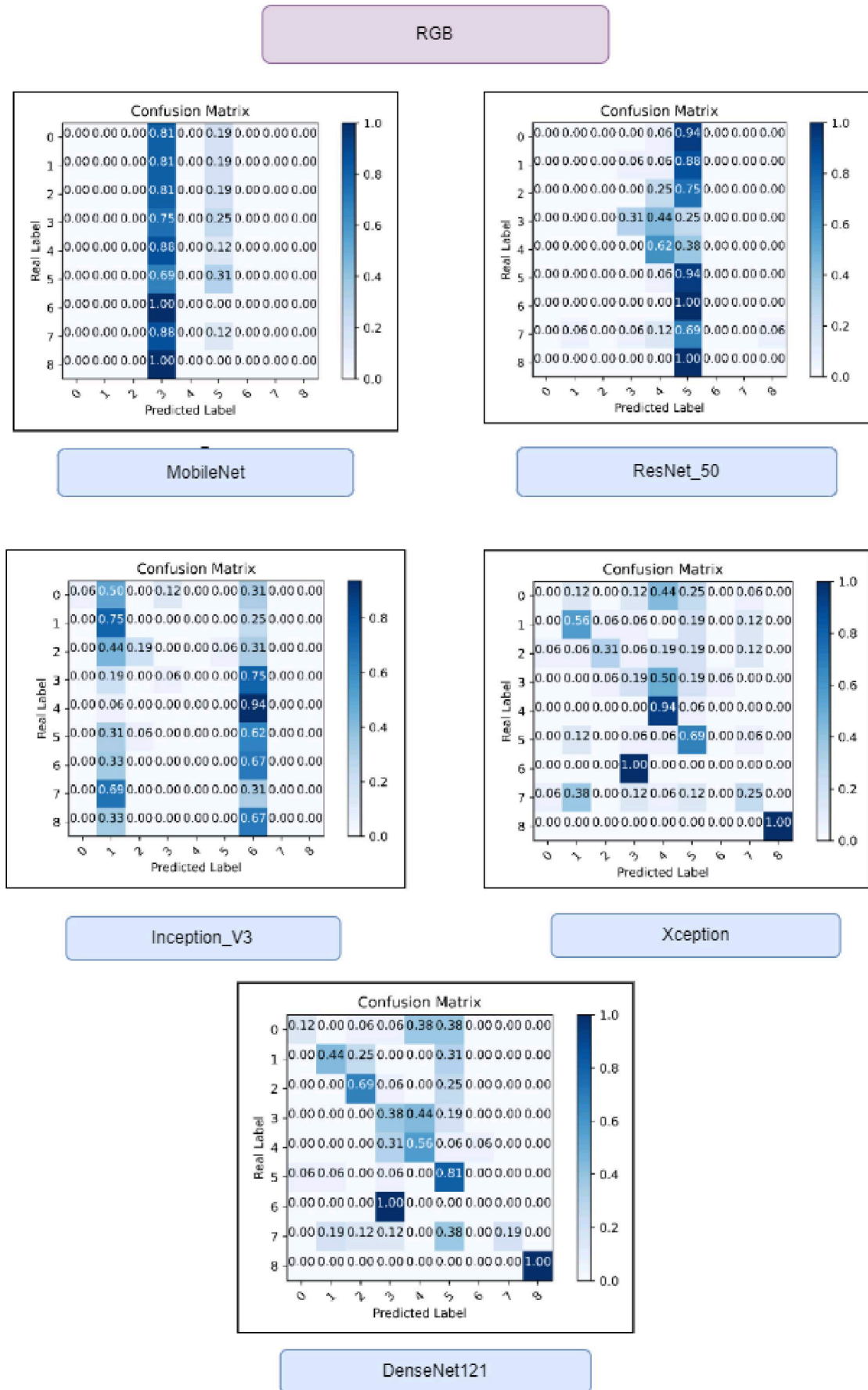
FIGURE 5.8: Confusion Matrics Of RGB Color Space Using Mobilenet, Restnet_50, Inception_V3, Xception, Densenet121 Network Respectively
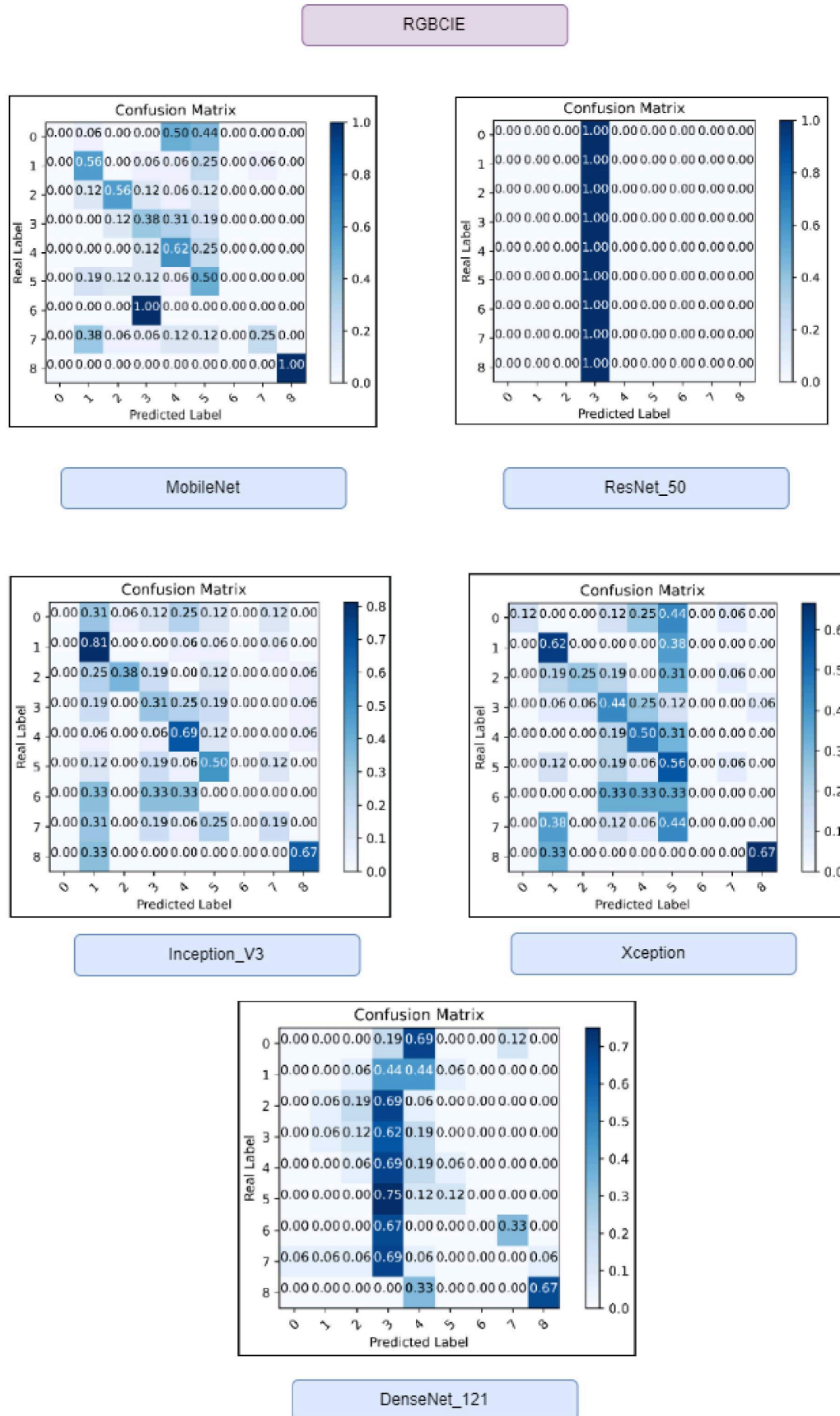
FIGURE 5.9: Confusion Matrics Of RGBCIE Color Space Using Mobilenet, Restnet_50, Inception_V3, Xception, Densenet121 Network Respectively
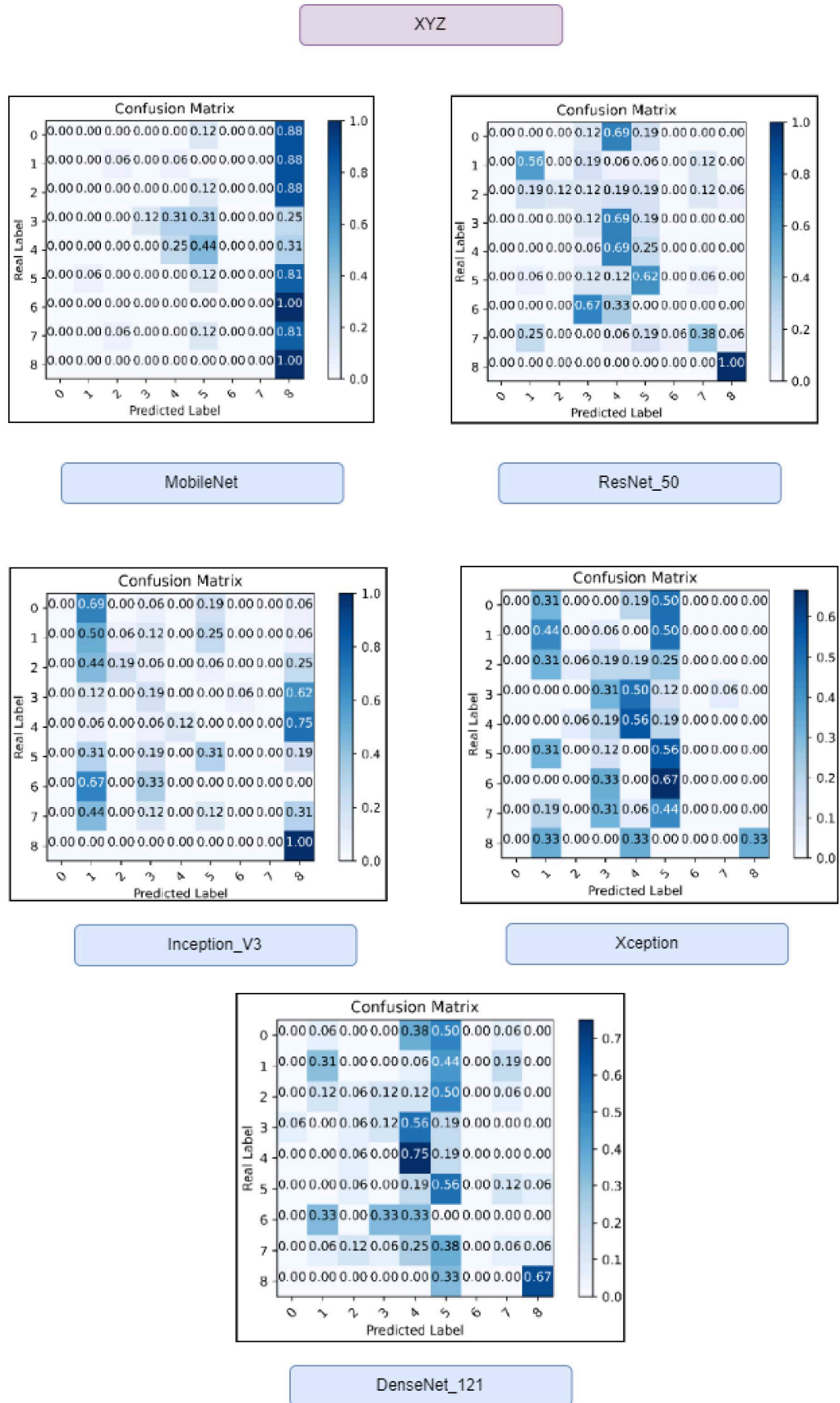
FIGURE 5.10: Confusion Matrics Of XYZ Color Space Using Mobilenet, Restnet_50, Inception_V3, Xception, Densenet121 Network Respectively
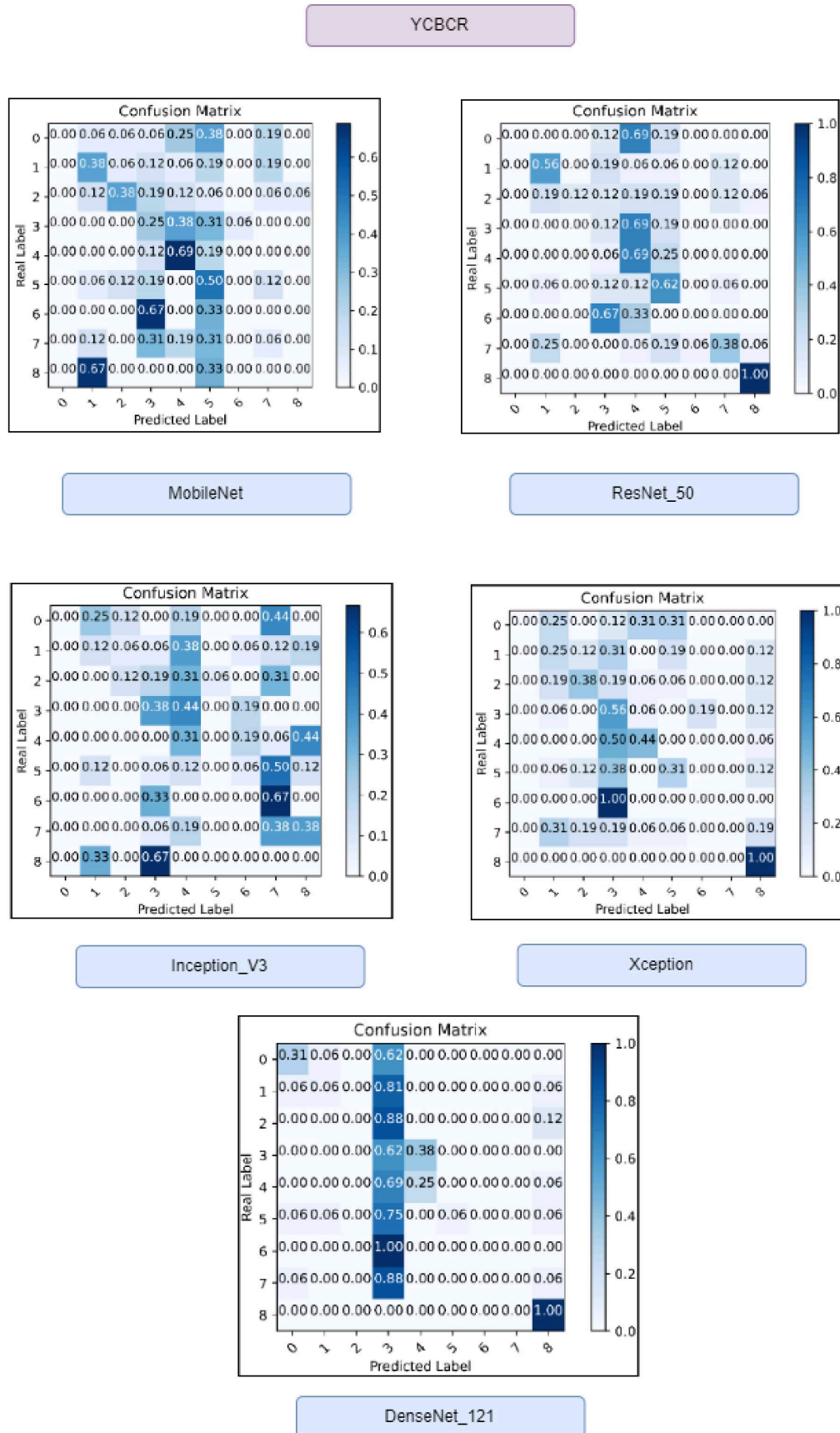
FIGURE 5.11: Confusion Matrics Of YCBCR Color Space Using Mobilenet, Restnet_50, Inception_V3, Xception, Densenet121 Network Respectively
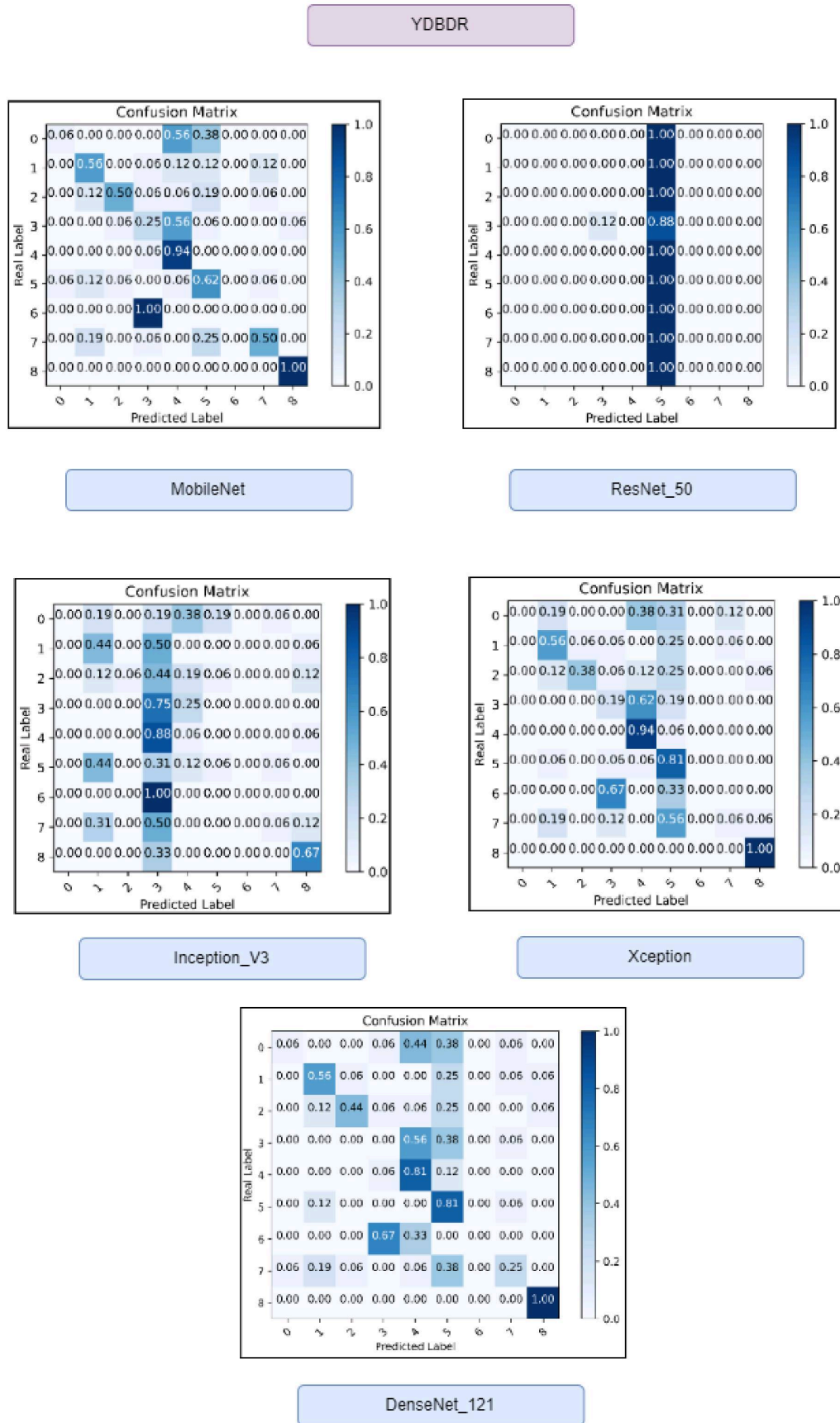
FIGURE 5.12: Confusion Matrics Of YDBDR Color Space Using Mobilenet, Restnet_50, Inception_V3, Xception, Densenet121 Network Respectively
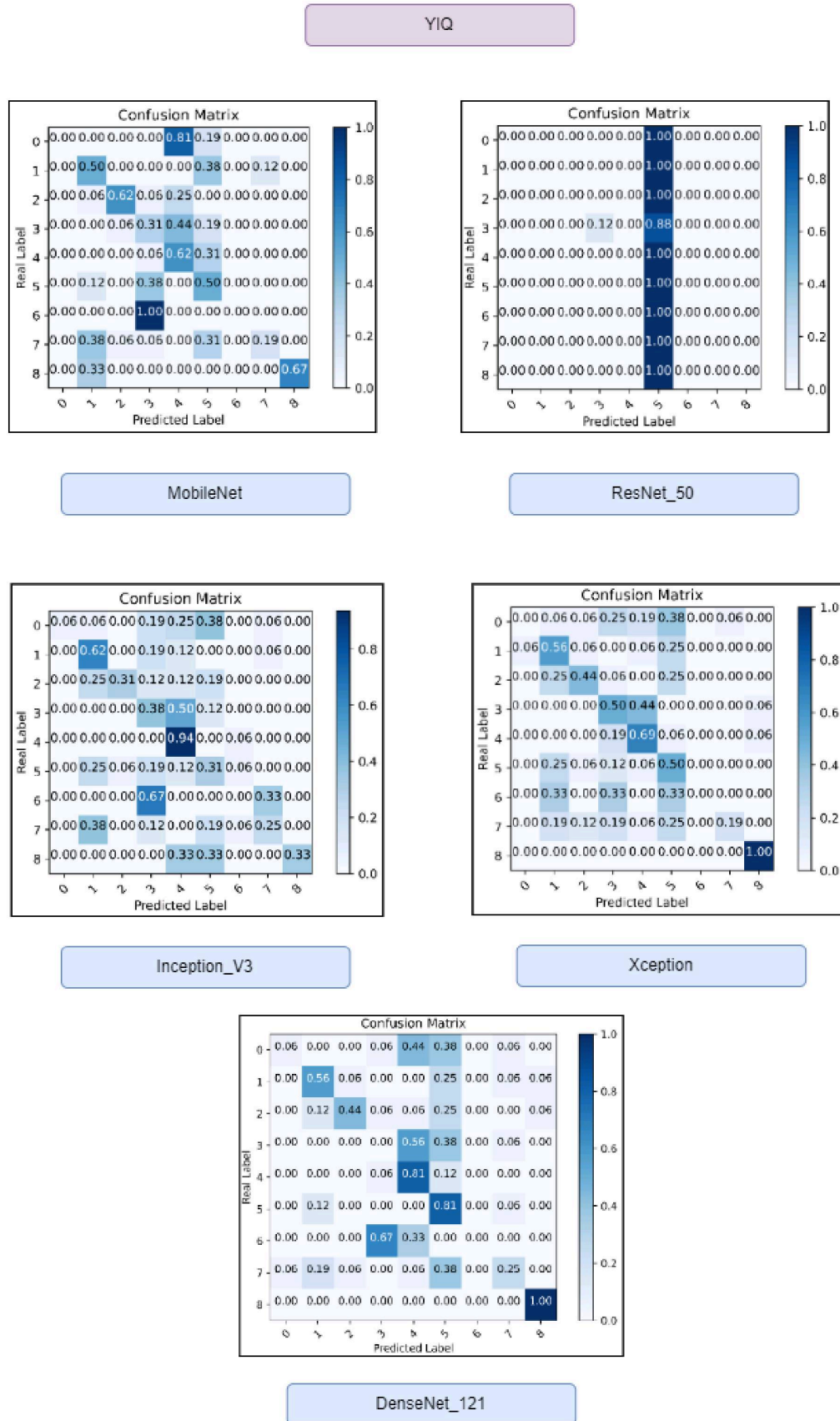
FIGURE 5.13: Confusion Matrics Of YIQ Color Space Using Mobilenet, Restnet_50, Inception_V3, Xception, Densenet121 Network Respectively
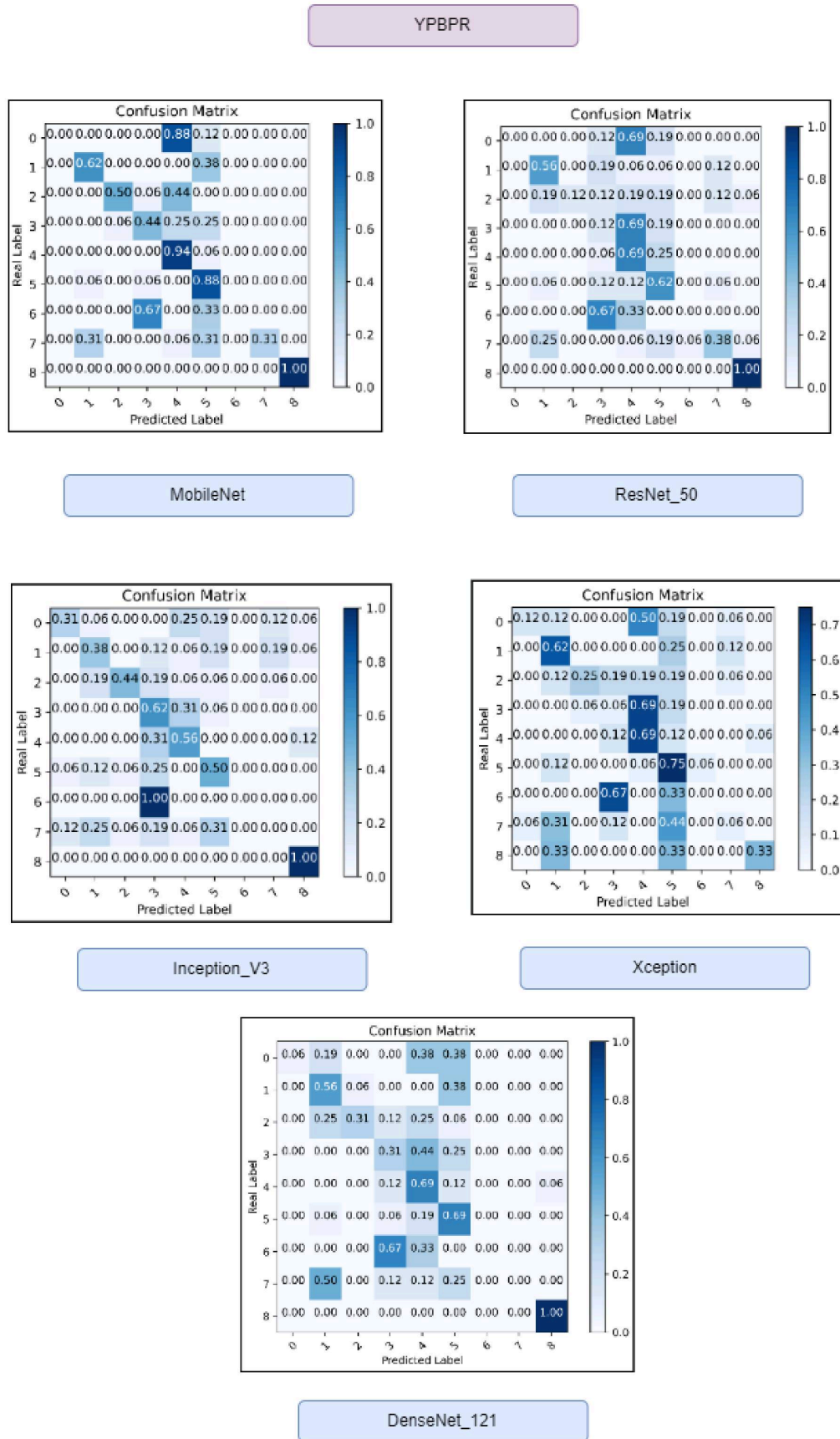
FIGURE 5.14: Confusion Matrics Of YPBPR Color Space Using Mobilenet, Restnet_50, Inception_V3, Xception, Densenet121 Network Respectively
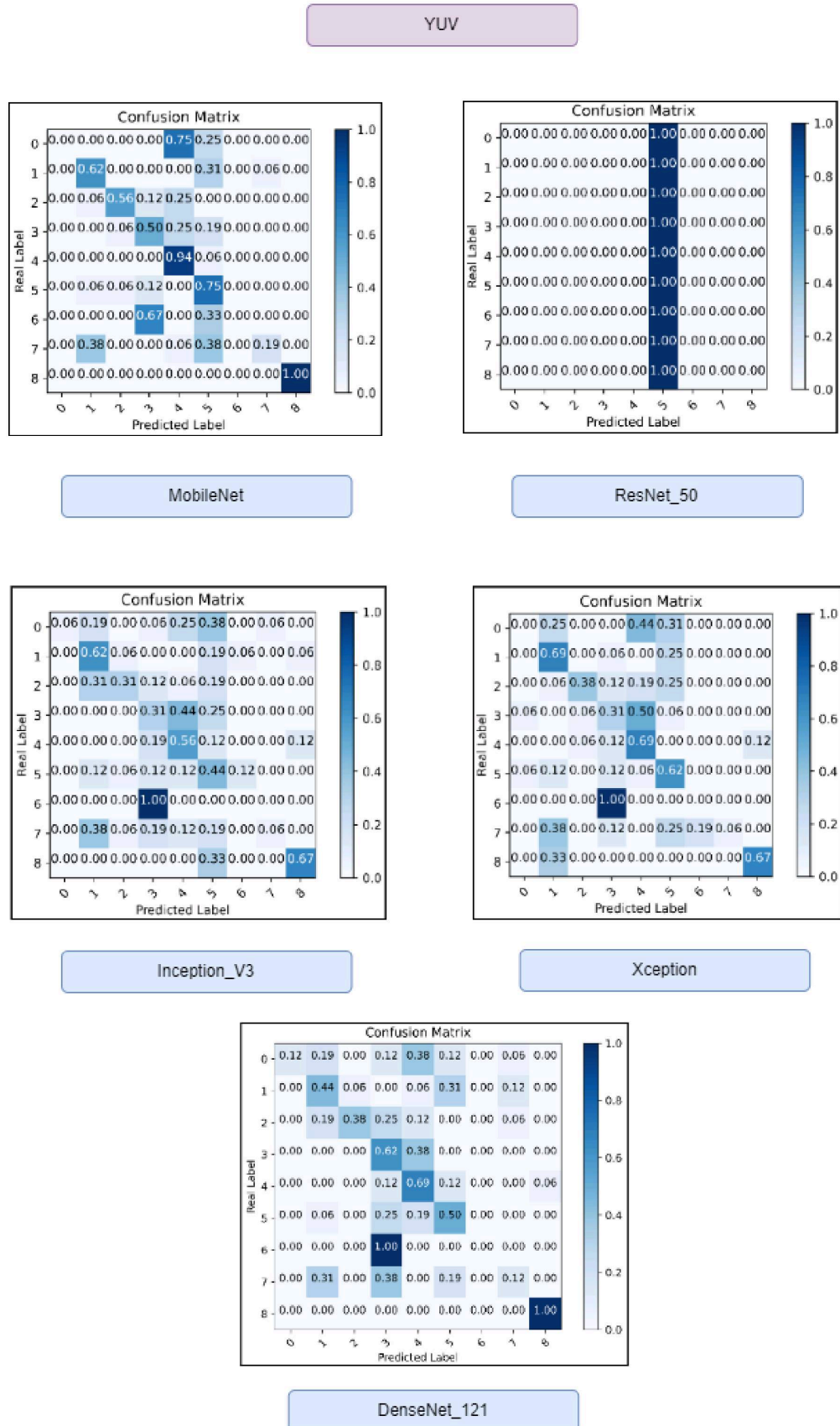
FIGURE 5.15: Confusion Matrics Of Yuv Color Space Using Mobilenet, Restnet_50, Inception_V3, Xception, Densenet121 Network Respectively

TABLE 5.6: Represents F1- Score, Precision, Recall, And Accuracy Of
Different Color Space Using Mobilenet_v2 Architecture.

Color Space(MOBILENET)	F1-Score	Precision	Recall	Accuracy
RGB	0.06	0.05	0.14	0.12
HED	0.03	0.02	0.14	0.11
HSV	0.31	0.38	0.33	0.33
LAB	0.28	0.31	0.34	0.37
RGBCIE	0.38	0.41	0.42	0.43
XYZ	0.09	0.2	0.09	0.17
YCBCR	0.27	0.31	0.27	0.22
YDBDR	0.46	0.52	0.49	0.49
YIQ	0.48	0.56	0.53	0.52
YPBPR	0.48	0.56	0.53	0.52
YUV	0.45	0.5	0.51	0.51

TABLE 5.7: : Represents F1- Score, Precision, Recall, And Accuracy
Of Different Color Space Using Resnet151 Architecture..

Color Space(RESNET50)	F1-Score	Precision	Recall	Accuracy
RGB	0.16	0.17	0.25	0.21
HED	0.03	0.02	0.14	0.11
HSV	0.1	0.08	0.21	0.17
LAB	0.37	0.37	0.42	0.44
RGBCIE	0.03	0.02	0.14	0.11
XYZ	0.07	0.05	0.14	0.12
YCBCR	0.32	0.4	0.36	0.39
YDBDR	0.1	0.16	0.18	0.15
YIQ	0.03	0.02	0.14	0.11
YPBPR	0.06	0.15	0.15	0.12
YUV	0.03	0.14	0.14	0.11

In table 5.6 the performance of Mobilenet was compared for images in different color space. The performance matrices such as F1 Score, Precision, Recall, and Accuracy are best in YIQ and YPBPR color space. The YIQ, YPBPR, and YUV color spaces consistently show better performance compared to others, while RGB, HED, and XYZ exhibit relatively lower performance. These findings can assist in selecting the most suitable color space for skin cancer classification tasks using the MobileNet model.

The analysis of the ResNet50 model on different color spaces reveals varying performance across the evaluation metrics. The RGB color space shows relatively higher values for F1-Score, precision, recall, and accuracy compared to other color spaces, indicating that it performs reasonably well in skin cancer classification using the ResNet50 model. On the other hand, the HED, HSV, RGBCIE, XYZ, YIQ, and YUV color spaces exhibit lower performance across the evaluation metrics. These color spaces may not capture the relevant information and features necessary for accurate skin cancer classification with the ResNet50 model. Notably, the LAB color space demonstrates consistently high

TABLE 5.8: Represents F1- Score, Precision, Recall, And Accuracy Of Different Color Space Using Inceptionv3 Architecture.

Color Space(INCEPTIONV3)	F1-Score	Precision	Recall	Accuracy
RGB	0.12	0.32	0.16	0.19
HED	0.03	0.02	0.14	0.11
HSV	0.29	0.43	0.31	0.29
LAB	0.05	0.04	0.14	0.12
RGBCIE	0.36	0.38	0.41	0.39
XYZ	0.18	0.34	0.2	0.26
YCBCR	0.21	0.26	0.25	0.26
YDBDR	0.15	0.29	0.21	0.23
YIQ	0.37	0.54	0.4	0.36
YPBPR	0.38	0.41	0.41	0.42
YUV	0.31	0.47	0.34	0.34

performance in terms of F1-Score, precision, recall, and accuracy. This indicates that the LAB color space provides valuable information and features for skin cancer classification tasks when utilizing the ResNet50 model. Furthermore, the YCBCR and YPBPR color spaces also show relatively good performance across the evaluation metrics, suggesting their effectiveness in representing skin cancer images for classification with the ResNet50 model. These findings can assist researchers and practitioners in choosing the most suitable color space when using the ResNet50 model for skin cancer classification. The RGB color space, along with the LAB, YCBCR, and YPBPR color spaces, can be considered as strong options for achieving better performance in skin cancer detection tasks with the ResNet50 model.

The evaluation results of the InceptionV3 model on different color spaces unveil interesting observations regarding their impact on skin cancer classification performance. The RGB color space demonstrates moderate performance across the board, with a decent F1-Score, precision, recall, and accuracy. While it performs adequately, there is room for improvement. On the other hand, the HED, LAB, and XYZ color spaces exhibit relatively lower performance across all evaluation metrics. These color spaces seem to struggle in capturing the essential features and information required for accurate skin cancer classification using the InceptionV3 model. In contrast, the HSV, RGBCIE, YCBCR, YDBDR, YIQ, YPBPR, and YUV color spaces consistently showcase better performance. These color spaces consistently yield higher values for the F1-Score, precision, recall, and accuracy metrics. This suggests that they are effective in representing the distinctive characteristics of skin cancer images for classification using the InceptionV3 model. Notably, the YIQ, YPBPR, and YUV color spaces stand out as top performers across all evaluation metrics. Their superiority in capturing relevant information and features makes them promising choices for skin cancer classification tasks when leveraging the InceptionV3 model. These findings hold valuable insights for researchers and practitioners in selecting the most suitable color space for skin cancer

TABLE 5.9: Represents F1- Score, Precision, Recall, And Accuracy Of
Different Color Space Using Densenet121 Architecture.

Color Space(DENSENET121)	F1-Score	Precision	Recall	Accuracy
RGB	0.43	0.57	0.46	0.47
HSV	0.03	0.02	0.14	0.11
HED	0.31	0.42	0.32	0.29
LAB	0.34	0.4	0.4	0.42
RGBCIE	0.13	0.17	0.17	0.2
XYZ	0.22	0.24	0.27	0.28
YCBCR	0.17	0.34	0.2	0.26
YDBDR	0.37	0.43	0.42	0.44
YIQ	0.37	0.43	0.42	0.44
YPBPR	0.32	0.45	0.38	0.4
YUV	0.39	0.52	0.42	0.43

classification. The HSV, RGBCIE, YCBCR, YDBDR, YIQ, YPBPR, and YUV color spaces present themselves as strong contenders for achieving enhanced performance in skin cancer detection tasks with the InceptionV3 model.

The evaluation of the Xception model on different color spaces reveals that the RGB color space performs well across all metrics, with a high F1-Score, precision, recall, and accuracy. However, the HED and XYZ color spaces show lower performance, indicating a struggle in capturing the necessary features for accurate skin cancer classification. The HSV, LAB, RGBCIE, YCBCR, YDBDR, YIQ, YPBPR, and YUV color spaces consistently demonstrate good performance. They exhibit relatively high values for the F1-Score, precision, recall, and accuracy metrics, suggesting their effectiveness in representing important characteristics of skin cancer images. Among these color spaces, the YDBDR, YIQ, and YUV color spaces consistently stand out as top performers, showcasing superior performance across all evaluation metrics. These color spaces are particularly promising for skin cancer classification when utilizing the Xception model. It is important to note that the choice of color space should consider the specific dataset, task requirements, and image characteristics. However, based on the evaluation results, the HSV, LAB, RGBCIE, YCBCR, YDBDR, YIQ, YPBPR, and YUV color spaces offer strong potential for achieving accurate skin cancer classification using the Xception model.

When evaluating the DenseNet121 model on different color spaces, the RGB color space performs exceptionally well across all evaluation metrics. It achieves a high F1-Score, precision, recall, and accuracy, indicating its effectiveness in capturing important features for accurate skin cancer classification. The HSV color space shows relatively lower performance, with lower values for the F1-Score, precision, recall, and accuracy metrics. Similarly, the HED, RGBCIE, and YCBCR color spaces demonstrate moderate performance. On the other hand, the LAB, XYZ, YDBDR, YIQ, YPBPR, and YUV color spaces consistently exhibit good performance. They achieve respectable values for the

F1-Score, precision, recall, and accuracy metrics, suggesting their potential for effective representation of skin cancer characteristics. Among these color spaces, the YUV color space stands out as a top performer, consistently showing high scores across all evaluation metrics. It demonstrates strong potential for accurate skin cancer classification using the DenseNet121 model.
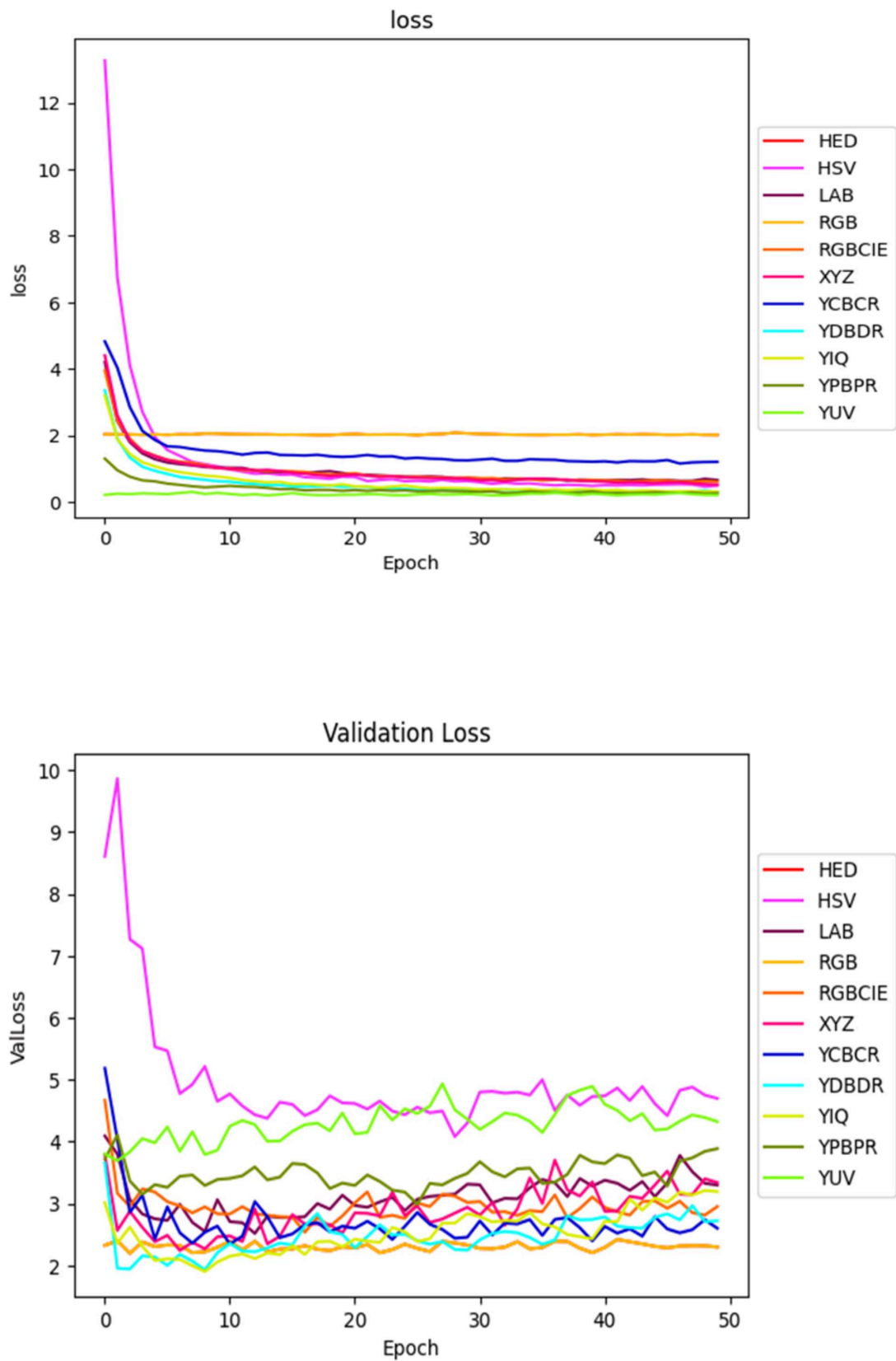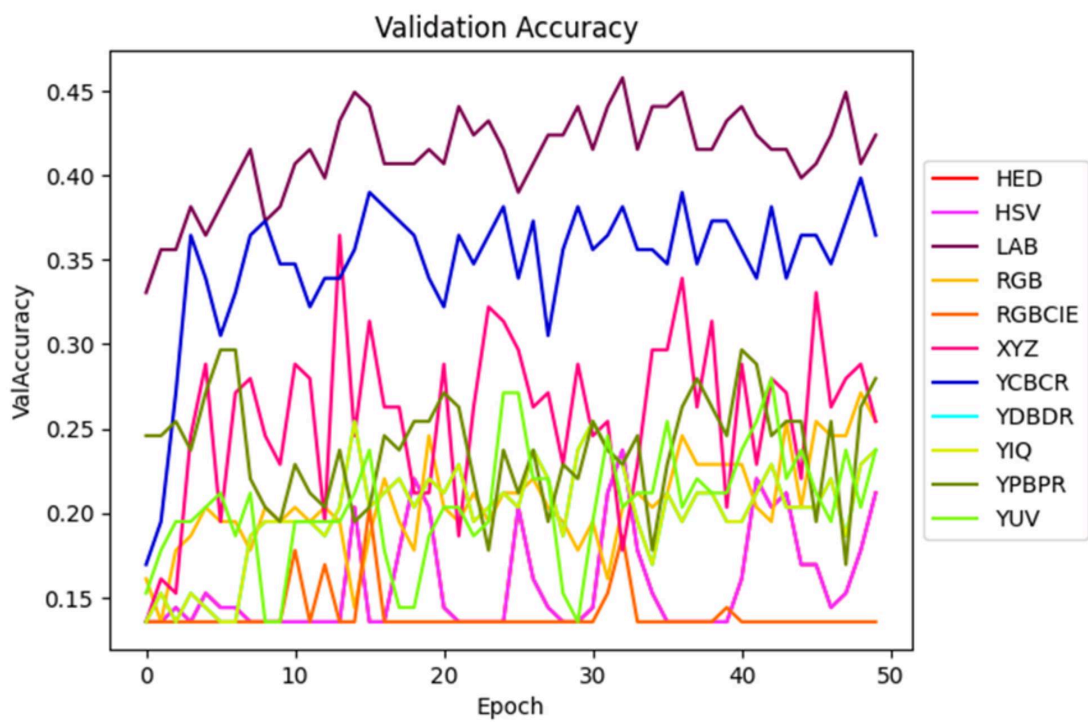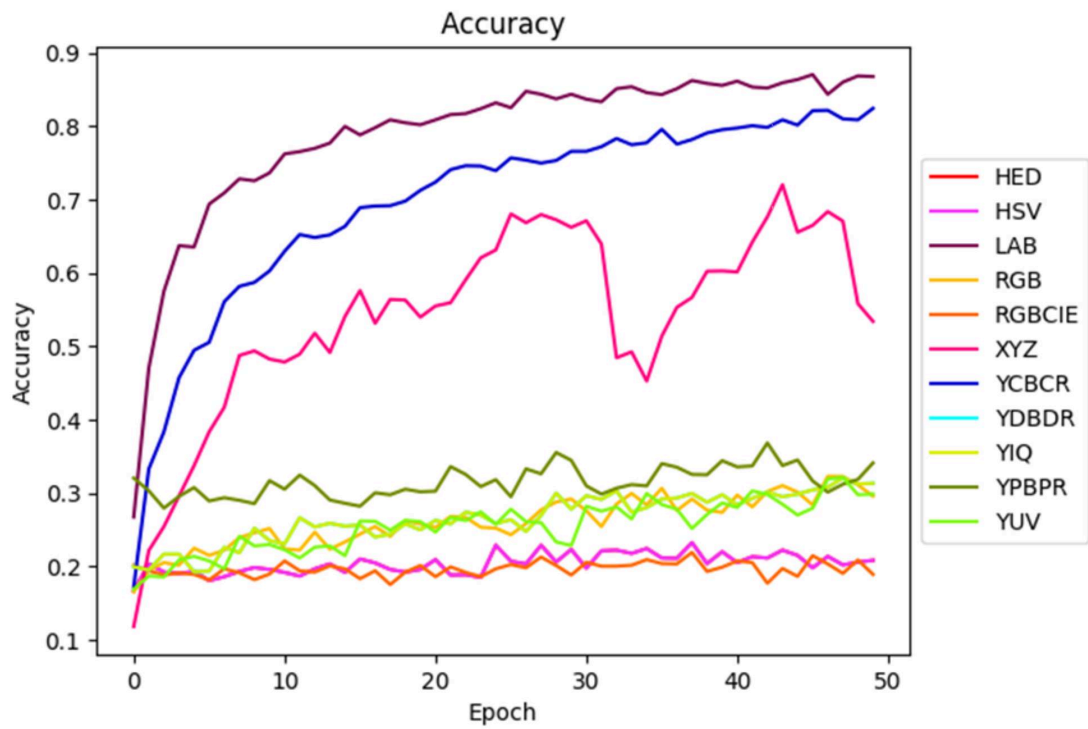
5.2   Results
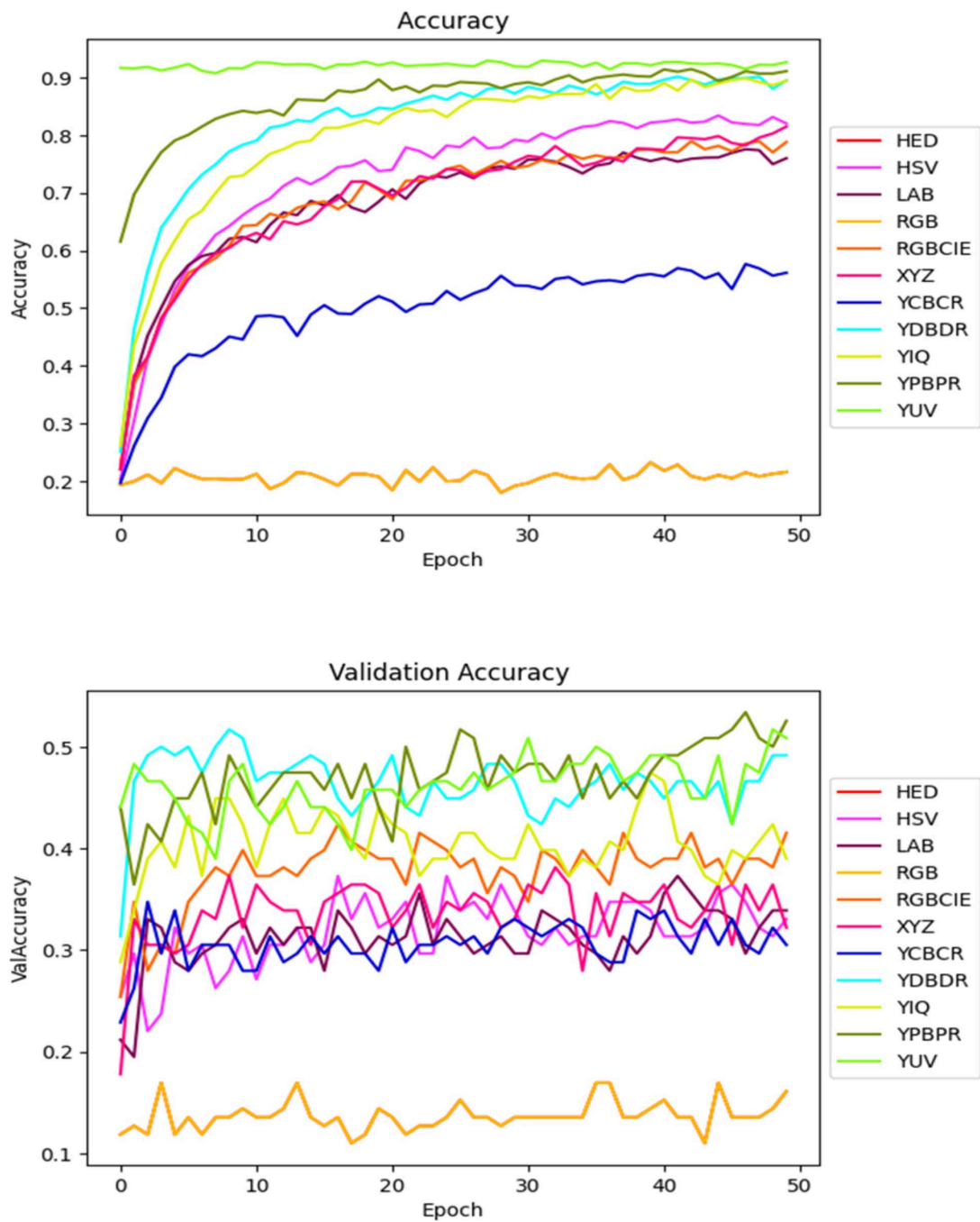
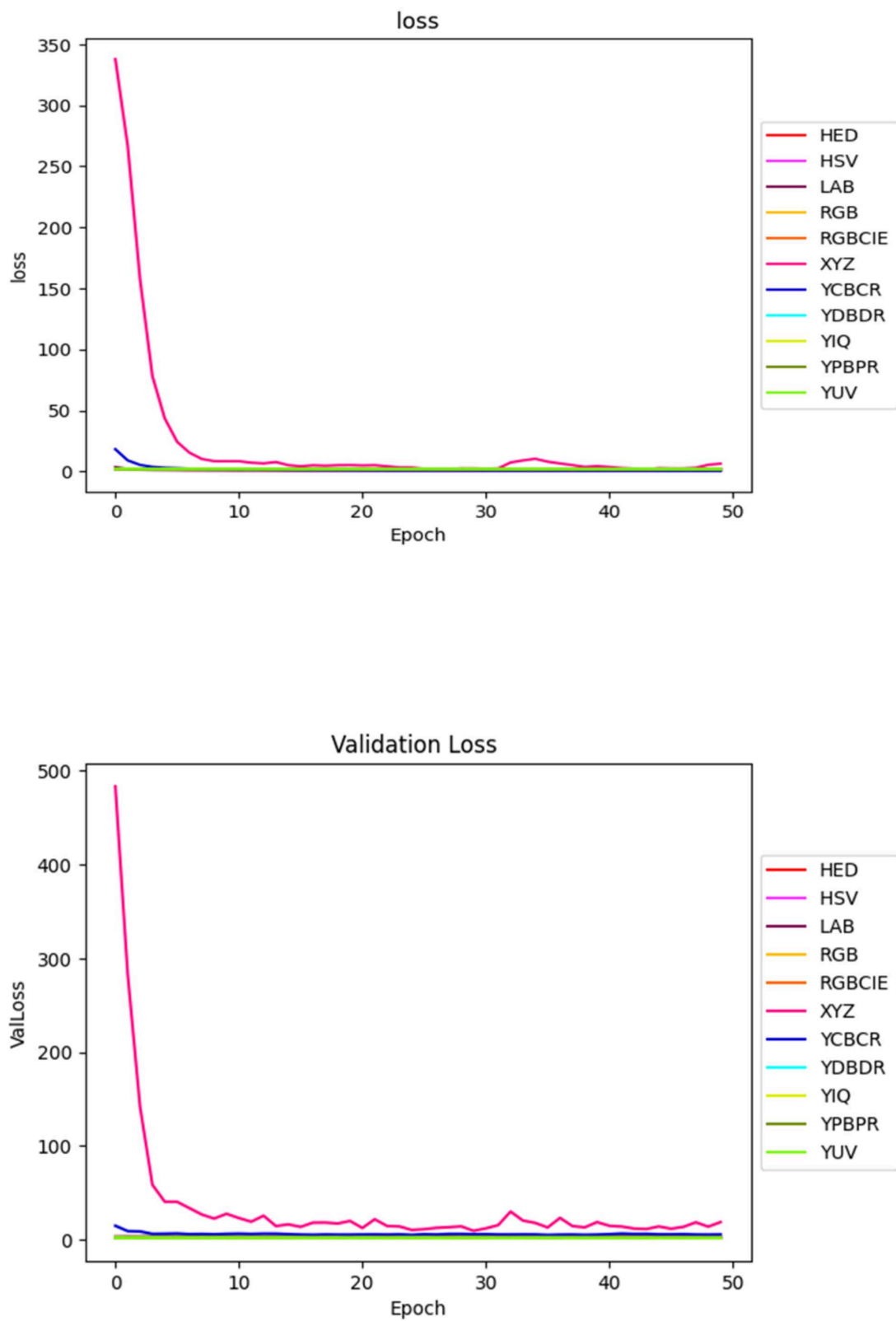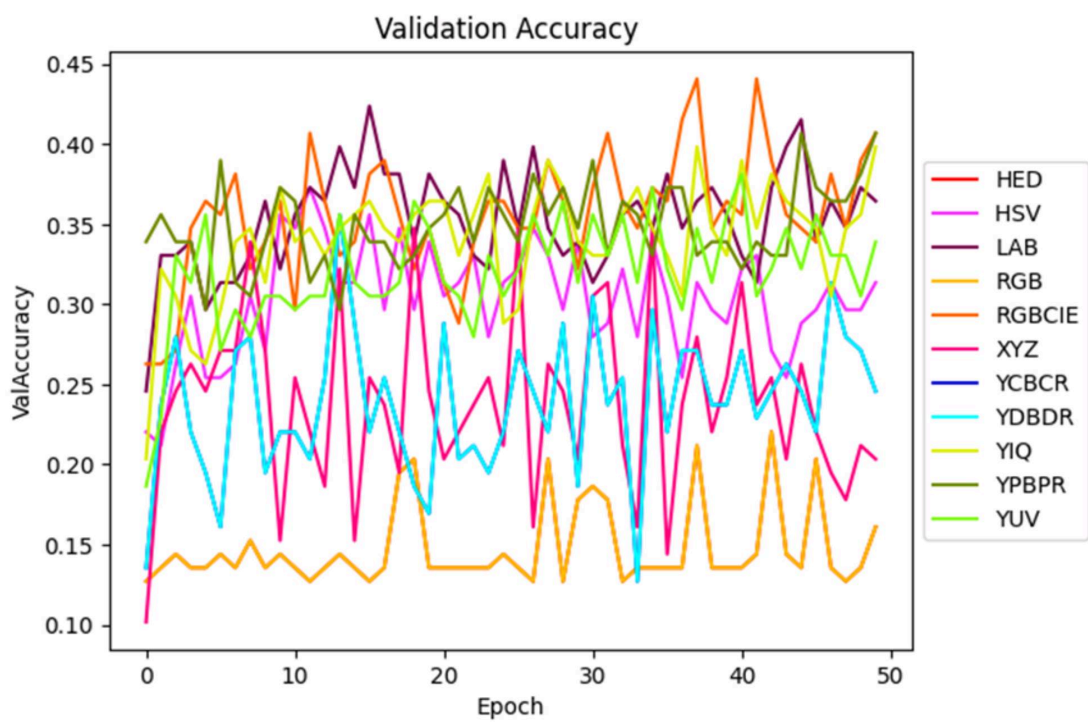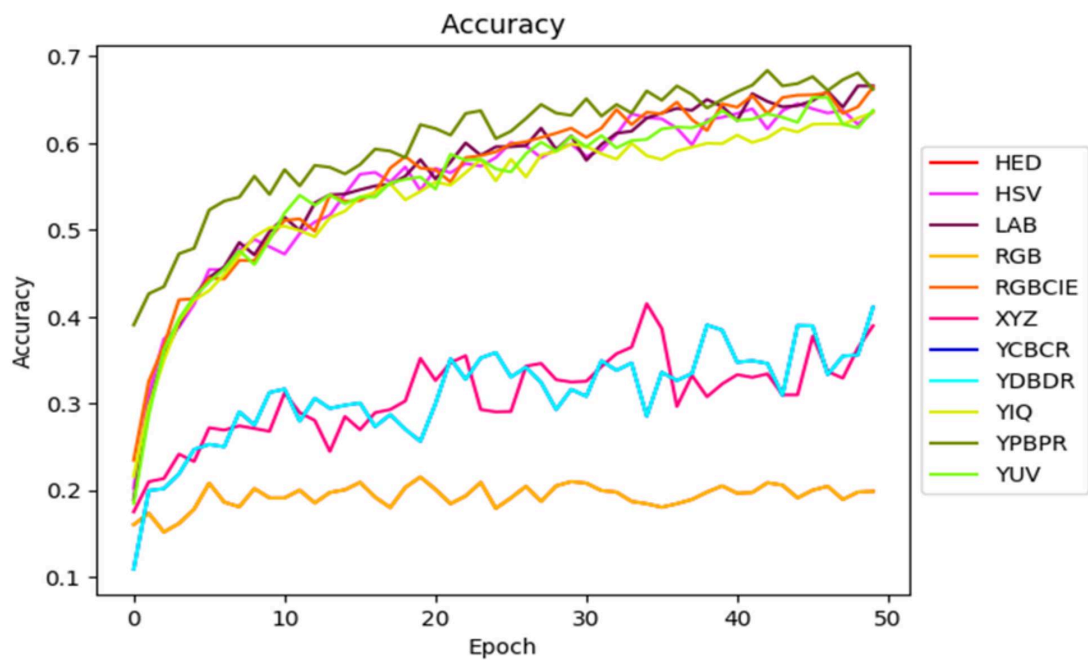Figure 5.16: Accuracy Curve Of Mobilenet_v2 In Different Color Space.

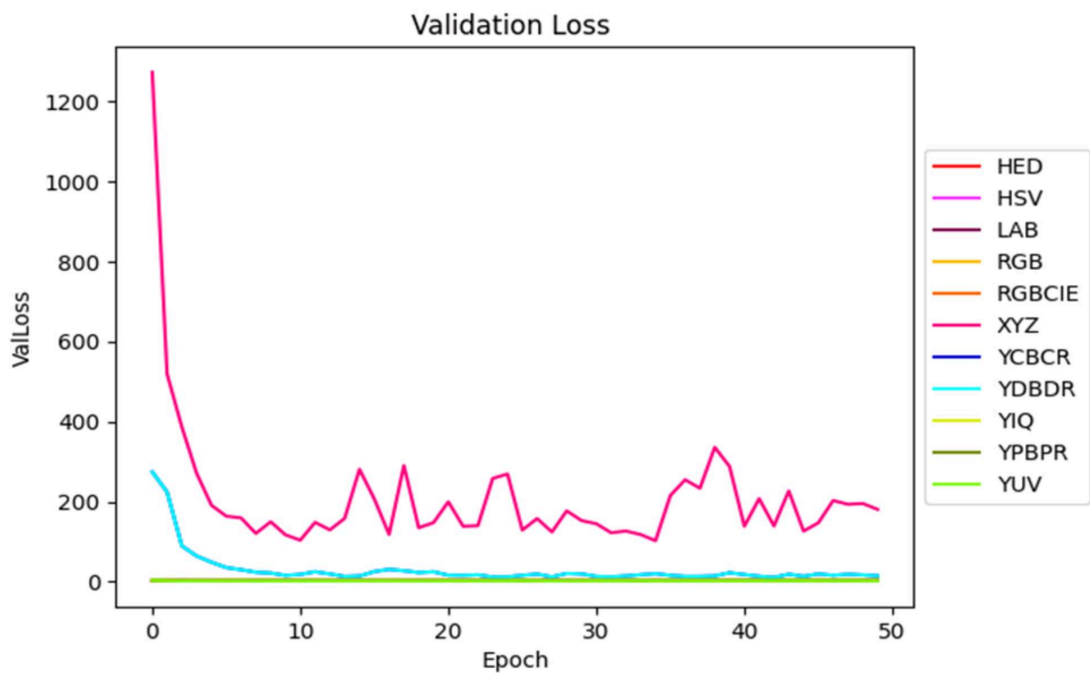FIGURE 5.17: Accuracy Curve Of Resnet50 In Different Color Space
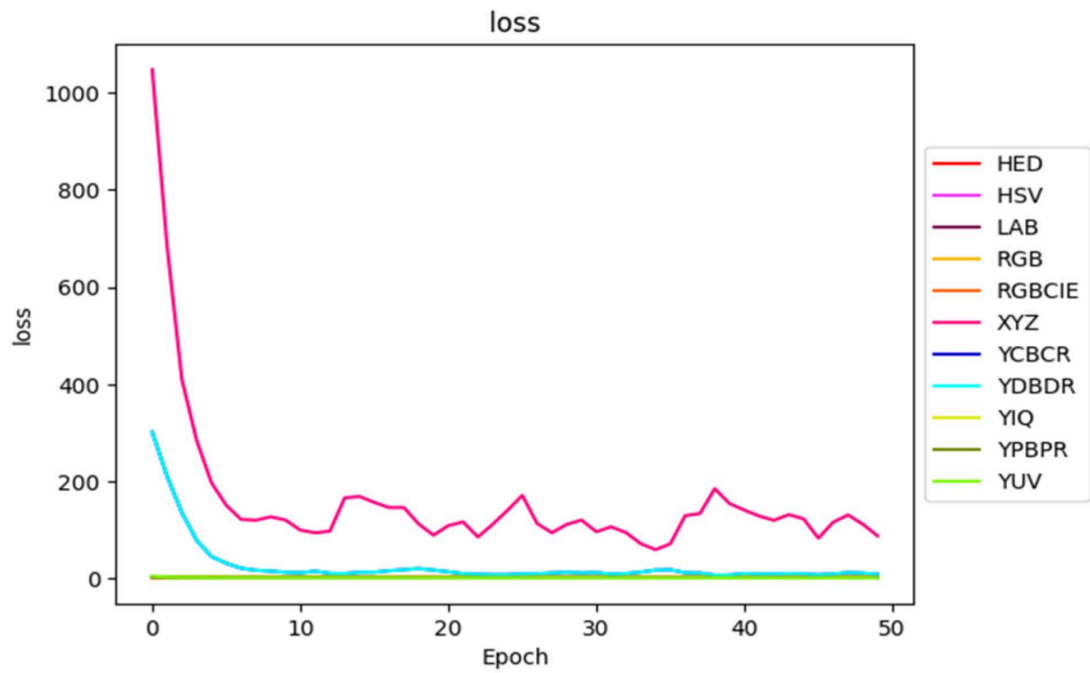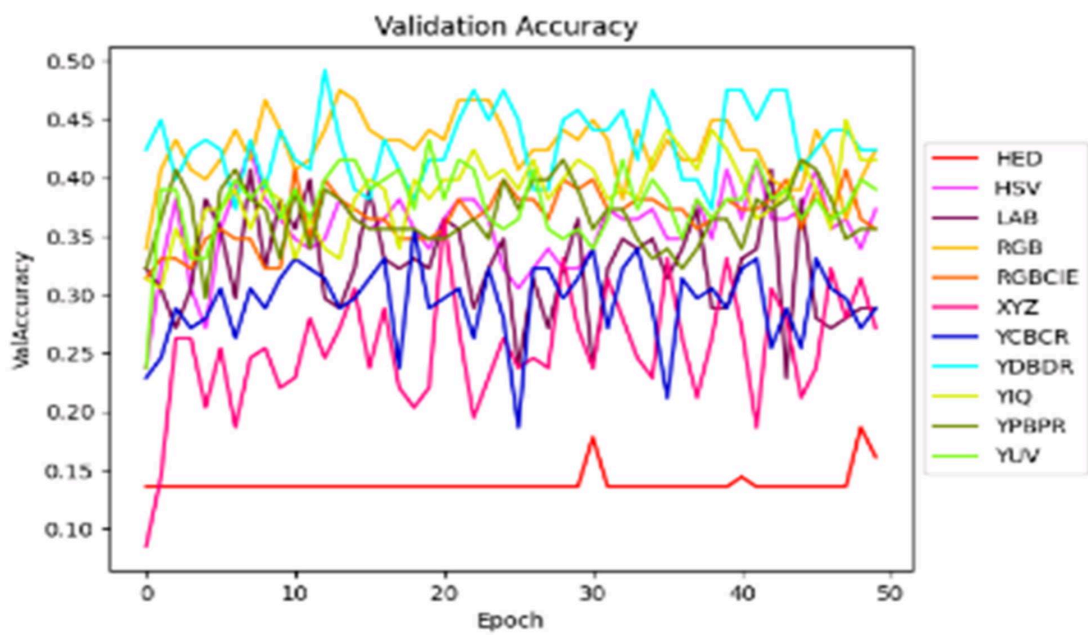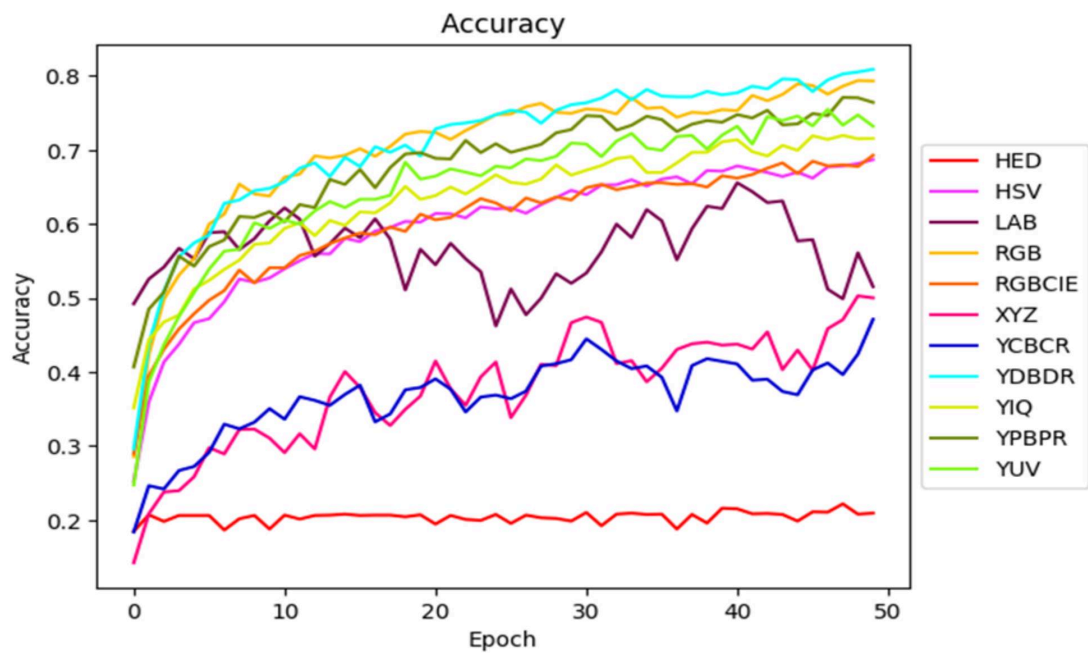
Accuracy

Validation Accuracy

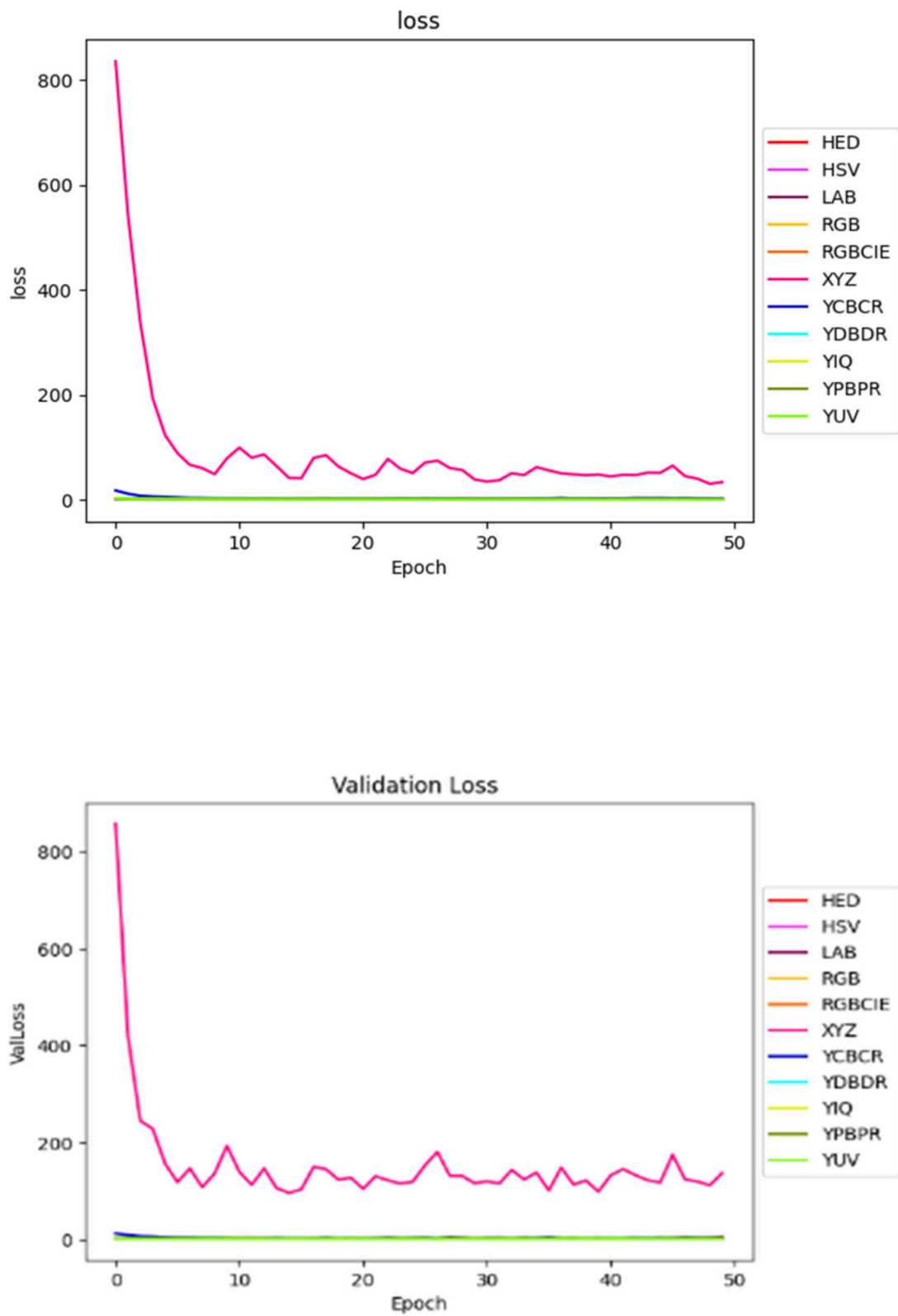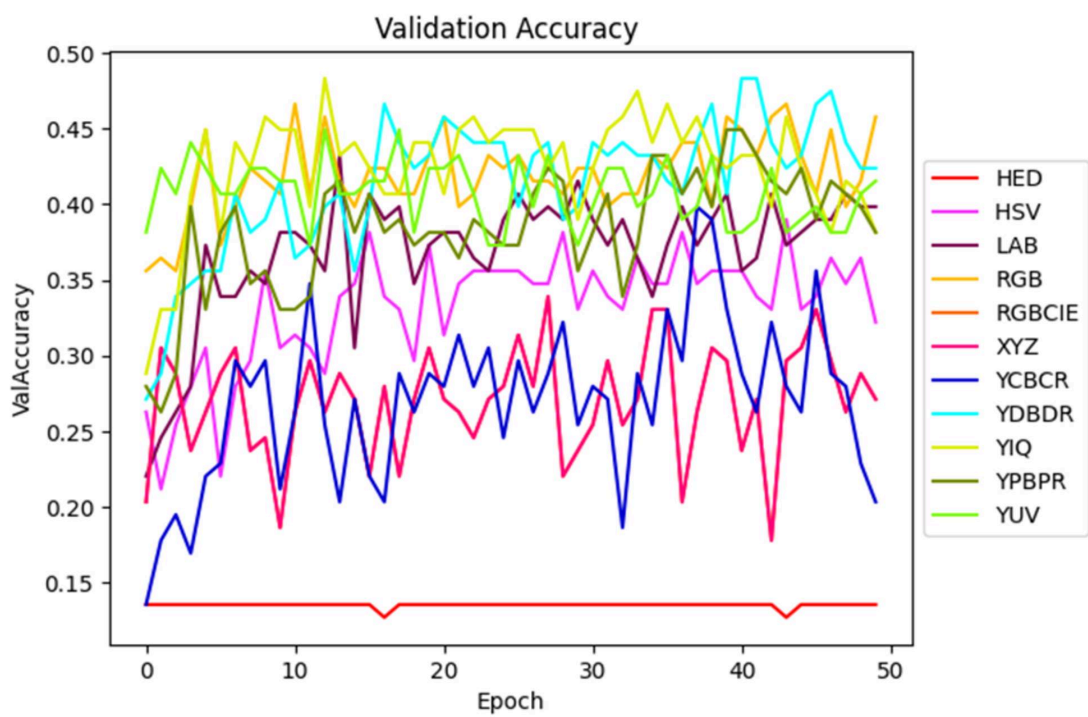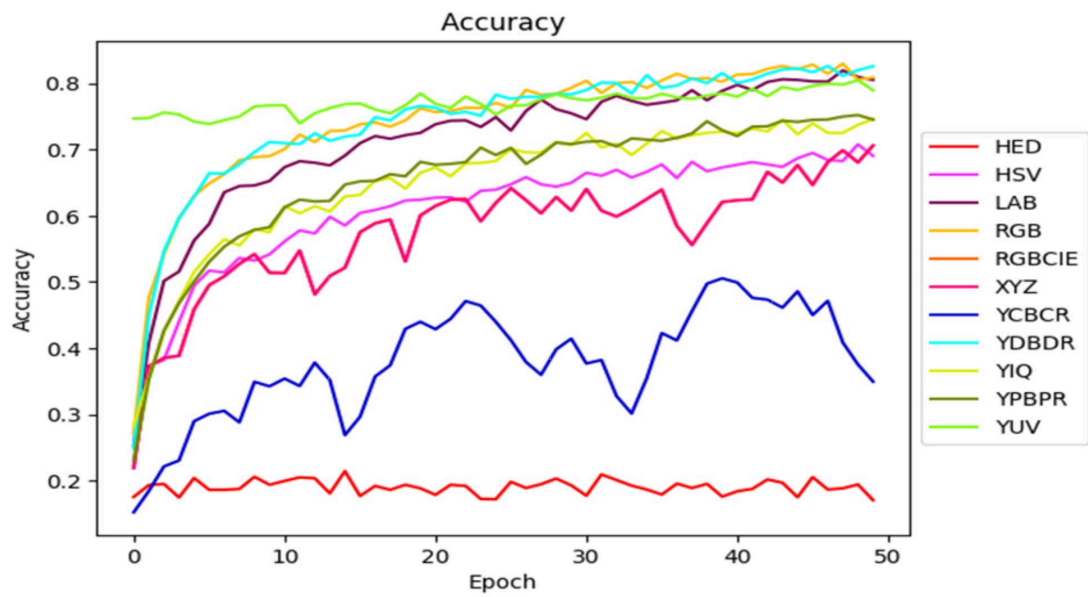FIGURE 5.18: Accuracy Curve Of Inception In Different Color Space

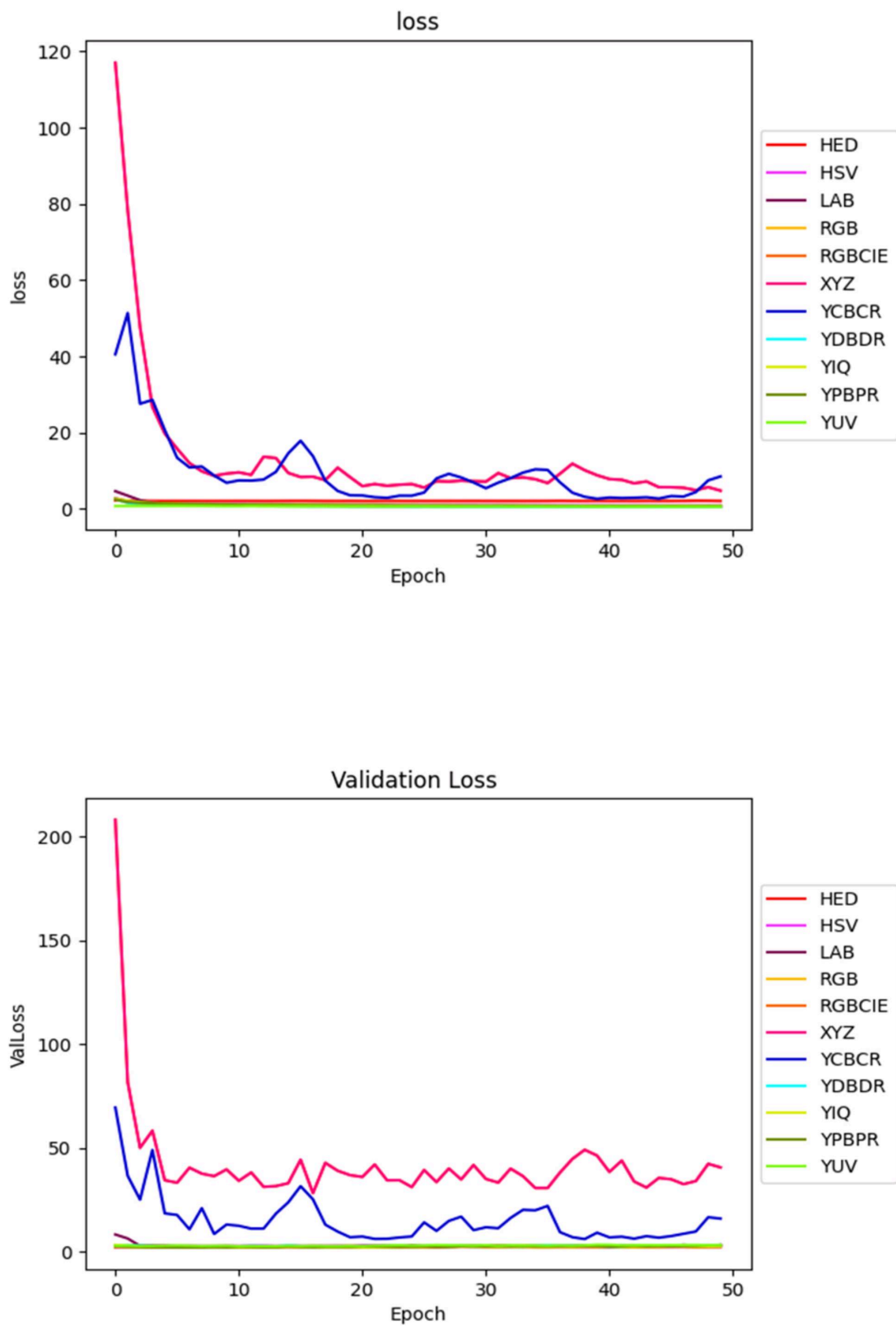FIGURE 5.19: Accuracy Curve Of Xception In Different Color Space

FIGURE 5.20: Accuracy Curve Of Densenet151 In Different Color Space

Chapter 6

Conclusion

In conclusion, this thesis aimed to classify skin cancer using different color spaces and explore their effectiveness in various convolutional neural networks. While the RGB color space is commonly regarded as the most effective, the findings of this study demonstrate that alternative color spaces, such as YUV and LAB, can yield superior accuracy results. By employing state-of-the-art classification models from The International Skin Imaging Collaboration (ISIC) dataset, the Color Space approach outperformed all other methods considered. Specifically, when using the MobileNet Architecture, the YUV color space achieved an impressive accuracy result of 92%. Similarly, the LAB color space, when utilized with the ResNet_50 model, yielded an accuracy of 86%. However, when employing the Inception_V3 model with the YPBPR color space, the accuracy decreased to 66%. The Xception architecture, when combined with the Color Space approach, achieved an accuracy of 80%, while the DenseNet121 model resulted in an accuracy of 82%.

The classification results reported in this study provide both quantitative and visual evidence of the effectiveness of the Color Space approach. These findings challenge the conventional belief that the RGB color space is universally superior for skin cancer classification. By considering alternative color spaces, researchers and practitioners can potentially enhance the accuracy and performance of skin cancer classification models. Further research and experimentation in this field are encouraged to explore the full potential of color spaces in medical image analysis and classification tasks.

6.1 FUTURE SCOPE

The future scope of using color space for skin cancer classification using deep learning holds immense potential for advancements in the field. There are several areas that offer opportunities for further exploration and development.

Firstly, researchers can delve deeper into integrating advanced color spaces beyond the commonly studied ones. By exploring color models like CMYK, LUV, LCH, and others, a more comprehensive understanding of skin cancer characteristics can be achieved. This exploration may uncover new features and relationships that contribute to improved classification accuracy.

Another avenue for future research is the investigation of hybrid color space models. By combining multiple color spaces, researchers can leverage the strengths of each model to capture a wider range of features. This can enhance classification accuracy by incorporating complementary information from different color spaces, leading to a more comprehensive representation of skin lesions. Adaptive color space selection is another promising area for future exploration. Developing techniques that dynamically determine the optimal color space for a given skin cancer image can enhance classification performance. By considering image-specific characteristics, such as lighting conditions and skin types, adaptive approaches can optimize the color space selection process and improve classification accuracy. Furthermore, the integration of color space with other modalities, such as texture, shape, and clinical metadata, holds the potential for more robust and accurate classification. By combining multiple modalities, researchers can capture a broader range of skin cancer characteristics, leading to more comprehensive diagnostic capabilities. To facilitate further advancements, the creation of large-scale, diverse datasets specifically designed for skin cancer classification in different color spaces is essential. Standardized datasets encompassing various skin types, lesion types, and color variations will enable better benchmarking and foster the development of more robust and generalizable deep-learning models.

Addressing the interpretability challenge in deep learning models for skin cancer classification is also crucial. Developing methods to understand and visualize the decision-making process of the models in different color spaces can provide valuable insights and increase trust in the classification results. Explainable AI techniques can help identify the color features and regions that contribute most significantly to the model's predictions.

Lastly, the real-world deployment and clinical integration of deep learning models for skin cancer classification using color space is an important future direction. Collaborations with healthcare professionals and dermatologists will enable the integration of these models into clinical workflows, allowing for improved skin cancer diagnosis, decision support, and ultimately enhancing patient care.

Chapter 7

REFERENCE

[1] Ganesan, P., B. S. Sathish, K. Vasanth, V. G. Sivakumar, M. Vadivel, and C. N. Ravi. "A comprehensive review of the impact of color space on image segmentation." In 2019 5th International Conference on Advanced Computing Communication Systems (ICACCS), pp. 962-967. IEEE, 2019.

[2] Tkalcic, Marko, and Jurij F. Tasic. Colour spaces: perceptual, historical and applicational background. Vol. 1. IEEE, 2003. [3] Asmare, Melkamu Hunegnaw, Vijanth Sagayan Asirvadam, and Lila Iznita. "Color space selection for color image enhancement applications." In 2009 International Conference on Signal Acquisition and Processing, pp. 208-212. IEEE, 2009.

[4] Zeileis, Achim, Jason C. Fisher, Kurt Hornik, Ross Ihaka, Claire D. McWhite, Paul Murrell, Reto Stauffer, and Claus O. Wilke. "colorspace: A toolbox for manipulating and assessing colors and palettes." arXiv preprint arXiv:1903.06490 (2019).

[5] Kuehni, Rolf G. "Color space and its divisions." Color Research Application: Endorsed by Inter-Society Color Council, The Colour Group (Great Britain), Canadian Society for Color, Color Science Association of Japan, Dutch Society for the Study of Color, The Swedish Colour Centre Foundation, Colour Society of Australia, Centre Français de la Couleur 26, no. 3 (2001): 209-222.

[6] Ballester, Coloma, Aurélie Bugeau, Hernan Carrillo, Michaël Clément, Rémi Giraud, Lara Raad, and Patricia Vitoria. "Influence of Color Spaces for Deep Learning Image Colorization." arXiv preprint arXiv:2204.02850 (2022).

[7] Zhang, Richard, Jun-Yan Zhu, Phillip Isola, Xinyang Geng, Angela S. Lin, Tianhe Yu, and Alexei A. Efros. "Real-time user-guided image colorization with learned deep priors." arXiv preprint arXiv:1705.02999 (2017).

[8] Kim, Hyun-Koo, Ju H. Park, and Ho-Youl Jung. "An efficient color space for deep-learning based traffic light recognition." Journal of Advanced Transportation 2018 (2018): 1-12.

[9] Al-Mohair, Hani K., Junita Mohamad-Saleh, and Shahrel Azmin Suandi. "Color space selection for human skin detection using color-texture features and neural networks." In 2014 International Conference on Computer and Information Sciences (IC-COINS), pp. 1-6. IEEE, 2014.

[10] Chavolla, Edgar, Daniel Zaldivar, Erik Cuevas, and Marco A. Perez. "Color spaces advantages and disadvantages in image color clustering segmentation." Advances in soft computing and machine learning in image processing (2018): 3-22.

[11] N. C. F. Codella et al., "Deep learning ensembles for melanoma recognition in dermoscopy images," in IBM Journal of Research and Development, vol. 61, no. 4/5, pp. 5:1-5:15, 1 July-Sept. 2017, doi: 10.1147/JRD.2017.2708299.

[12] A. Mahbod, G. Schaefer, C. Wang, R. Ecker and I. Ellinge, "Skin Lesion Classification Using Hybrid Deep Neural Networks," ICASSP 2019 - 2019 IEEE International Conference on Acoustics, Speech and Signal Processing (ICASSP), Brighton, UK, 2019, pp. 1229-1233, doi: 10.1109/ICASSP.2019.8683352.

[13] Li, Yuexiang, and Linlin Shen. 2018. "Skin Lesion Analysis towards Melanoma Detection Using Deep Learning Network" Sensors 18, no. 2: 556.
https://doi.org/10.3390/s18020556

[14] Esteva, A., Kuprel, B., Novoa, R. et al. Dermatologist-level classification of skin cancer with deep neural networks. Nature 542, 115–118 (2017).
https://doi.org/10.1038/nature21056.

[15] A. Arik, M. Gölcük and E. M. Karslıgil, "Deep learning based skin cancer diagnosis," 2017 25th Signal Processing and Communications Applications Conference (SIU), Antalya, Turkey, 2017, pp. 1-4, doi: 10.1109/SIU.2017.7960452.

[16] K. M. Hosny, M. A. Kassem and M. M. Foaud, "Skin Cancer Classification using Deep Learning and Transfer Learning," 2018 9th Cairo International Biomedical Engineering Conference (CIBEC), Cairo, Egypt, 2018, pp. 90-93,
doi: 10.1109/CIBEC.2018.8641762.

[17] Y. Fujisawa and others, Deep-learning-based, computer-aided classifier developed with a small dataset of clinical images surpasses board-certified dermatologists in skin tumour diagnosis, British Journal of Dermatology, Volume 180, Issue 2, 1 February 2019, Pages 373–381, https://doi.org/10.1111/bjd.16924

[18] Fooladi, Saber, Hassan Farsi, and Sajad Mohamadzadeh. "Detection and classification of skin cancer using deep learning." J Birjand Univ Med Sci 26, no. 1 (2019): 44-53.

[19] A. Demir, F. Yilmaz and O. Kose, "Early detection of skin cancer using deep learning architectures: resnet-101 and inception-v3," 2019 Medical Technologies Congress (TIPTEKNO), Izmir, Turkey, 2019, pp. 1-4, doi: 10.1109/TIPTEKNO47231.2019.8972045.

[20] Zekry, Abdelhalim. (2019). Deep Learning Can Improve Early Skin Cancer Detection. International Journal of Electronics and Telecommunications. 65. 10.24425/ijet.2019.129806.

[21] Kanani, Pratik. (2019). Deep Learning to Detect Skin Cancer using Google Colab. International Journal of Engineering and Advanced Technology. 8. 2176-2183. 10.35940/ijeat.F8587.088619.

[22] D, Seeja A, Suresh. (2019). Deep Learning Based Skin Lesion Segmentation and Classification of Melanoma Using Support Vector Machine (SVM). Asian Pacific Journal of Cancer Prevention. 20. 1555-1561. 10.31557/APJCP.2019.20.5.1555.

[23] M. M. I. Rahi, F. T. Khan, M. T. Mahtab, A. K. M. Amanat Ullah, M. G. R. Alam and M. A. Alam, "Detection Of Skin Cancer Using Deep Neural Networks," 2019 IEEE Asia-Pacific Conference on Computer Science and Data Engineering (CSDE), Melbourne, VIC, Australia, 2019, pp. 1-7, doi: 10.1109/CSDE48274.2019.9162400.

[24] C. Barata and J. S. Marques, "Deep Learning For Skin Cancer Diagnosis With Hierarchical Architectures," 2019 IEEE 16th International Symposium on Biomedical Imaging (ISBI 2019), Venice, Italy, 2019, pp. 841-845, doi: 10.1109/ISBI.2019.8759561.

[25] Garg, S., H. Garg, V. Tripathi, B. Pant, and K. Pant. "An Efficient Framework using Deep Learning for Skin Cancer Classification." Int. J. Innov. Technol. Explor. Eng. 9, no. 2 (2019): 1947-1951.

[26] Teck Yan Tan, Li Zhang, Chee Peng Lim, Intelligent skin cancer diagnosis using improved particle swarm optimization and deep learning models, Applied Soft Computing, Volume 84, 2019, 105725, ISSN 1568-4946, https://doi.org/10.1016/j.asoc.2019.105725.

[27] Khamparia, Aditya, Prakash Kumar Singh, Poonam Rani, Debabrata Samanta, Ashish Khanna, and Bharat Bhushan. "An internet of health things-driven deep learning framework for detection and classification of skin cancer using transfer learning." Transactions on Emerging Telecommunications Technologies 32, no. 7 (2021): e3963.

[28] Manne, Ravi, Snigdha Kantheti, and Sneha Kantheti. "Classification of Skin cancer using deep learning, ConvolutionalNeural Networks-Opportunities and vulnerabilities-A systematic Review." International Journal for Modern Trends in Science and Technology, ISSN 6 (2020): 2455-3778.

[29] Kadampur, Mohammad Ali, and Sulaiman Al Riyaee. "Skin cancer detection: Applying a deep learning based model driven architecture in the cloud for classifying dermal cell images." Informatics in Medicine Unlocked 18 (2020): 100282.

[30] Ameri, A. "A deep learning approach to skin cancer detection in dermoscopy images." Journal of Biomedical Physics and Engineering 10, no. 6 (2020): 801-806.

[31] R. Ashraf, I. Kiran, T. Mahmood, A. Ur Rehman Butt, N. Razzaq and Z. Farooq, "An efficient technique for skin cancer classification using deep learning," 2020 IEEE 23rd International Multitopic Conference (INMIC), Bahawalpur, Pakistan, 2020, pp. 1-5, doi: 10.1109/INMIC50486.2020.9318164.

[32] M. A. Hossin, F. F. Rupom, H. R. Mahi, A. Sarker, F. Ahsan and S. Warech, "Melanoma Skin Cancer Detection Using Deep Learning and Advanced Regularizer," 2020 International Conference on Advanced Computer Science and Information Systems (ICACSIS), Depok, Indonesia, 2020, pp. 89-94, doi: 10.1109/ICACSIS51025.2020.9263118.

[33] A. C. Salian, S. Vaze, P. Singh, G. N. Shaikh, S. Chapaneri and D. Jayaswal, "Skin Lesion Classification using Deep Learning Architectures," 2020 3rd International Conference on Communication System, Computing and IT Applications (CSCITA), Mumbai, India, 2020, pp. 168-173, doi: 10.1109/CSCITA47329.2020.9137810.

[34] Dildar, Mehwish, Shumaila Akram, Muhammad Irfan, Hikmat Ullah Khan, Muhammad Ramzan, Abdur Rehman Mahmood, Soliman Ayed Alsaiari, Abdul Hakeem M Saeed, Mohammed Olaythah Alraddadi, and Mater Hussen Mahnashi. 2021. "Skin Cancer Detection: A Review Using Deep Learning Techniques" International Journal of Environmental Research and Public Health 18, no. 10: 5479.
https://doi.org/10.3390/ijerph18105479

[35] Kareem, O. S., Abdulazeez, A. M., Zeebaree, D. Q. (2021). Skin Lesions Classification Using Deep Learning Techniques: Review. Asian Journal of Research in Computer Science, 9(1), 1–22. https://doi.org/10.9734/ajrcos/2021/v9i130210.

[36] J. Bethanney Janney, N. R. Krishnamoorthy, S. Divakaran, T. Sudhakar, S. Krishnakumar and V. Akshya., "Diagnosis of Skin Malignancy using Deep Learning Approaches," 2021 International Conference on Advancements in Electrical, Electronics, Communication, Computing and Automation (ICAECA), Coimbatore, India, 2021, pp. 1-4, doi: 10.1109/ICAECA52838.2021.9675722.

[37] Li, Hongfeng, Yini Pan, Jie Zhao, and Li Zhang. "Skin disease diagnosis with deep learning: a review." Neurocomputing 464 (2021): 364-393. [38] Juboori, Husam Khalaf Salih. "Detection of skin melanoma using deep learning approach." Sci. Arch 2, no. 4: 330-334.

[39] V. Rawat, D. P. Singh, N. Singh, P. Kumar and T. Goyal, "A Comparative Study of various Skin Cancer using Deep Learning Techniques," 2022 International Conference

on Computational Intelligence and Sustainable Engineering Solutions (CISES), Greater Noida, India, 2022, pp. 505-511, doi: 10.1109/CISES54857.2022.9844409.

[40] Wu, Yinhao, Bin Chen, An Zeng, Dan Pan, Ruixuan Wang, and Shen Zhao. "Skin Cancer Classification With Deep Learning: A Systematic Review." Frontiers in Oncology 12 (2022).

[41] Sweta, S., Mishra, N., Chaturvedi, S. (2022). Diagnosis of skin cancer using deep learning. International Journal of Health Sciences, 6(S5), 3374–3380. https://doi.org/10.53730/ijhs.v6nS5.9368.

[42] Gouda, Walaa, Najm Us Sama, Ghada Al-Waakid, Mamoona Humayun, and Noor Zaman Jhanjhi. "Detection of skin cancer based on skin lesion images using deep learning." In Healthcare, vol. 10, no. 7, p. 1183. MDPI, 2022.

[43] Montaha, Sidratul, Sami Azam, AKM Rakibul Haque Rafid, Sayma Islam, Pronab Ghosh, and Mirjam Jonkman. "A shallow deep learning approach to classify skin cancer using down-scaling method to minimize time and space complexity." PLoS One 17, no. 8 (2022): e0269826.

[44] R. S. Kumar, A. Singh, S. Srinath, N. K. Thomas and V. Arasu, "Skin Cancer Detection using Deep Learning," 2022 International Conference on Electronics and Renewable Systems (ICEARS), Tuticorin, India, 2022, pp. 1724-1730, doi: 10.1109/ICEARS53579.2022.9751826.